VOLUME 40, NUMBER 1, MARCH 2017

HADRONIC JOURNAL

Founded in 1978 by Prof. R. M. Santilli at Harvard University. Some of the past Editors include Professors S. L. Adler, A. 0. Barut, L. C. Biedenharn, N. N. Bogoliubov, M. Froissart, J.Lohmus, S. Okubo, Nobel Laureate Ilya Prigogine, M. L. Tomber, J. P.Vigier, J. Wess, Nobel Laureate Chen Ning Yang.

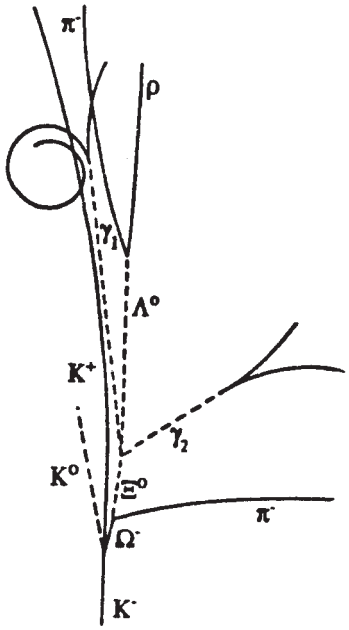

EDITORIAL BOARD

A.O.ANIMALU
A. K. ARINGAZIN
A. A. BHALEKAR
S. J. DHOBLE
J. DUNNING-DAVIES
T. L. GILL
L. P. HORWITZ
S. L. KALLA
S. I. KRUGLOV
M. NISHIOKA
R. F. O'CONNELL
Z. OZIEWICZ
E. RECAMI
M. SALEEM
B. G. SIDHARTH
S. SILVESTROV
H. M. SRIVASTAVA
E. TRELL
R.I. TSONCHEV
QI-REN ZHANG
C.A.WOLF
YI-ZHONG ZHUO

Founder and
Editor In Chief
R. M. SANTILLI

HADRONIC JOURNAL Volume 40, Number 1, March 2017

H/P HADRONIC PRESS, INC.

HADRONIC JOURNAL

VOLUME 40, NUMBER 1, MARCH 2017

THE STATUS OF PARTICLE THEORY, 1
E.L. Koschmieder
Center for Statistical Mechanics
The University of Texas at Austin
Austin, TX 78712 USA
THE SIGNIFICANCE OF THE NEUTRINOS AND THE MAGNETIC MONOPOLES FOR THE UNIVERSE, 13
H. Strusny
Hohenschoenhauser Str. 1, 10369 Berlin, Germany
PARTICLES AND GENERAL COORDINATE TRANSFORMATIONS, 57
Simon Davis
Research Foundation of Southern California
8861 Villa La Jolla Drive #13595
La Jolla, CA 92039 USA
STUDY OF COMBUSTION OF COAL WITH MAGNEGAS AS AN ADDITIVE FOR IMPROVING COMBUSTION EFFICIENCY: A REVIEW OF PRESENT SCENARIO AND FUTURE SCOPE, 71
Sachin Wazalwar
Department of Applied Chemistry
Rajiv Gandhi College of Engineering
Research & Technology, Chandrapur
Vijay Tangde and Anil Bhalekar
Department of Chemistry
Rashtrasant Tukadoji Maharaj Nagpur University
Amravati Road Campus, Nagpur
CONNECTION PRESERVING MAPS AND SOME APPLICATIONS, 85
Feray Bayar and Ayhan Sarioğlugil
Ondokuz Mayis University, Faculty of Sciences and Arts
Department of Mathematics, 55139, Samsun, Türkiye
MAGNECULAR STRUCTURE OF NEW CLEAN FUELS, 97
Chandrashekhar P. Pandhurnekar
Department of Applied Chemistry
Shri Ramdeobaba College of Engineering and Management
Nagpur, India

THE STATUS OF PARTICLE THEORY

E.L. Koschmieder
Center for Statistical Mechanics
The University of Texas at Austin
Austin, TX 78712 USA
koschmieder@utexas.edu

Received February 27, 2017
Revised March 14, 2017

Abstract

The long-lasting problem with the understanding of the masses of the elementary particles is investigated. The results of the well-known Standard Model of the particles and of a newer theory of the elementary particles are compared.

Copyright © 2017 by Hadronic Press, Inc., Palm Harbor, FL 34684, USA

Introduction

Feynman [1] wrote on the final page of his book about quantum-electrodynamics: "There remains one especially unsatisfactory feature: the observed masses of the particles, m. There is no theory that adequately explains these numbers. We use the numbers in all our theories, but we do not understand them - what they are, or where they come from. I believe that from a fundamental point of view, this is a very interesting and serious problem". That was 30 years ago and has not changed in the meantime.

If we discuss the status of the explanation of the particles we have to define what is meant by 'elementary particle'. In this article the elementary particles are the "stable" mesons and baryons and the charged leptons. The leptons are of the same importance as the mesons and baryons, because there are as many charged leptons in the world as charged mesons and baryons. The experimentally measured masses of the elementary particles are listed in the Review of Particle Physics [2]. We have also to say what we want to have explained about the elementary particles. That means that we want to know the parts of which the particles are made. Mass, charge and spin are the fundamental parts of the particles.

1 The Masses of the Mesons and Baryons

When the elementary particles are brought up, the theory usually referred to is the standard model (SM) of the particles, which came into being in the 1970s, after Gell-Mann [3] had introduced the quarks. A review of the SM can be found in [2] under the title "Electroweak Model and ..." Over the years the SM has bloomed into a model with 61 new particles, using 20 parameters in the process. More new hypothetical particles are introduced by the SM than the 20 stable elementary particles we know with certainty, and try to understand. None of the 61 particles predicted by the SM has been confirmed experimentally. Among the 20 parameters the SM uses are the measured masses of the mesons and baryons. If one uses one of these as a parameter one can then, of course, not explain with the same theory the masses one wants to understand. After the amount of time and effort spent on the SM, and after there has been no experimental verification of

the existence of the quarks, as well as of the existence of the fractional electrical charges which are supposed to be in the quarks, and since the SM does not deal with the leptons, and since the SM has not explained why a particular particle has its particular mass, it appears to be necessary to explore new ways to understand the elementary particles.

Two other theories have tried to explain the elementary particles, the string theory and supersymmetry. In spite of enormous efforts, both theories have, so far, not come up with experimentally realizable results. They are therefore not a part of this paper.

In the paper "Theory of the Elementary Particles", henceforth abbreviated to TEP, Koschmieder [4] has suggested that, quote: *"the elementary particles consist of the same particles into which they decay"*, directly or ultimately. A simple composition rule. That means that the particles are made of electromagnetic waves or photons, neutrinos and charge, whose existence in the particles is unquestionable. The particles are assumed to be held together by the weak nuclear force, because neutrinos interact through the weak force.

Another principal aspect of the TEP is the *integer multiple rule* of the particle masses. The integer multiple rule reads: "the measured rest masses of the stable mesons and baryons are, in a very good approximation, integer multiples of the π^0 or $\pi^{\pm}$ mesons". See Fig. 1

For example, the mass of the η meson, the first neutral meson heavier than the π^0 meson, is $m(\eta) = 1.0147 \cdot 4 \cdot m(\pi^0)$, which is followed by $m(\Lambda) = 1.0332 \cdot 8 \cdot m(\pi^0) = 1.0182 \cdot 2 \cdot m(\eta)$. And the mass of the heavy neutral baryon Ω_c^0 is $m(\Omega_c^0) = 0.9984 \cdot 20 \cdot m(\pi^0)$. The nine neutral particles whose masses are approximately integer multiples of the mass of π^0 are referred to as the γ-branch of the particle spectrum. The fundamental integer multiple rule is a summary of experimental facts and is consequently unquestionable.

It is incomprehensible that the simple integer multiple rule has escaped the attention of a generation of particle physicists. It is likewise very odd that this rule has been ignored since its publication in the arXiv in 2000, or in later papers as in [4].

The composition rule runs immediately into trouble with the π^0 meson.

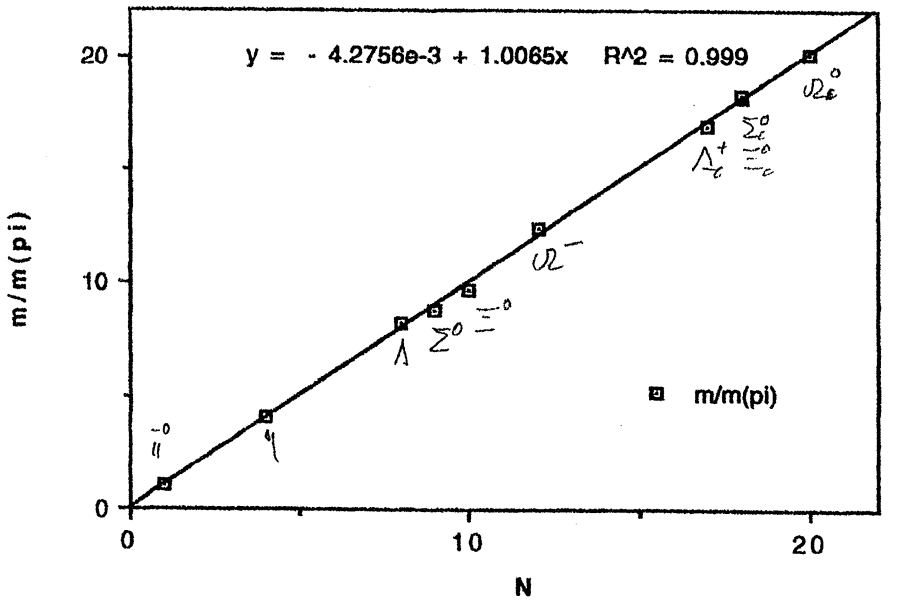

Figure 1: The Masses of the particles of the γ-branch, from a least-square analysis, with $m_i = 1.0065\ N_i \cdot m(\pi^0)$.

The π^0 meson has the smallest mass and presumably the most simple composition of all mesons. The π^0 meson decays into two γ-rays, $\pi^0 \rightarrow \gamma\gamma$. According to the composition rule the π^0 meson should consist of γ-rays. That is, however, impossible. γ-rays move with the velocity of light, which they cannot do in a particle which has a rest mass. However, there exist also *"standing electromagnetic waves"*. The existence of standing electromagnetic waves is unquestionable. If the γ-rays in the π^0 meson are standing waves, then the composition rule is satisfied.

The *explanation of the integer multiple rule* of the particle masses follows immediately, if the π^0 meson and its multiples do, indeed, consist of standing waves. The frequencies of standing waves are integer multiples of the basic frequency of the wave. That means that the multiples of the π^0 meson mass are filled with waves with integer multiples of the basic frequency of π^0.

Since the mass of a particle is proportional to the sum of its frequencies, the mass of any particle of the γ-branch must be an integer multiple of the mass with the basic frequency.

The mass of the π^0 meson can be calculated from the sum of the frequencies of the standing waves in the π^0 meson, if one uses Plancks classical equation for the energy of a linear oscillator E_ν. The mass of the π^0 meson is

$$m(\pi^0)(theor) = N \cdot \overline{E_\nu} = 1.005 \cdot m(\pi^0)(exp).$$

N is the number of the waves in the π^0 meson, $N = 4\pi {r_p}^3/3a^3 = 2.854 \cdot 10^9$, where r_p is the measured charge radius of the proton, and a is the lattice constant, set to be $a = 10^{-16}$ cm. To quote: "the π^0 meson is like a cubic black body filled with standing electromagnetic waves". The masses of the other nine particles of the γ-branch can be explained as higher modes or the sum of superposed modes of the standing waves in the π^0 meson.

According to the composition rule the $\pi^\pm$ mesons should consist of muon neutrinos, electron neutrinos, their antiparticles, plus a charge $e^\pm$, as the $\pi^\pm$ decay sequence tells. Neutrinos interact with the weak force, which has the very short range of $O(10^{-16})$ cm. Assuming that the weak force holds the neutrinos in the pion together, it follows, quote: *"A particle held together by the weak force is not spherical but cubic"*. Something unheard of.

If the $\pi^\pm$ mesons are like cubic crystals, then classical lattice theory, Born und v.Karman [5], applies. To quote [4] "The $\pi^\pm$ mesons are like cubic black bodies, filled with oscillating neutrinos". The theoretical rest mass of the $\pi^\pm$ neutrino lattice is equal to the measured mass of the $\pi^\pm$ mesons, if the consequences of the charge for the mass of $\pi^\pm$ are neglected and the oscillation energy is taken into account. The five elementary particles with a cubic neutrino lattice, which make up the neutrino branch of the particles, are the $\pi^\pm$ mesons, K mesons, the neutron, the proton, and the D mesons. They consist of cubic neutrino lattices and the oscillation energies of the neutrinos in their lattice. In the lattice of the K^0 meson one encounters neutrino dipoles, $\nu_e, \bar{\nu}_e$ or $\nu_\mu, \bar{\nu}_\mu$, together with a charge dipole e^+, e^-. The lattice of the neutron consists of neutrino quadrupoles $\nu_\mu, \bar{\nu}_\mu, \nu_e, \bar{\nu}_e$, not individual neutrinos as e.g. electron neutrinos ν_e or muon neutrinos ν_μ, and of a charge quadrupole e^-, e^+, e^-, e^+. The neutrino quadrupoles oscillate in their cubic lattices following the same laws as the individual neutrinos. The

proton is a consequence of the β-decay of the neutron, $n \rightarrow p + e^- + \bar{\nu}_e$ (100%). The reversal of the β-decay, the synthesis of the neutron $p + e^- + \bar{\nu}_e \rightarrow n$, has also been observed experimentally. The consequences and importance of the synthesis of the neutron has been shown by Santilli [6]. The β-decay of the neutron means that neutrino triplets like $\bar{\nu}_\mu,\nu_e,\nu_\mu$ and also an electric triplet e^+,e^-,e^+ must be in the proton. All particles of the neutrino branch of the particles have a cubic oscillating neutrino lattice with N lattice points, whose oscillation energy can be calculated.

All "stable" mesons and baryons are thus accounted for. For each of these particles one can calculate its rest mass. For example:

$$m(\pi^\pm)(theor) = N(m(\nu_\mu) + m(\nu_e)) = 1.028\, m(\pi^\pm)(exp),$$

without considering the charge. The calculated masses of the stable mesons and baryons are integer multiples of either the π^0 meson mass or of the $\pi^\pm$ meson mass, complying with the integer multiple rule.

2 The Masses of the Leptons

The leptons e, μ, τ and the neutrinos pose new problems. The e, μ and τ particles are supposed to be *point particles.* Since the electron, muon and tau lepton have very accurately measured rest masses, the point particle concept would mean that the density of these particles is infinite. That does not make much sense.

The muon was discovered 80 years ago by Anderson and Neddermeyer [7] and Street and Stevenson [8], and has been a puzzle ever since, because it does not react strongly with other particles. The key to the explanation of the muon is the fact that, quote: "the mass of the muons is in a good approximation 3/4 of the mass of the $\pi^\pm$ mesons", $m(\mu^\pm) = 1.00937 \cdot 3/4 \cdot m(\pi^\pm)$. Heretofore the muon has been considered to be a multiple of the electron mass, $m(\mu) = 207\, m(e)$. The decay $\pi^\pm \rightarrow \mu^\pm + \nu_\mu(\bar{\nu}_\mu)$, which produces the muon, tells what the muons are made of. In the decay of the pion all muon neutrinos or anti-muon neutrinos in its lattice annihilate into kinetic energy, but for one single muon- or anti-muon neutrino, which was in the center of the pion lattice, and is the single muon- or anti-muon neutrino in $\pi^\pm \rightarrow \mu^\pm + \nu_\mu(\bar{\nu}_\mu)$. The mass of N/4 muon

neutrinos is nearly 1/2 of the mass of all neutrinos in the pion lattice, if the mass of the electron (m(e) = m($\pi^{\pm}$)/273) and of all electron neutrinos is negligible. All N/4 ν_μ plus all N/4 $\bar{\nu}_\mu$ neutrinos in the pion make up approximately m($\pi^{\pm}$)/2, the other half of the mass of $\pi^{\pm}$ is in the oscillation energy of the neutrinos, which can be calculated. Since N/4·m(ν_μ) = m($\pi^{\pm}$)/4, N/4 muon neutrinos have to be subtracted from m($\pi^{\pm}$). Then

$$m(\mu^{\pm})(theor) = 3/4\,N{\cdot}m(\nu_\mu) + N{\cdot}m(\nu_e) = 1.020 \cdot 3/4 \cdot m(\pi^{\pm})(exp),$$

without considering the charge. The muon mass is 3/4 of the pion mass when the pion has lost all ν_μ or $\bar{\nu}_\mu$ neutrinos in the decay, in order to explain why the mass of the muon is equal to 3/4 m($\pi^{\pm}$). It has thus been explained why m($\mu^{\pm}$) is practically $3/4 \cdot$ m($\pi^{\pm}$).

In order to verify the validity of the explanation of the equation for the mass of the muon, one has to know the masses of the neutrinos, whose masses are controversial. In general it is believed that the neutrinos do not have mass, although it is, of course, $E = mc^2$. If the pion has indeed a cubic neutrino lattice consisting of equal numbers of muon neutrinos, electron neutrinos and their antiparticles, then the mass of the muon neutrino follows directly from the mass of the pion. As shown in the preceding paragraph the sum of the masses of the muon neutrinos in the cubic lattice of $\pi^{\pm}$ is m($\pi^{\pm}$)/4. That means that N/4·m(ν_μ) = m($\pi^{\pm}$)/4. From the exactly known m($\pi^{\pm}$)/4 follows that m(ν_μ) $\approx$ 50 milli-eV/c^2. In other words, the mass of a muon neutrino in the pion is $\approx$ 50 milli-eV/c^2.

The mass of the electron neutrino follows from the energy released in the β-decay of the neutron, $n \rightarrow p + e^- + \bar{\nu}_e$. We have m(n) - m(p) = 1.29333 MeV/c^2 [2], and N anti-electron neutrinos are in the neutrino quadrupole lattice of the neutron. One finds that m(ν_e) = m($\bar{\nu}_e$) = 0.365 milli-eV/c^2. This may or may not be so, but this value of m(ν_e) brings about a stunning result. With m(ν_μ) = 49.91 milli-eV/c^2 and m(ν_e) = 0.365 milli-eV/c^2 follows from the ratio m(ν_e)/m(ν_μ) that $m(\nu_e)(theor) = 1.0022 \cdot \alpha_f \cdot m(\nu_\mu)$, with the fine-structure constant α_f = 1/137.036. The equation m(ν_e) = α_fm(ν_μ) is unparalled. It poses the question how it can be that the masses of the electron neutrino and the muon neutrino are coupled through the fine-structure constant α_f, which originates from atomic theory.

After the discovery of the electron by Thomson [9] in 1897, there was an intensive effort to explain the existence of the electron. Some of the most distinguished physicists participated in this work. Nevertheless, one hundred years later we still do not have an accepted theory of the electron. The SM does not solve the electron problem either, it just does not deal with that.

From the decay sequence of the $\pi^{\pm}$ mesons $\pi^{\pm} \rightarrow \mu^{\pm} + \nu_{\mu}(\bar{\nu}_{\mu})$ and $\mu^{\pm} \rightarrow e^{\pm} + \bar{\nu}_{\mu}(\nu_{\mu}) + \bar{\nu}_{e}(\nu_{e})$ seems to follow that there are *neutrinos in the electron.* There are four neutrino types $\nu_{\mu}, \bar{\nu}_{\mu}, \nu_{e}, \bar{\nu}_{e}$ in the cubic lattice of the pion. Three of the neutrino types $\nu_{\mu}, \bar{\nu}_{\mu}, \bar{\nu}_{e}$ are accounted for in the decay sequence of the pion, but after the decay the electron neutrinos which were in the $\pi^{\pm}$ meson are missing. They cannot simply disappear, that would violate conservation of energy. There is no other place where, after the decay of the muon, the missing electron neutrinos can be, but in the electron. Since N/4 electron neutrinos must be in the cubic π^{-} lattice, it follows that N/4 electron neutrinos must be in the electron emitted in the decay of the muon. Each of the missing electron neutrinos carries the mass $m(\nu_{e})$, the sum of which is $N/4 \cdot m(\nu_{e}) = 1.019\, m(e^{\pm})/2$. The neutral sum of the electron neutrinos in the electron is what in modern parlance is called the "bare" part of the electron, it is now $m_{b} = \Sigma\, m(\nu_{e}) = m(e^{\pm})/2$. It seems, therefore, to be justified to believe that the N/4 electron neutrinos missing after the $\pi^{\pm}$ decay are indeed in the electron emitted in the subsequent muon decay.

Electron neutrinos make up 1/2 of the mass of the electron.

The other half of the energy in the electron is in the oscillation energy of its neutrinos, which oscillate in their cubic lattice. The oscillation frequencies are determined by a simple equation of classical lattice theory. In order to determine the oscillation energy in the electron from the sum of the frequencies one cannot use the equation used for the oscillation energy in the case of the pion, because this equation leads to a mistaken result. If, however, the equation used for the oscillation energy in the pion is multiplied with the fine-structure constant α_{f}, then one arrives at an oscillation energy in the electron $E_{\nu}(e^{\pm}) = 0.996\, m(e^{\pm})c^{2}/2$. That means that the oscillation energy in the neutrino lattice of the electron is, in a good approximation, the same as the energy in the sum of the electron neutrino masses in the electron, which is $N/4 \cdot m(\nu_{e})c^{2} \cong m(e^{\pm})c^{2}/2$. The sum of both, of the mass

of all electron neutrinos plus the mass in the oscillation energy of all electron neutrinos in $e^{\pm}$, or the total energy in the rest mass of the electron or positron is then $m(e^{\pm})(theor) \cong N/2 \cdot m(\nu_e) = 1.019\, m(e^{\pm})(exp)$.

This equation says nothing about the charge, the other fundamental property of the electron. But this problem has already been taken care of when the equation used for the oscillation energy in $\pi^{\pm}$ was modified by multiplication with the fine-structure constant, in order to arrive at the correct value of the oscillation energy of the neutrinos in the electron. When the energy $h\nu$ of the lattice oscillations with frequency ν is multiplied with the fine-structure constant $\alpha_f = e^2/\hbar c$, the oscillation energy turns out to be electric energy. The electric energy is given by the equation $h\nu_0\alpha_f = e^2/a$; a being the lattice constant, $a = 10^{-16}$ cm. That means that the oscillation energy of the neutrinos in the electron is actually electrical energy, which must be caused by an electrical charge Q, whose charge is found to be $Q = \pm 1.047 \cdot e$. The sum of the masses of the electron neutrinos in $e^{\pm}$, plus the mass in the sum of the oscillations energies in $e^{\pm}$ is, within the accuracy of the parameters N and $m(\nu_e)$, equal to

the rest mass of the electron $\quad m(e)(theor) \cong N/2 \cdot m(\nu_e)$.

If the electron has, indeed, been explained by this equation, then it is part of the explanation of the ratios $m(\mu^{\pm})/m(e^{\pm}) = 207$ and $m(\pi^{\pm})/m(e^{\pm}) = 273$, and also of $m(p^{\pm})/m(e^{\pm}) = 1836$, for which an explanation has been looked for since about 100 years. The first step towards the explanation of these ratios was taken by Nambu [10] in 1952, who noted empirically that $m(\mu^{\pm})/m(e^{\pm})$ is approximately $3/2\alpha_f$, where α_f is the fine-structure constant, and that $m(\pi^{\pm})/m(e^{\pm})$ is approximately $2/\alpha_f$. 25 years later Barut [11] found that both ratios can be described by similar but more accurate equations, $m(\mu^{\pm})/m(e^{\pm}) = 3/2\alpha_f + 1 = 0.9989\, m(\mu^{\pm})/m(e^{\pm})(exp)$ and $m(\pi^{\pm})/m(e^{\pm}) = 2/\alpha_f - 1 = 0.9998\, m(\pi^{\pm})/m(e^{\pm})(exp)$. Afterwards the Nambu-Barut equations have been forgotten.

If one now uses the TEP equations for the masses of the muon and pion and divides them by the equation for the mass of the electron, then one arrives theoretically at the N-B equations. The theoretical mass ratios then differ from the measured mass ratios by 0.38% in the case of $m(\mu^{\pm})/m(e^{\pm})$, and by 1.08% in the case of $m(\pi^{\pm})/m(e^{\pm})$. In other words: "The theoretical values of $m(\mu^{\pm})/m(e^{\pm})$ and $m(\pi^{\pm})/m(e^{\pm})$ prove, within a percent, the

validity of the explanation of $m(\mu^{\pm})$, of $m(\pi^{\pm})$, and of $m(e^{\pm})$, as well as the validity of the relation $m(\nu_e) = \alpha_f \cdot m(\nu_\mu)$".

The explanation of the spin of the particles has been disappointing. The spin was discovered 90 years ago by Uhlenbeck and Goudsmit [12], but there is at the present time no accepted explanation of the spin, even for the spin of the quarks in the SM. But the spin is one of the fundamental properties of all elementary particles, from the electron to the Higgs boson. At the end the TEP showed that the spin of the particles is determined by the center particle of the cubic lattice of the particles. To quote: "The center of the lattice alone determines the angular momentum of the oscillations and of the spin of the neutrinos in the lattice". The symmetry of cubic lattices is crucial for the explanation of the spin. Adding to that the spin vector of one or more charges $e^{\pm}$ one arrives at the total intrinsic angular momentum of a particle. The spin can be explained through the structure of the particles.

Conclusions

The extraordinary experimental efforts in the investigation of the elementary particles ask for an explanation of the results of these experiments. At the present time it seems to be questionable that we have a theory which would explain the reason for which the mass of a particular particle, say the proton, has the value which has been measured. It is usually maintained that the standard model takes care of this. In order to explain the particles, the SM reduces the multitude of observed particles to a few hypothetical basic particles, the quarks. The proton, for example, is said to consist of three quarks. This apparently simple model brings problems with it. The proton carries one positive electrical charge. The charge has then to be distributed somehow on the three quarks. That introduces the so-called fractional electrical charges, which are $2/3\,e^{\pm}$ and $-1/3\,e^{\pm}$, for the u and d quarks. However, fractional electric charges are not known in traditional electricity. This concept has to be verified experimentally.

The SM treats the interactions of the elementary particles successfully, but the model stumbles when it comes to the explanation of the masses of the particles. In order to do that one would have to know the masses of

the quarks. Elaborate experiments to find and thereby determine a quark mass have not been successful. The failure to do so has been justified with the argument that the quarks are "confined". But a rigorous theoretical justification of confinement has not been found. That means, after 40 years of searching, that the SM does not provide an explanation of the mass of the elementary particles. There is also the problem, that it has not been possible to confirm experimentally the existence of the fractional charges. And there is the problem that the SM does not deal with the leptons. For the validity of the SM, or any other model of the elementary particles, it is necessary that the model can explain, to a certain degree of accuracy, the value of the mass of a particular particle. No way has yet been found to solve the crucial problem the SM has with the masses of the particles.

It appears that we have to try a different way in order to arrive at a correct explanation of the masses of the elementary particles. An alternative solution of this problem is suggested in the TEP. One advantage of this theory is that it does not use hypothetical particles. Instead it uses, as it reads in the abstract of [4]: *"Only photons, neutrinos, charge and the weak nuclear force are needed to explain the masses of the elementary particles"*. Another fundamental feature of the TEP is the *integer multiple rule* of the masses of the stable mesons and baryons. The rule is a summary of unquestionable experimental facts. The masses of all stable mesons and baryons have been calculated by the TEP. They agree, within a small uncertainty, with the measured values of the particle masses, and thereby follow the integer multiple rule. Surprisingly one can also explain the muon from the decay sequence of the pion. The muon is a fragment of the pion, its mass is

$$\mathrm{m}(\mu^{\pm})(\mathit{theor}) = 1.021{\cdot}3/4 \cdot \mathrm{m}(\pi^{\pm}).$$

And even more surprising is that one can explain the electron. The title of chapter 11 of [4] reads: *"Neutrinos in the electron"*, a concept that has apparently not been considered before. The sum of the masses of the electron neutrinos in the electron is equal to one half of the mass of the electron. The other half of the mass of the electron is in the oscillation energy of the charge of the electron. The sum of both masses is

$$\mathrm{m(e)}(\mathit{theor}) = \mathrm{N}/2{\cdot}\mathrm{m}(\nu_e) = 1.019\,\mathrm{m(e)}(\mathit{exp}).$$

And finally, the spin of the particles has been explained through the lattice structure of the particles. The center particle of the lattice deter-

mines the sum of the angular momentum of the lattice oscillations, and the sum of the spin of all neutrinos in the lattice. Mass, charge, and spin of the elementary particles have in common one elementary feature, the cubic lattice.

It is time to answer Feynmans challenge for an explanation of the masses of the particles m. Progress has been slow. Even the simple integer multiple rule has not been noticed over the years. The TEP offers an explanation of the masses of the stable mesons and baryons, as well as of the leptons, using only photons, neutrinos, charge, the weak nuclear force, and lattice theory. The masses of the particles explained this way agree with the measured masses of the particles within about a percent, which is crucial for the validity of the model. If we can finally calculate the values of the masses of the particles, we will have come one step further in the understanding of the elementary particles.

Acknowledgement
I thank Prof. L. Frommhold for suggesting the abbreviation TEP.

References

[1] Feynman, R.P. 1985. *QED. The Strange Theory of Light and Matter.* Princeton University Press, p.152.
[2] Olive, K.A. et al. 2014. Review of Particle Physics. Chin.Phys.C. **38**,090001.
[3] Gell-Mann, M. 1964. Phys.Lett.B. **11**,1.
[4] Koschmieder, E.L. 2008. arXiv.org 0804.4848. 2014. Hadr.J. **37**,361.
[5] Born, M. und v.Karman, Th. 1912. Phys.Z. **13**,297.
[6] Santilli, R.M: *Clifford Analysis , Clifford Algebras and their Applications*, in Press (2017).
[7] Anderson, C.D. and Neddermeyer, S. 1937. Phys.Rev. **51**,884.
[8] Street, J.C. and Stevenson, E.C. 1937. Phys.Rev. **52**,1003.
[9] Thomson, J.J. 1897. Phil.Mag. **44**,293.
[10] Nambu,Y. 1952. Prog.Th.Phys. **7**,595.
[11] Barut, A.O. 1979. Phys.Rev.Lett. **42**,1251.
[12] Uhlenbeck, G.E. and Goudsmit, S. 1925. Naturwiss. **13**,953.

THE SIGNIFICANCE OF THE NEUTRINOS AND THE MAGNETIC MONOPOLES FOR THE UNIVERSE

H. Strusny
Hohenschoenhauser Str. 1
10369 Berlin, Germany
p.ressel@freenet.de

Received March 28, 2017

Abstract

We present a new estimation for the neutrino masses and the neutrino density of the universe. For the X and Y gauge bosons as well as the magnetic monopoles, which are predicted by the (supersymmetric) grand unified theories ((SUSY) GUTs) for the early universe, we derive their mass on a new way, so that in agreement with the particle physics we can uniquely determine the coupling constant of the (SUSY) GUTs. We find an exact and unique description of the inflation and its transition to the standard model. For the redshift, we calculate quantitatively two different scale factors of the absorption of light prior to and after this inflation. We derive the exact value of the curvature of the universe. We explain the influence of the dark energy which in first approximation yields effectively a "final" state for the universe as a function of a blueshift via a negative acceleration determined by the electron neutrino density of the universe, so that we can explain the Pioneer anomaly and the flyby anomaly as well as the astronomical unit changing. By the neutrinos, plausible values of the redshifts for the beginning, the half and the end of the reionization are obtained. We have explained the physical meaning of the effective influence of the dark energy via the "final" state of the universe. Thus, we can show that in future after the (present) exponential expansion (defined by the dark energy) we will observe a slow linear expansion of the universe. All these results were mainly obtained by the big bang model, so that they show the significance of the light neutrinos and the extremely heavy hypothetical magnetic monopoles for the universe.

PACS numbers: 14.70.-e, 14.80.Hv, 95.85.Ry, 98.80.Cq

Copyright © 2017 by Hadronic Press, Inc., Palm Harbor, FL 34684, USA

1 Introduction

The neutrino masses and the neutrino densities of the universe are still unknown [1, 2]. The masses of the X and Y gauge bosons as well as the magnetic monopoles, which are predicted for the early universe by the supersymmetric grand unified theories (SUSY GUTs), can only approximately be estimated [2]. Therefore, for the universe, in spite of the SUSY GUTs, the significance of the light neutrinos and the extremely heavy hypothetical magnetic monopoles is not clear [1, 2]. Further, there is no exact description of the inflationary cosmology and its transition to the standard cosmology, so that pressing problems of the standard model (as for example the horizon problem, the monopole problem, the flatness problem and the initial condition problem) can only qualitatively be explained [1, 3]. At the redshift defined by the Friedmann-Robertson-Walker metric, the value of the scale factor of the absorption of light is not known [3, 4]. The exact value of the curvature of the universe is not clear [1, 3]. The question of the "end" of the universe is still open. The Pioneer anomaly [5] and the flyby anomaly [6] as well as the astronomical unit changing [7-9] are still unsolved. The exact values of the redshifts for the beginning, the half and the end of the reionization are still unclear [1]. The physical meaning of the influence of the dark energy is still unknown [3].

Therefore, in this work, we try to solve the above-mentioned problems on the basis of the results of the big bang model and the supersymmetric grand unified theories. Thus, this work is organized as follows. In Sec. 2, we describe shortly the results of the big-bang cosmology (Sec. 2.1), the pressing problems of the standard model (Sec. 2.2) and the results of the supersymmetric grand unified theories (Sec. 2.3). In Sec. 3, we estimate the neutrino masses (Sec. 3.1) and the neutrino densities of the universe (Sec. 3.2). In Sec. 4, we derive the rest energy of the X and Y gauge bosons. In Sec. 5, we treat the inflationary cosmology, whereat we determine the values of the scale factors of the absorption of light at the redshift "before" and after the inflation (Sec. 5.1), calculate the rest energy of the magnetic monopoles (Sec. 5.2) as well as solve the inflation problem (Sec. 5.3). In Sec. 6, we find the exact value of the curvature for the universe. In Sec. 7, we describe the Planck units (Sec. 7.1),

explain qualitatively in first approximation the "final" state of the universe by a mean negative acceleration as a function of a blueshift via the electron neutrino density (Sec. 7.2), determine quantitatively the characteristic values of this "final" state and of this mean negative acceleration interpreted as the Pioneer anomaly (Sec. 7.3) as well as estimate the redshifts for the beginning, the half and the end of the reionization (Sec. 7.4). In Sec. 8, we treat the flyby anomaly (Sec. 8.1), the astronomical unit changing (Sec. 8.2) and the physical meaning of the influence of the dark energy on the "final" state of the universe (Sec. 8.3). In Sec. 9, we give a short summary. The values used for the fundamental constants, are given in Refs. [2, 10].

2 Results of the models used

2.1 The results of the big-bang model

In this chapter, the considerations are based on Refs. [1-4, 10, 11]. In agreement with all of those parts of the universe, which are accessible by observations, we can assume that at (very) early times and today on a sufficiently large scale the universe is very nearly homogeneous and isotropic. For such a space, the most general four-dimensional line element ds is determined by the Friedmann-Robertson-Walker metric in the form

$$ds^2 = c^2 dt^2 - R^2(t)\left[\frac{dr^2}{1-\mathrm{k}r^2} + r^2(d\vartheta^2 + \sin^2\vartheta\, d\varphi^2\right], \qquad (2.1)$$

where c is the velocity of light in vacuum and t is the time, whereas the dimensionless Lagrange coordinates r, ϑ and φ are constant because of the expansion of the universe, so that $R(t)$ determines alone the time dependence of this metric, i.e. $R = R(t)$ is the scale factor for distances in comoving coordinates. By appropriate rescaling of the radial coordinate, the constant k can be chosen to be $+1$ (closed geometry with finite volume), -1 (open hyperbolic space) or 0 (Euclidian (spatially flat) geometry with infinite volume).

In such an expanding universe, the observed wavelength λ of the light emitted (e) from a distant source with λ_e, is shifted towards the red. Via the Friedmann-Robertson-Walker metric, this so-called redshift z is defined by

$$1+z=\frac{\lambda}{\lambda_e}=\frac{R_0}{R}, \tag{2.2}$$

where R_0 and R are the scale factors of absorption and emission of light, respectively.

In this important metric, Einstein's equations lead to the Friedmann equation

$$H^2=\left(\frac{\dot{R}}{R}\right)^2=-\mathrm{k}\frac{c^2}{R^2}+\frac{8\pi G_N}{3}\rho+\frac{c^2}{3}\Lambda \tag{2.3}$$

as well as to the equation

$$\frac{\ddot{R}}{R}=-\frac{4\pi G_N}{3}\left(\rho+\frac{3P}{c^2}\right)+\frac{c^2}{3}\Lambda \tag{2.4}$$

as the so-called Friedmann-Lemaitre Equations, where $H=H(t)$ is the Hubble parameter, G_N is the gravitational constant, ρ is the mean mass density, P is the isotropic pressure and Λ is the cosmological constant. For $\Lambda=0$, we obtain the so-called standard model (of the relativistic cosmology). From Eqs. (2.3) and (2.4), we can derive a third useful equation

$$\dot{\rho}=-3\frac{\dot{R}}{R}(\rho+\frac{P}{c^2})=-3\frac{\dot{R}}{R}\rho(1+w), \tag{2.5}$$

where $w=P/\rho c^2$ is the so-called state parameter. Additional to the Hubble parameter, it is useful to define also several other measurable cosmological parameters. For this goal, at $\mathrm{k}=0$ and $\Lambda=0$, via the Friedmann equation, a critical (C) density can be defined by

$$\rho_C=\frac{3H^2}{8\pi G_N}=1.87847(23)\times10^{-29}h^2\,\mathrm{g\,cm^{-3}}=$$
$$=1.05375(13)\times10^4h^2(\mathrm{eV}/c^2)\,\mathrm{cm^{-3}}, \tag{2.6}$$

where the scaled Hubble parameter h is defined by the expression

$$H = 100h \text{ km s}^{-1} \text{ Mpc}^{-1} = \frac{h}{9.777752 \text{ Gyr}} =$$

$$= 3.240779 \times 10^{-18} h \text{ s}^{-1}. \tag{2.7}$$

Then, we can rewrite the Friedmann equation as

$$\mathrm{k}\frac{c^2}{R^2} = H^2(\Omega - 1) \tag{2.8}$$

with

$$\Omega = \frac{\rho}{\rho_{\mathrm{C}}}. \tag{2.9}$$

Because it is often necessary to distinguish between different contributions to the density ρ, it is usual to define present-day density parameters for dark energy (Ω_Λ), pressureless matter (Ω_{m}) and relativistic particles (Ω_{r}), so that the very important Friedmann equation (2.8) can be written in the form

$$\mathrm{k}\frac{c^2}{R_0^2} = H_0^2(\Omega_\Lambda + \Omega_{\mathrm{m}} + \Omega_{\mathrm{r}} - 1) = H_0^2(\Omega_{\mathrm{tot}} - 1), \tag{2.10}$$

where the subscript "0" characterizes the present-day values for $\Omega_{\mathrm{tot}} = \Omega_\Lambda + \Omega_{\mathrm{m}} + \Omega_{\mathrm{r}}$. Instead of the expression (2.10), it is often used the quantity

$$\Omega_{\mathrm{k}} = -\mathrm{k}\frac{c^2}{R_0^2 H_0^2} = \Omega_{\mathrm{tot}} - 1. \tag{2.11}$$

In Eq. (2.10), Ω_{r} is defined by

$$\Omega_{\mathrm{r}} = \frac{1}{2} N(T)\, \Omega_\gamma, \tag{2.12}$$

where the statistical quantity $N(T)$, which has here the value $N(T) = 3.362644$ for photons with neutrinos and antineutrinos of three different types, counts generally the massless degrees of freedom of bosons and fermions, whereat $\Omega_\gamma = 2.4728 \times 10^{-5} h^{-2}$ is defined by the present-day ratio of the photon density to the critical density (see Eq. (3.20)).

For constant w, Eq. (2.5) can easily be integrated, so that we get

$$\rho \propto R^{-3(1+w)}. \tag{2.13}$$

In Eq. (2.3), at early times when R is small, the term $-\mathrm{k}c^2/R^2$ can be neglected for $w > -\frac{1}{3}$. Then, for $w \neq -1$, the Friedmann equation can be written as $(\dot{R}/R)^2 \propto R^{-3(1+w)}$ and is easily integrated to yield

$$R \propto t^{2/[3(1+w)]}. \tag{2.14}$$

For the radiation-dominated universe, in Eqs. (2.13) and (2.14), we can substitute $w = \frac{1}{3}$, so that we obtain

$$\rho \propto R^{-4}; \qquad R \propto t^{1/2}; \qquad H = 1/2t. \tag{2.15}$$

At the matter-dominated universe, in Eqs. (2.13) and (2.14), we must substitute $w = 0$, so that we get

$$\rho \propto R^{-3}; \qquad R \propto t^{2/3} \quad (\text{if } \mathrm{k} = 0); \qquad H = 2/3t. \tag{2.16}$$

If there is an universe with a dominant source of constant vacuum (V) mass density ρ_V, we would observe this mass density as cosmological vacuum constant $\Lambda_\mathrm{V} = 8\pi G_\mathrm{N}\rho_\mathrm{V}/c^2$ and state $w = -1$. In this case (denoted as inflationary cosmology), Eq. (2.3) yields an extremely rapid exponential expansion of the universe

$$R \propto \mathrm{e}^{\sqrt{c^2\Lambda_\mathrm{V}/3}\,\Delta t} = \mathrm{e}^{H_\mathrm{V}\Delta t}, \tag{2.17}$$

where Δt describes thus the period of the inflationary phase, whereas H_V denotes the vacuum Hubble constant.

More generally, via the present-day critical density (see Eq. (2.6)), we may introduce the density

$$\rho = \rho_\Lambda + \rho_\mathrm{m} + \rho_\mathrm{r} = \left[\Omega_\Lambda + \Omega_\mathrm{m}(R_0/R)^3 + \Omega_\mathrm{r}(R_0/R)^4\right]\frac{3H_0^2}{8\pi G_N}. \tag{2.18}$$

Then, the relativistic formalism (2.3) yields

$$H^2 = \left(\frac{\dot{R}}{R}\right)^2 = H_0^2\left[\Omega_\Lambda + \Omega_\mathrm{m}\left(\frac{R_0}{R}\right)^3 + \Omega_\mathrm{r}\left(\frac{R_0}{R}\right)^4\right] - \mathrm{k}\frac{c^2}{R^2} \tag{2.19}$$

with the general solution

$$t = t(z) = \frac{1}{H_0}\int_0^{1/(1+z)} \frac{dx}{x\,(\Omega_\Lambda + \Omega_k x^{-2} + \Omega_m x^{-3} + \Omega_r x^{-4})^{1/2}}, \qquad (2.20)$$

where $x \equiv (R/R_0) = (1/[1+z])$. In Eq. (2.20), for a flat universe ($\Omega_k = 0$), at $z \to 0$, because of the very small value Ω_r compared with Ω_Λ and Ω_m, the term $\Omega_r x^{-4}$ can be neglected, since at present most of the integral (2.20) comes from an epoch when the expansion is dominated by the matter and the dark energy.

Then, by Eq. (2.20), for $z = 0$, the age of the present universe (see below) is defined by

$$t_0 = \frac{1}{H_0}\int_0^1 \frac{dx}{x\,(\Omega_\Lambda + \Omega_m x^{-3})^{1/2}}. \qquad (2.21)$$

For an universe, which expands adiabatically, the entropy per comoving volume is constant, so that we can describe the mass density of the radiation-dominated universe for $T > 3\cdot 10^5$ K by

$$\rho_r = \{\pi^2/30(\hbar^3 c^5)\}(kT)^4 N(T), \qquad (2.22)$$

where $\hbar$ is the Planck constant and k is the Boltzmann constant. Comparing ρ_r from Eqs. (2.18) and (2.22), for the redshift we can also write

$$1 + z = \frac{T}{T_0}, \qquad (2.23)$$

where T_0 is the present-day mean temperature of the cosmic microwave background (CMB).

For Eq. (2.22), the values of $N(T)$, taken from Ref. [10], are given in Table I. At higher temperatures, the values $N(T)$ depend on the particle physics models (for example, $N(T)$ for the X and Y gauge bosons (minimal SU(5) model (SUSY GUTs))) [10].

Using the expressions (2.15) and (2.22), the Friedmann equation (2.3) yields the time for the radiation-dominated universe ($z > 10^5$) as a function of the thermal energy kT, the temperature T or the redshift z by the following expression

$$t = t(z) = \frac{1}{2}\left(\frac{90\hbar^3 c^5}{8\pi^3 G_N}\right)^{1/2} \frac{1}{\sqrt{N(T)}\,(kT)^2} =$$

$$= \frac{(2.42035 \pm 0.00015)}{\sqrt{N(T)}}\left(\frac{\text{MeV}}{kT}\right)^2 \text{s} =$$

$$= \frac{(3.25936 \pm 0.00021)}{\sqrt{N(T)}}\left(\frac{10^{10}\,\text{K}}{T}\right)^2 \text{s} =$$

$$= \frac{(0.438773 \pm 0.000028)}{\sqrt{N(T)}}\left(\frac{10^{10}}{1+z}\right)^2 \text{s}. \qquad (2.24)$$

According to Eqs. (2.2) and (2.18), for the matter-dominated universe, at $z_{\text{eq}} = 3360 >> z >> 1$ (see Tables II and IV) and $\text{k} = 0$, we observe as dominant density

$$\rho_{\text{m}} = \left[\Omega_{\text{m}}(R_0/R)^3\right]\frac{3H_0^2}{8\pi G_N} = \left[\Omega_{\text{m}}(1+z)^3\right]\frac{3H_0^2}{8\pi G_N}, \qquad (2.25)$$

whereas for $z_{\text{eq}} >> z$ we cannot more neglect Ω_Λ, so that here we have

$$\rho_\Lambda + \rho_{\text{m}} = \left[\Omega_\Lambda + \Omega_{\text{m}}(R_0/R)^3\right]\frac{3H_0^2}{8\pi G_N} =$$

$$= \left[\Omega_\Lambda + \Omega_{\text{m}}(1+z)^3\right]\frac{3H_0^2}{8\pi G_N}. \qquad (2.26)$$

In chapter 7.3, both these cases (2.25) and (2.26) are treated.

For $\text{k} = 0$, at the dominant term $\Omega_\Lambda H_0^2$, Eq. (2.19) yields the (present) exponential expansion

$$R = R_0\, \text{e}^{\Omega_\Lambda^{1/2} H_0 (t - t_0)} = R_0\, \text{e}^{H_\Lambda (t - t_0)} \quad \text{at} \quad H_\Lambda = \Omega_\Lambda^{1/2} H_0, \qquad (2.27)$$

where t_0 is the age of the present-day universe (see Table IV).

TABLE I. The important $N(T)$ values. [a] T_c corresponds to the confinement-deconfinement transition between quarks and hadrons. [b] For $T > m_{X,Y}$, the minimal SU(5) model (SUSY GUTs) yields $N(T) = 160.75$.

Temperature	**New particles**	$4N(T)$ [b]
$T < m_e$	photons (γ)+neutrinos (ν)	29
$m_e < T < m_\mu$	$e^{\pm}$	43
$m_\mu < T < m_\pi$	$\mu^{\pm}$	57
$m_\pi < T < T_c$ [a]	$\pi^{\pm}$, π^0	69
$T_c < T < m_{strange}$	$\pi^{\pm}$, $\pi^0 + u, \bar{u}, d, \bar{d}$ + gluons	205
$m_s < T < m_{charm}$	$s, \bar{s}$	247
$m_c < T < m_\tau$	$c, \bar{c}$	289
$m_\tau < T < m_{bottom}$	$\tau^{\pm}$	303
$m_b < T < m_{W,Z}$	$b, \bar{b}$	345
$m_{W,Z} < T < m_{Higgs}$	$W^{\pm}$, Z^0	381
$m_H < T < m_{top}$	H^0	385
$m_t < T$	$t, \bar{t}$	427

The necessary values of the cosmological parameters are given in the Tables II to IV. The most recent data of the cosmological parameters are given by the Planck 2013 results [12], which are summarized in the Tables II and III.

TABLE II. The cosmological parameter values of Planck 2013. In column 1, z_{eq} and z_{reion} are the redshift of the matter-radiation equality (eq) and the redshift of the half reionization (reion), respectively. The column 2 gives results for the Planck temperature data alone. Column 3 combines these Planck data and the WMAP polarization data at low multipoles as Planck+WP.

	Planck	**Planck+WP**
Parameter	**Best fit [68% limits]**	**Best fit [68% limits]**
H_0 [km/s Mpc]	67.11 [67.4 ± 1.4]	67.04 [67.3 ± 1.2]
Ω_Λ	0.6825 [0.686 ± 0.020]	0.6817 [$0.685^{+0.018}_{-0.016}$]
$100\,\Omega_b h^2$	2.2068 [2.207 ± 0.033]	2.2032 [2.205 ± 0.028]
$\Omega_{dm} h^2$	0.12029 [0.1196 ± 0.0031]	0.12038 [0.1199 ± 0.0027]
$\Omega_m h^2$	0.14300 [0.1423 ± 0.0029]	0.14305 [0.1426 ± 0.0025]
Ω_m	0.3175 [0.314 ± 0.020]	0.3183 [$0.315^{+0.016}_{-0.018}$]
Age t_0 [Gyr]	13.819 [13.813 ± 0.058]	13.8242 [13.817 ± 0.048]
z_{eq}	3402 [3386 ± 69]	3403 [3391 ± 60]
z_{reion}		11.37 [11.1 ± 1.1]

TABLE III. The cosmological parameter values of Planck 2013, continued. Column 2 gives the combination of the Planck+WP likelihoods with the ACT and SPT likelihoods, denoted as Planck+WP+highL. The column 3 defines the combination of the Planck+WP+highL and the BAO data, denoted as Planck+WP+highL+BAO.

	Planck+WP+highL	**Planck+WP+highL+BAO**
Parameter	**Best fit**	**Best fit**
	[68% limits]	**[68% limits]**
H_0 [km/s Mpc]	67.15	67.77
	$[67.3 \pm 1.2]$	$[67.80 \pm 0.77]$
h	0.6715	0.6777
	$[0.673 \pm 0.012]$	$[0.6780 \pm 0.0077]$
Ω_Λ	0.6830	0.6914
	$[0.685^{+0.017}_{-0.016}]$	$[0.692 \pm 0.010]$
$100\ \Omega_b\ h^2$	2.2069	2.2161
	$[2.207 \pm 0.027]$	$[2.214 \pm 0.024]$
$\Omega_{dm}\ h^2$	0.12025	0.11889
	$[0.1198 \pm 0.0026]$	$[0.1187 \pm 0.0017]$
Age t_0 [Gyr]	13.8170	13.7965
	$[13.813 \pm 0.047]$	$[13.798 \pm 0.037]$
z_{reion}	11.38	11.52
	$[11.1 \pm 1.1]$	$[11.3 \pm 1.1]$

TABLE IV. Important astrophysical parameters for the big bang cosmology [2].

Quantity	Symbol, equation	Value
present day CMB temperature	T_0	$2.7255(6)\ \mathrm{K}$
present day Hubble expansion rate	H_0	$67.3 \pm 1.2\ \mathrm{km\ s^{-1}\ Mpc^{-1}} =$ $= h \times (9.777752\ \mathrm{Gyr})^{-1} =$ $= (2.181 \pm 0.039) \cdot 10^{-18}\ \mathrm{s^{-1}}$
scale factor for Hubble expansion rate	h	0.673 ± 0.012
critical present density of the universe	$\rho_{0\mathrm{C}} = 3H_0^2/8\pi G_N$	$1.05375(13) \cdot 10^{-5} h^2\ (\mathrm{GeV}/c^2)\ \mathrm{cm^{-3}} =$ $= 4.77(17) \cdot 10^3\ (\mathrm{eV}/c^2)\ \mathrm{cm^{-3}}$
baryon (proton) density of the universe	$\Omega_\mathrm{b} = \rho_\mathrm{b}/\rho_{0\mathrm{C}}$	$0.02207(27)\, h^{-2} = 0.0499(22)$
(cold) dark matter density of the universe	$\Omega_\mathrm{dm} = \rho_\mathrm{dm}/\rho_{0\mathrm{C}}$	$0.1198(26)\, h^{-2} = 0.265(11)$
dark energy density of the ΛCDM universe	Ω_Λ	$0.685^{+0.017}_{-0.016}$

TABLE IV, continued.

Quantity	Symbol, equation	Value
pressureless matter density of the universe	$\Omega_{\mathrm{m}} = \Omega_{\mathrm{dm}} + \Omega_{\mathrm{b}}$	$0.315^{+0.016}_{-0.017}$
CMB radiation density of the universe	$\Omega_\gamma = \rho_\gamma / \rho_{0\mathrm{C}}$	$2.473 \cdot 10^{-5} (T/2.7255\ \mathrm{K})^4 h^{-2} =$ $= 5.46(19) \cdot 10^{-5}$
curvature	$\Omega_{\mathrm{tot}} = \Omega_{\mathrm{m}} + \cdots + \Omega_\Lambda$	$0.96^{+0.4}_{-0.5}$; $1.000(7)$ (CMB + BAO)
sum of neutrino masses	$\sum m_\nu c^2$	< 0.23 eV
neutrino density of the universe	Ω_ν	$< 0.0025 h^{-2}$; < 0.0055
redshift of matter-radiation equality	z_{eq}	3360 ± 70
redshift at half reionization	z_{reion}	11.1 ± 1.1
age of the universe	t_0	13.81 ± 0.05 Gyr = $= (4.358 \pm 0.016) \cdot 10^{17}$ s

2.2 Problems of the standard model

The standard cosmology [2] provides a very successful framework for the explanation of the cosmic observations. However, there are a number of

problems, which cannot simply be solved within the standard cosmology. These problems are the horizon problem, the monopole problem, the flatness problem and the initial condition problem, which are treated in detail in Refs. [1, 3].

A way out of these problems is the inflation [1, 3], which in the early universe enlarges the scale factor by a factor of about 10^{30} [3, 4, 11]. However, this inflationary cosmology and its transition to the standard model are quantitatively still an open problem [4].

For a better understanding, in the chapters 2.2.1 to 2.2.4, we explain shortly the above-mentioned problems of the standard model.

2.2.1 The horizon problem

The temperature of the cosmic microwave background (CMB) is the same in all directions of the universe with an accuracy better than about 10^{-5}. The question is how all these disconnected and non-interacted regions can have this extremely high temperature isotropy. This problem is the so-called horizon problem of the standard cosmology.

By the inflation, this isotropy of the CMB can be explained because prior to the inflation the universe occupied such a small volume, so that after the inflation these very small regions rapidly attain gigantic dimensions and cannot longer interact [4].

2.2.2 The monopole problem

Using the SUSY GUT transition for the early universe, the formation of magnetic monopoles is expected with a density of about one per horizon volume at that epoch [1]. This enormous density dominates the present cosmic matter density in a fatal conflict with the measurements [1]. This is the so-called monopole problem of the standard cosmology. At the end of the inflation this monopole density would be reduced by a factor of about $(10^{-30})^3$, so that the contribution of the monopoles to the present cosmic density would be completely negligible in accordance with the observations [1]. However, this inflation is only qualitatively solved (see Sec. 2.2).

2.2.3 The flatness problem

In spite of the Planck 2013 results [12], which favor $\Omega_k = 0$ (see Eq. (2.11)), the assumption that Ω_{tot} (see Eqs. (2.8) and (2.10)) differs mildly from unity, leads to the so-called flatness problem of the standard cosmology, which at the Planck time requires an extreme "fine-tuning" of Ω_{tot}.

A trivial way out of this problem is to postulate $\Omega_{tot} \equiv 1$ throughout the history of the universe [1].

2.2.4 The initial condition problem

All above-mentioned problems do not falsify the standard cosmology. However, they can be interpreted into the standard cosmology as initial conditions. Therefore, the standard cosmology provides only a consistent model to explain the observable universe with some assumed initial conditions without to explain their origin [1].

For many years it was assumed that the initial conditions for the standard cosmology could arise from the quantum cosmology at very early times, where the universe was so small that the classical cosmology model is no longer valid. Unfortunately, the quantum cosmology cannot present up to now reliable predictions. However, the situation changed in the early 1980s by the new inflation concept, which solves all these problems within the classical cosmology because the inflation operates at an energy scale that is much lower than the Planck energy, so that the cosmology can be treated classically [1].

2.3 Results of the supersymmetric grand unified theories (SUSY GUTs)

For the early universe, the SUSY GUTs require that the three low energy gauge couplings of the strong and electroweak interactions unify at the gauge coupling unification $E_G \approx 3 \times 10^{16}\,\mathrm{GeV}$ [2], whereby the GUT coupling constant has a value of $\alpha_{GUT} \approx 0.04$ [13-17].

The rest energies of the X and Y gauge bosons are given by $E_0(\mathrm{X}) = E_G$ and $E_0(\mathrm{Y}) = E_G$ [18]. The SUSY GUTs predict also the existence of magnetic

monopoles (M), for which according to Refs. [2, 18] the rest energy is defined by $E_0(\mathrm{M}) = E_\mathrm{G} / \alpha_\mathrm{GUT} \approx 7.5 \cdot 10^{17}\,\mathrm{GeV}$.

In SUSY GUTs, the baryon number is violated [2], so that they predict a proton (p) decay with the very large lifetime $\tau_\mathrm{p} \propto E_\mathrm{G}^4 / \left[\alpha_\mathrm{GUT}^2 E_0^5(\mathrm{p})\right]$, where $E_0(\mathrm{p})$ is the proton rest energy. Then, non-SUSY GUTs (e.g., non-SUSY SU(5)), which predict a proton lifetime $\tau_\mathrm{p} \approx 10^{31}\,\mathrm{yr}$ at $E_\mathrm{G} \approx 10^{15}\,\mathrm{GeV}$ [17], are ruled out by the non-observation of the proton decay in the allowed range [2].

3 The neutrino problem

3.1 The estimation of the neutrino masses

There are three neutrinos (tauon neutrino ν_τ, muon neutrino ν_μ and electron neutrino ν_e).

According to Beringer et al. [10], the best values of the 3-neutrino oscillation parameters, derived from global neutrino oscillation data, yield for the square mass differences of the neutrino rest energies:

$$\Delta m_{\tau\mu}^2 c^4 = E_0^2(\nu_\tau) - E_0^2(\nu_\mu) = (2.35^{+0.12}_{-0.09}) \cdot 10^{-3}\,\mathrm{eV}^2, \tag{3.1}$$

$$\Delta m_{\mu\mathrm{e}}^2 c^4 = E_0^2(\nu_\mu) - E_0^2(\nu_\mathrm{e}) = (7.58^{+0.22}_{-0.26}) \cdot 10^{-5}\,\mathrm{eV}^2. \tag{3.2}$$

From Eqs. (3.1) and (3.2), we can form the equations

$$E_0(\nu_\tau) = \left(\Delta m_{\tau\mu}^2 c^4 + E_0^2(\nu_\mu)\right)^{1/2} =$$

$$= \left(\Delta m_{\tau\mu}^2 c^4 + \Delta m_{\mu\mathrm{e}}^2 c^4 + E_0^2(\nu_\mathrm{e})\right)^{1/2} \tag{3.3}$$

and

$$E_0(\nu_\mu) = \left(\Delta m_{\mu\mathrm{e}}^2 c^4 + E_0^2(\nu_\mathrm{e})\right)^{1/2}. \tag{3.4}$$

By Beringer et al. [10], for the normal hierarchy $E_0(\nu_\tau) > E_0(\nu_\mu) > E_0(\nu_\mathrm{e})$, from Eqs. (3.1) to (3.4), the neutrino rest energies $E_0(\nu_\tau)$ and $E_0(\nu_\mu)$ were estimated to

$$E_0(\nu_\tau) \approx \left|\Delta m^2_{\tau\mu} c^4\right|^{1/2} \approx 4.8 \cdot 10^{-2}\,\mathrm{eV} \tag{3.5}$$

and

$$E_0(\nu_\mu) \approx \left|\Delta m^2_{\mu e} c^4\right|^{1/2} \approx 8.6 \cdot 10^{-3}\,\mathrm{eV}. \tag{3.6}$$

Using the upper conditions (3.5) and (3.6) for normal hierarchy, we can assume as new approach

$$E_0(\nu_\mu) \cong \left[E_0(\nu_\tau)\, E_0(\nu_e)\right]^{1/2}, \tag{3.7}$$

so that by Eqs. (3.3) and (3.4) via Eq. (3.7) we obtain

$$E_0(\nu_e) \cong \frac{E_0^2(\nu_\mu)}{E_0(\nu_\tau)} = \frac{\Delta m^2_{\mu e} c^4}{\left[\Delta m^2_{\tau\mu} c^4 - \Delta m^2_{\mu e} c^4\right]^{1/2}} =$$

$$= (1.589^{+0.078}_{-0.098}) \cdot 10^{-3}\,\mathrm{eV}. \tag{3.8}$$

Consequently, by Eq. (3.8), the expressions (3.3) and (3.4) yield

$$E_0(\nu_\tau) = \left(\Delta m^2_{\tau\mu} c^4 + \Delta m^2_{\mu e} c^4 + E_0^2(\nu_e)\right)^{1/2} \cong (4.93^{+0.12}_{-0.10}) \cdot 10^{-2}\,\mathrm{eV} \tag{3.9}$$

and

$$E_0(\nu_\mu) = \left(\Delta m^2_{\mu e} c^4 + E_0^2(\nu_e)\right)^{1/2} \cong (8.85^{+0.14}_{-0.16}) \cdot 10^{-3}\,\mathrm{eV} \tag{3.10}$$

in accordance with Eqs. (3.5) and (3.6). Then, the sum of the neutrino rest energies (see Eqs. (3.8) to (3.10)) gives the approximate solution

$$\sum_i E_0(\nu_i) = E_0(\nu_\tau) + E_0(\nu_\mu) + E_0(\nu_e) \cong (5.97^{+0.14}_{-0.13}) \cdot 10^{-2}\,\mathrm{eV}, \tag{3.11}$$

where the subscript $i = e, \mu, \tau$ characterizes the e, μ and τ neutrino. The sum (3.11) does not contradict the observed limit $\sum_i E_0(\nu_i) < 0.23\,\mathrm{eV}$ [2, 12].

3.2 The estimation of the neutrino densities of the universe

First we must explain the radiation density of the universe. These considerations are based on Refs. [3, 10, 11]. The cosmic microwave (radiation) background (CMB) is observed as a black-body spectrum with the mean temperature

$$T = T_0 = 2.7255 \pm 0.0006\,\mathrm{K}. \tag{3.12}$$

Consequently, this observation is consistent with a Planck distribution at the temperature (3.12). The Planck distribution of photons is quantum statistically characterized by the energy density

$$\rho(\gamma)c^2 = \frac{\pi^2}{15}\frac{(kT)^4}{(\hbar c)^3} =$$

$$= (4.722158 \pm 0.000017)\cdot 10^{-3}\left(\frac{T}{\mathrm{K}}\right)^4 \mathrm{eV/cm^3} \qquad (3.13)$$

and the number density

$$n(\gamma) = \frac{2.404113806}{\pi^2}\left(\frac{kT}{\hbar c}\right)^3 =$$

$$= (20.286843 \pm 0.000057)\left(\frac{T}{\mathrm{K}}\right)^3 \mathrm{cm^{-3}}, \qquad (3.14)$$

where the value 2.404113806 corresponds to the integral $\int_0^\infty [x^2/(e^x - 1)]\mathrm{dx}$.

The radiation density of the universe is defined by

$$\Omega_\gamma = \frac{\rho_0(\gamma)}{\rho_{0\mathrm{C}}}, \qquad (3.15)$$

where the present photon density $\rho_0(\gamma)$ and the critical present density $\rho_{0\mathrm{C}}$ are given by

$$\rho_0(\gamma) = \frac{\pi^2}{15}\frac{(kT_0)^4}{\hbar^3 c^5} \qquad (\text{see Eq. (3.13)}), \qquad (3.16)$$

$$\rho_{0\mathrm{C}} = \frac{3H_0^2}{8\pi G_N} \qquad (\text{see Eq. (2.6)}). \qquad (3.17)$$

Thus, Eq. (3.16) gives

$$\rho_0(\gamma)\,c^2 = \frac{\pi^2}{15}\frac{(kT_0)^4}{(\hbar c)^3} = (0.26057 \pm 0.00023)\ \mathrm{eV\,cm^{-3}}. \qquad (3.18)$$

For Eq. (3.17), we get

$$\rho_{0\mathrm{C}}c^2 = \frac{3c^2H_0^2}{8\pi G_N} = (1.05375 \pm 0.00013)\cdot 10^4 h^2\ \mathrm{eV\,cm^{-3}}. \qquad (3.19)$$

Then, via Eqs. (3.18) and (3.19), Eq. (3.15) yields the present radiation density of the universe to

$$\Omega_\gamma = \frac{\rho_0(\gamma)}{\rho_{0C}} = (2.4728 \pm 0.0025) \cdot 10^{-5} h^{-2} . \tag{3.20}$$

More generally, we have

$$\Omega_\gamma(T) = \Omega_\gamma \cdot \left(\frac{T}{T_0} \right)^4 . \tag{3.21}$$

Now, analogously to the baryon number density [3], we can introduce the present neutrino number densities

$$n_0(\nu_i) = \Omega_\nu(\nu_i) \frac{\rho_{0C} c^2}{E_0(\nu_i)} , \tag{3.22}$$

so that the neutrino densities of the universe are determined by

$$\Omega_\nu(\nu_i) = E_0(\nu_i) \frac{n_0(\nu_i)}{\rho_{0C} c^2} . \tag{3.23}$$

For the neutrino temperature $T_0(\nu_i) = (4/11)^{1/3} T_0 = (1.94537 \pm 0.00043)\,\mathrm{K}$ [3, 10], we find the present neutrino number densities (for every subscript $i = \mathrm{e}, \mu, \tau$) to

$$n_0(\nu_i) = \frac{3}{4} \frac{2.404113806}{\pi^2} \frac{(k[(4/11)^{1/3} T_0])^3}{(\hbar c)^3} =$$

$$= (112.016 \pm 0.074)/\mathrm{cm}^3 . \tag{3.24}$$

Analogous to Ref. [2], the expressions (3.15) as well as (3.23) and (3.24) yield

$$\Omega_\nu(\nu_i) = E_0(\nu_i) \frac{n_0(\nu_i)}{\rho_0(\gamma) c^2} \Omega_\gamma = \frac{45}{11} \frac{2.4041138}{\pi^4} \frac{E_0(\nu_i)}{k T_0} \Omega_\gamma =$$

$$= (429.889 \pm 0.095)\, E_0(\nu_i)\, \Omega_\gamma =$$

$$= (0.010630 \pm 0.000011)\, E_0(\nu_i)\, h^{-2} . \tag{3.25}$$

Using the rest energies (3.8) to (3.10) together with the radiation density $\Omega_\gamma = (5.46 \pm 0.19) \cdot 10^{-5}$ (see Table 4), by Eq. (3.25), we get

$$\Omega_\nu(\nu_e) \cong (0.683^{+0.034}_{-0.042})\Omega_\gamma =$$

$$= (1.69^{+0.09}_{-0.11})\cdot 10^{-5} h^{-2} = (3.73^{+0.32}_{-0.36})\cdot 10^{-5}, \quad (3.26)$$

$$\Omega_\nu(\nu_\mu) \cong (3.805^{+0.061}_{-0.070})\Omega_\gamma =$$

$$= (9.41^{+0.16}_{-0.18})\cdot 10^{-5} h^{-2} = (2.08 \pm 0.11)\cdot 10^{-4}, \quad (3.27)$$

$$\Omega_\nu(\nu_\tau) \cong (21.19^{+0.52}_{-0.44})\Omega_\gamma =$$

$$= (5.24^{+0.13}_{-0.11})\cdot 10^{-4} h^{-2} = (1.157^{+0.069}_{-0.064})\cdot 10^{-3}. \quad (3.28)$$

The sum of Eqs. (3.26) to (3.28) gives

$$\Omega_\nu = \sum_i \Omega_\nu(\nu_i) \cong (25.68^{+0.62}_{-0.55})\Omega_\gamma =$$

$$= (6.35^{+0.16}_{-0.14})\cdot 10^{-4} h^{-2} = (1.402^{+0.083}_{-0.079})\cdot 10^{-3}. \quad (3.29)$$

The sum (3.29) does not contradict the observed limiting values $\Omega_\nu < 0.0055$ and $\Omega_\nu < 0.0025 h^{-2}$ (see Table IV). Then, the deviations amount to only a factor 4.

4 The rest energy of the X and Y gauge bosons

For the Standard $\mathrm{SU(2)} \times \mathrm{U(1)}$ electroweak theory, Fujikawa and Shrock [19] (see also Ref. 10) have derived the magnetic moment of massive neutrinos to

$$\mu_\nu(\nu_i) = \frac{3}{8\pi^2\sqrt{2}} e[G_F/(\hbar c)^3]\hbar c^2 E_0(\nu_i) =$$

$$= 3.203\cdot 10^{-19}(E_0(\nu_i)/\mathrm{eV})\mu_B, \quad (4.1)$$

where $[G_F/(\hbar c)^3] \doteq 1.1663787\cdot 10^{-23}\,\mathrm{eV}^{-2}$ describes the Fermi coupling constant [10]. The Bohr magneton μ_B [10] is defined by

$$\mu_B = \frac{e\hbar c^2}{2E_0(\mathrm{e})} = (5.7883818066(38)\cdot 10^{-11}\,\mathrm{MeV/T}, \quad (4.2)$$

where $E_0(\mathrm{e})$ is the rest energy of the electron (e). The magnetic moment of the electron is given by $\mu_\mathrm{e} = \mathrm{C_e}\mu_B$, where $\mathrm{C_e} \cong 1.00116$ [10]. Similar to the

nucleon magneton $\mu_N = (E_0(\mathrm{e})/E_0(p))\mu_B$, the X magneton (SUSY grand unification magneton) is assumed to

$$\mu_{\mathrm{X}} = \frac{E_0(\mathrm{e})}{E_0(\mathrm{X})}\mu_B\,, \tag{4.3}$$

so that analogous to the magnetic moment of the electron (see above) the magnetic moment of the neutrinos, using reasonably $1 \le \mathrm{C}_\nu \le \mathrm{C}_\mathrm{e}$, may be assumed to

$$\mu_\nu(\nu_i) \cong \mathrm{C}_\nu \frac{E_0(\nu_i)}{\sum_i E_0(\nu_i)}\mu_{\mathrm{X}} = \mathrm{C}_\nu \frac{E_0(\nu_i)}{\sum_i E_0(\nu_i)}\frac{E_0(\mathrm{e})}{E_0(\mathrm{X})}\mu_B\,. \tag{4.4}$$

Then, the derivation of Eq. (4.4) is clear because the expression $\sum_i \mu_\nu(\nu_i)/\mathrm{C}_\nu$ gives again the grand unification magneton μ_{X} (see Eq. (4.3)). By Eqs. (4.1) and (4.4), if we assume as the maximum value $\mathrm{C}_\nu = \mathrm{C}_\mathrm{e}$ in Eq. (4.4), we may estimate the rest energy of the X gauge boson to

$$E_0(\mathrm{X}) \cong \mathrm{C}_\mathrm{e}\frac{E_0(\nu_i)}{\sum_i E_0(\nu_i)}\frac{E_0(\mathrm{e})}{\mu_\nu(\nu_i)}\mu_B =$$

$$= \mathrm{C}_\mathrm{e}\frac{E_0(\mathrm{e})}{\sum_i E_0(\nu_i)}\frac{\mathrm{eV}}{3.203\cdot 10^{-19}} = (2.675^{+0.058}_{-0.063})\cdot 10^{16}\,\mathrm{GeV}. \tag{4.5}$$

The value (4.5) agrees excellently with the gauge coupling unification $E_\mathrm{G} \approx 3\times 10^{16}\,\mathrm{GeV}$, which is identical with $E_0(\mathrm{X}) = E_\mathrm{G}$ and $E_0(\mathrm{Y}) = E_\mathrm{G}$ (see Sec. 2.3), so that we have $E_0(\mathrm{X}) = E_0(\mathrm{Y})$.

By Eqs. (2.24) and (4.5) as well as $N(T) = N_{\mathrm{X,Y}}(T) = 160.75$ (see Table I), we obtain the time $t_{\mathrm{X,Y}}$ and correspondingly the temperature $T_{\mathrm{X,Y}}$ for these X and Y gauge bosons:

$$t = t_{\mathrm{X,Y}} = \frac{2.42035}{\sqrt{N_{\mathrm{X,Y}}(T)}}\left[\frac{\mathrm{MeV}}{E_0(\mathrm{X})}\right]^2 \mathrm{s} = (2.67^{+0.13}_{-0.12})\cdot 10^{-40}\,\mathrm{s} \tag{4.6}$$

and

$$T = T_{\mathrm{X,Y}} = E_0(\mathrm{X})/k = (3.104^{+0.067}_{-0.073})\cdot 10^{29}\,\mathrm{K} \propto t_{\mathrm{X,Y}}^{-1/2}\,. \tag{4.7}$$

Taking Eqs. (2.23) and (4.7), we find the redshift of the X and Y gauge bosons to

$$1+z_{\mathrm{X,Y}}=\frac{T_{\mathrm{X,Y}}}{T_0}=(1.139^{+0.025}_{-0.027})\cdot 10^{29}. \tag{4.8}$$

5 The inflationary cosmology

5.1 The scale factor of absorption of light "before" and after the inflation

Using $H_0=(2.181\pm 0.039)\cdot 10^{-18}\,\mathrm{s}^{-1}$ (see Table IV), for the present critical density $\rho_{0\mathrm{C}}$ (see Eq. (2.6)), we can introduce

$$\rho_{0\mathrm{C}}=\frac{3H_0^2}{8\pi G_N}\left[\frac{R_{\mathrm{Pl}}^2}{R_{\mathrm{Pl}}^2}\right]=\frac{3H_0^2}{8\pi G_N}\left[\frac{\hbar\, G_N/c^3}{R_{\mathrm{Pl}}^2}\right]=$$
$$=\frac{3\hbar}{8\pi c(R_{\mathrm{Pl}}c/H_0)^2}=\frac{3\hbar}{8\pi c\,\widetilde{R}_0^4}, \tag{5.1}$$

where the Planck radius R_{Pl} is defined by Eq. (7.1), so that the scale factor $\widetilde{R}_0$ is given by

$$\widetilde{R}_0=(R_{\mathrm{Pl}}c/H_0)^{1/2}=(4.713\pm 0.042)\cdot 10^{-5}\,\mathrm{m}. \tag{5.2}$$

Similar to Eq. (5.1), we can also introduce

$$\rho_{0\mathrm{C}}=\frac{3H_0^2}{8\pi G_N}\left[\frac{c^2}{c^2}\right]=\frac{3}{8\pi G_N}\frac{c^2}{[c/H_0]^2}=\frac{3c^2}{8\pi G_N R_0^2} \tag{5.3}$$

with

$$R_0=c/H_0=(1.375\pm 0.025)\cdot 10^{26}\,\mathrm{m}. \tag{5.4}$$

Between Eqs. (5.2) and (5.4), we have trivially the connection $\widetilde{R}_0=(R_{\mathrm{Pl}}R_0)^{1/2}$. Because of $\widetilde{R}_0 << R_0$, we assume that Eqs. (5.2) and (5.4) represent the "two" unknown scale factors of the absorption of light at the redshift (see Eq. (2.2)) "before" and after the inflation, respectively. In Sec. 5.2 and 5.3, we explain these assumptions.

5.2 The rest energy of the magnetic monopoles

Using "both" scale factors of the absorption of light at the redshift "before" (see Eq. (5.2)) and after (see Eq. (5.4)) the inflation, because of Eqs. (2.2) and (2.23), we can define

$$1+z_{\mathrm{M}}=\frac{T_{\mathrm{M}}}{T_0}=\frac{\widetilde{R}_0}{R_{\mathrm{Pl}}}=\frac{R_0}{\widetilde{R}_0}=(2.916\pm 0.026)\cdot 10^{30}. \tag{5.5}$$

In Eq. (5.5), because of Eq. (4.8), for $E_0(\mathrm{M})>E_0(\mathrm{X})$ (see Sec. 2.3), the subscript M is assumed to define the magnetic monopoles, so that via Eqs. (2.23) and (3.12) we can determine their temperature as follows:

$$T_{\mathrm{M}}=(1+z_{\mathrm{M}})T_0=(7.948\pm 0.073)\cdot 10^{30}\,\mathrm{K}. \tag{5.6}$$

Consequently, the rest energy of the magnetic monopoles is defined by

$$E_0(\mathrm{M})=kT_{\mathrm{M}}=(1+z_{\mathrm{M}})kT_0=(6.849\pm 0.063)\cdot 10^{17}\,\mathrm{GeV}. \tag{5.7}$$

Then, by Eqs. (4.5) and (5.7), the coupling constant of the SUSY GUTs is found to

$$\alpha_{\mathrm{GUT}}=\frac{E_0(\mathrm{X})}{E_0(\mathrm{M})}=0.0391^{+0.0012}_{-0.0013} \tag{5.8}$$

in excellent agreement with the value $\alpha_{\mathrm{GUT}}\approx 0.04$, which was obtained by a completely other way (see Sec. 2.3). Therefore, the result (5.8) confirms the assumption (5.6) and the estimation (3.11) as well as the solutions (5.2) and (5.4) as the unknown scale factor of the absorption of light at the redshift (see Eq. (2.2)) "before" and after the inflation (see also Sec. 5.3).

In SUSY GUTs the baryon number is violated, so that they predict a proton decay. By Eqs. (4.5) and (5.8), the proton lifetime (see Sec. 2.3) is estimated to

$$\tau_{\mathrm{p}}=\frac{\hbar}{2\alpha_{\mathrm{GUT}}^2\left[E_0(\mathrm{p})\right]^5/\left[E_0(\mathrm{X})\right]^4}=4.803\cdot 10^{36}\,\mathrm{yr} \tag{5.9}$$

in accordance with the experimental limiting value of the proton lifetime $\tau_{\mathrm{p}}(\mathrm{p}\to\pi^0\mathrm{e}^+)\geq 1.0\cdot 10^{34}\,\mathrm{yr}$ [10].

Using Eqs. (2.24) and (5.7), for the magnetic monopoles, we can determine the time

$$t_{\mathrm{M}} = \frac{2.42035}{\sqrt{N_{\mathrm{M}}(T)}}\left[\frac{\mathrm{MeV}}{kT_{\mathrm{M}}}\right]^2 \mathrm{s} = \frac{(5.160 \pm 0.095)\cdot 10^{-42}}{\sqrt{N_{\mathrm{M}}(T)}}\,\mathrm{s}\,. \tag{5.10}$$

5.3 The inflation problem

In this chapter, we investigate the connections

$$1 + z_{\mathrm{M}} = \frac{T_{\mathrm{M}}}{T_0} = \frac{\widetilde{R}_0}{R_{\mathrm{Pl}}} = \mathrm{e}^{H_{\mathrm{V}}\Delta t} = (2.916 \pm 0.026)\cdot 10^{30} \tag{5.11}$$

and

$$1 + z_{\mathrm{M}} = \frac{T_{\mathrm{M}}}{T_0} = \frac{R_0}{\widetilde{R}_0} = \mathrm{e}^{H_{\mathrm{V}}\Delta t} = (2.916 \pm 0.026)\cdot 10^{30}\,, \tag{5.12}$$

where H_{V} and Δt are defined by Eq. (2.17). For this goal, we use the radiation-dominated universe ($z > 10^5$). Then, by Eqs. (2.2) and (2.22) as well as (2.23) and (3.15), we can write

$$\rho_{\mathrm{r}} = \{\pi^2/30(\hbar^3 c^5)\}(kT)^4 N(T) = \frac{1}{2}N(T)\,\rho_0(\gamma)\left(\frac{T}{T_0}\right)^4 =$$

$$= \frac{1}{2}N(T)\,\Omega_\gamma\,\rho_{0\mathrm{C}}\left(\frac{T}{T_0}\right)^4 =$$

$$= \frac{1}{2}N(T)\,\Omega_\gamma\,\rho_{0\mathrm{C}}\left(\frac{R_0}{R}\right)^4 = \frac{1}{2}N(T)\,\Omega_\gamma\,\rho_{0\mathrm{C}}\,(1+z)^4\,. \tag{5.13}$$

Taking $R_0 \to \widetilde{R}_0$ (see Eq. (5.2)) in Eq. (5.13), Eq. (2.3) yields

$$\widetilde{R} = (2\,N(T)\,\Omega_\gamma)^{1/4}(R_{\mathrm{Pl}}\,ct)^{1/2} \propto t^{1/2}\,, \tag{5.14}$$

whereas for R_0 (see Eq. (5.4)) in Eq. (5.13) the Friedmann equation (see Eq. (2.3)) gives

$$R = (2\,N(T)\,\Omega_\gamma)^{1/4}(R_0\,ct)^{1/2} \propto t^{1/2}\,, \tag{5.15}$$

so that for the radiation-dominated universe ($z > 10^5$) by Eqs. (5.14) and (5.15) we can derive

$$t = t(z) = \frac{1/H_0}{(2\,N(T)\;\Omega_\gamma)^{1/2}\,(1+z)^2} \quad (z > 10^5)\,. \tag{5.16}$$

At the matter-dominated universe, for Eqs. (2.25) and (2.26), the time $t = t(z)$ is determined by Eqs. (7.9) and (7.12), respectively.

Then, using $t = t_{\mathrm{M}}$ (see Eq. (5.10)) and $t = t_{\mathrm{X,Y}}$ (see Eqs. (4.6) and (4.7)) in Eqs. (5.14) and (5.15), we find

$$\widetilde{R} = \widetilde{R}_{\mathrm{M}} = (2\,N_{\mathrm{M}}(T)\,\Omega_\gamma)^{1/4}(R_{\mathrm{Pl}}\,c\,t_{\mathrm{M}})^{1/2} = R_{\mathrm{Pl}} = \frac{\widetilde{R}_0}{1+z_{\mathrm{M}}}\,, \tag{5.17}$$

$$R = R_{\mathrm{M}} = (2\,N_{\mathrm{M}}(T)\,\Omega_\gamma)^{1/4}(R_0\,c\,t_{\mathrm{M}})^{1/2} = \widetilde{R}_0 = \frac{R_0}{1+z_{\mathrm{M}}}\,, \tag{5.18}$$

$$\widetilde{R} = \widetilde{R}_{\mathrm{X,Y}} = (2\,N_{\mathrm{X,Y}}(T)\,\Omega_\gamma)^{1/4}(R_{\mathrm{Pl}}\,c\,t_{\mathrm{X,Y}})^{1/2} =$$

$$= \frac{\widetilde{R}_0}{1+z_{\mathrm{X,Y}}} = 4.138\cdot 10^{-34}\ \mathrm{m} \tag{5.19}$$

and

$$R = R_{\mathrm{X,Y}} = (2\,N_{\mathrm{X,Y}}(T)\,\Omega_\gamma)^{1/4}(R_0\,c\,t_{\mathrm{X,Y}})^{1/2} =$$

$$= \frac{R_0}{1+z_{\mathrm{X,Y}}} = 1.207\cdot 10^{-3}\ \mathrm{m}\,. \tag{5.20}$$

Now, we can interpret Eqs. (5.11) and (5.12), using Eqs. (5.17) to (5.20). Eq. (5.11) means that during the inflationary phase Δt the dimension R_{Pl} of the beginning of the universe is enlarged by the enormous factor of $1+z_{\mathrm{M}} = \mathrm{e}^{H_{\mathrm{V}}\Delta t} = 2.916\cdot 10^{30}$ to the scale factor $\widetilde{R}_0 = R_{\mathrm{Pl}}\,\mathrm{e}^{H_{\mathrm{V}}\Delta t}$ of absorption of light at the redshift before the inflation, if we assume $\widetilde{R} = \widetilde{R}_0/(1+z)$ for every z value (see Eqs. (5.17) and (5.19)), i.e., we have more generally the connection $R = \widetilde{R}(1+z_{\mathrm{M}}) = R_0/(1+z)$ with the scale factor $R_0 = \widetilde{R}_0(1+z_{\mathrm{M}})$ of absorption of light at the redshift after the inflation (see Eqs. (5.12), (5.18) and (5.20)). Thus, because of Eqs. (5.17) to (5.20), the two scale factors $\widetilde{R}_0$

and R_0 are characteristical quantities (see Sec. 5.1), so that the two scale factors $\widetilde{R}$ and R for the emission of light can be assumed for every z value as follows:

$$\widetilde{R} = \frac{R}{1+z_{\mathrm{M}}} = \frac{\widetilde{R}_0}{1+z} \quad \text{(see below)} \tag{5.21}$$

and

$$R = (1+z_{\mathrm{M}})\widetilde{R} = \frac{R_0}{1+z}. \tag{5.22}$$

After the inflation, by the magnetic monopoles, we have the scale factor $\widetilde{R}_0 = R_{\mathrm{Pl}}\,\mathrm{e}^{H_{\mathrm{V}}\Delta t}$ at $\widetilde{t}_{\mathrm{H}} = \widetilde{R}_0/c = (R_{\mathrm{Pl}}R_0)^{1/2}/c = (t_{\mathrm{Pl}}/H_0)^{1/2} = 1.572\cdot 10^{-13}\,\mathrm{s}$ (as a reduced Hubble time) in the universe, i.e., more generally Eq. (5.22) is useful, since Eq. (5.21) must be multiplied by the enormous factor $1+z_{\mathrm{M}} = \mathrm{e}^{H_{\mathrm{V}}\Delta t} = 2.916\cdot 10^{30}$ because of the inflation, so that we obtain again Eq. (5.22). Therefore, this inflation determines the significance of the magnetic monopoles for the universe. Using Eqs. (5.17) and (5.19), we can also assume that in the space region $R_{\mathrm{Pl}} \le \widetilde{R} \le \widetilde{R}_0$ the quantum fluctuations kT (for $T \le T_{\mathrm{Pl}}$) lead to the important separation of matter (universe ($R \ge R_{\mathrm{Pl}}$)) and antimatter (vacuum ($R \le R_{\mathrm{Pl}}$)), which is converted into a stable state by the inflation. Thus, the relativistic energy of the magnetic monopoles is $E(\mathrm{M}) = E_{\mathrm{K}}(\mathrm{M}) + E_0(\mathrm{M}) \le E_{\mathrm{Pl}}$, whereat their kinetic energy is determined by $E_{\mathrm{K}}(\mathrm{M})$. Then, by Eq. (5.17), via the relativistic energy E_{Pl}, the rest energy of the magnetic monopoles is connected with the Planck radius. To this point, we will return in Sec. 7.2.

By this inflation model we have also confirmed the solution of the pressing problems of the standard model as the horizon problem (see Sec. 2.2.1) and the monopole problem (see Sec. 2.2.2), whereat because of the rest energy of the magnetic monopoles $E_0(\mathrm{M}) << E_{\mathrm{Pl}}$ (see Eqs. (5.7) and (7.3)) the initial condition problem (see Sec. 2.2.4) can be treated by the classical cosmology. To the flatness problem (see Sec. 2.2.3), we will return in Sec. 6.

Because of Eqs. (5.11) and (5.12), we can calculate $H_{\mathrm{V}}\Delta t$ to

$$\ln(1+z_M) = H_V \Delta t = 70.148 . \tag{5.23}$$

Suppose that the inflation begins at some very early time t_i and ends at some later time t_e, so that the period of inflation is $\Delta t = t_e - t_i$. Using Eqs. (5.17) to (5.20), we can again assume that Δt is defined by the very short period of the SUSY GUTs, so that we obtain $\Delta t = t_{X,Y} - t_M$, where $t_{X,Y}$ and t_M are given by Eqs. (4.6) and (5.10), respectively. Assuming $t_{X,Y} >> t_M$, we get

$$H_V \cong \frac{1}{t_{X,Y}} \ln(1+z_M) = (2.63^{+0.14}_{-0.15}) \cdot 10^{41}\,\mathrm{s}^{-1} . \tag{5.24}$$

Then, according to Eq. (2.17), we find the cosmological vacuum constant to

$$\Lambda_V = \frac{3H_V^2}{c^2} \cong (2.31^{+0.25}_{-0.26}) \cdot 10^{66}\,\mathrm{m}^{-2} . \tag{5.25}$$

6 The exact value of the curvature for the universe

By the inflation, the dimension of the universe, enlarges by the enormous factor $e^{H_V \Delta t} = 2.916 \cdot 10^{30}$ (see Sec. 5.3), so that any deviation from the flat geometry is quickly levelled out, i.e., the present-day universe ($z = 0$) can be assumed as Euclidian ($\Omega_{tot} = 1$ and $k = 0$). This conclusion is supported by the relation (2.10), which for the new scale factor $R_0 = c/H_0$ (see Eq. (5.4)) because of $R = R_0/(1+z)$ (see Eq. (5.22)) yields

$$k \frac{c^2}{R_0^2 H_0^2} = k = (\Omega_{tot} - 1) . \tag{6.1}$$

Then, via (6.1), the Planck 2013 results [12], which were used at the determination of the experimental limit $\Omega_{tot} \approx 1$ for the curvature in Table IV, permit uniquely to exclude the values $\Omega_{tot} = 2$ ($k = +1$) and $\Omega_{tot} = 0$ ($k = -1$), so that we must assume the exact value $\Omega_{tot} = 1$ ($k = 0$). Therefore, in the Friedmann equation (see Eq. (2.3)), we have $k = 0$.

Thus, the exact value $\Omega_{tot} = 1$ solves the flatness problem (see Sec. 2.2.3).

7 The "final" state and the reionization of the universe

7.1 The Planck units

The modern relativistic cosmology is based on the General Relativity ($R_{\mathrm{Pl}} \leq R \leq \infty$) and the quantum theory ($0 \leq R \leq \infty$). However, the different ranges of validity for the General Relativity and the quantum theory lead to an incompatibility between these theories, so that the Friedmann-Lemaitre equations (see Sec. 2.1), which are based on the (classical) General Relativity, have a limit of their applicability on massive particles at the Planck radius. Then, for massive particles of the energy E, the uncertainty relation $R = \hbar c/2E$, multiplied by their Schwarzschild radius $R = 2G_N E/c^4$, which describes the massive particles (matter), yields this limit as the so-called Planck radius (see Sec. 7.2):

$$R_{\mathrm{Pl}} = c\,t_{\mathrm{Pl}} = \sqrt{\frac{\hbar G_N}{c^3}} = (1.616200 \pm 0.000096) \cdot 10^{-35}\ \mathrm{m}\,. \tag{7.1}$$

Then, derived Planck units are the Planck time, the Planck energy and the Planck temperature:

$$t_{\mathrm{Pl}} = \frac{R_{\mathrm{Pl}}}{c} = \sqrt{\frac{\hbar G_N}{c^5}} = (5.39106 \pm 0.00032) \cdot 10^{-44}\ \mathrm{s}\,, \tag{7.2}$$

$$E_{\mathrm{Pl}} = \frac{\hbar c}{R_{\mathrm{Pl}}} = \frac{\hbar}{t_{\mathrm{Pl}}} = \sqrt{\frac{\hbar c^5}{G_N}} = (1.220932 \pm 0.000073) \cdot 10^{28}\ \mathrm{eV}\,, \tag{7.3}$$

$$T_{\mathrm{Pl}} = \frac{E_{\mathrm{Pl}}}{k} = \sqrt{\frac{\hbar c^5}{G_N k^2}} = (1.416833 \pm 0.000086) \cdot 10^{32}\ \mathrm{K}\,. \tag{7.4}$$

The above-mentioned incompatibility between the General Relativity and the quantum theory can only be solved by the quantum gravity, which must reconcile the gravitation with the quantum theory. Unfortunately, the quantum gravity is still highly incomplete and no reliable predictions can be presented [1].

7.2 The "final" state of the universe

For the estimation of the Planck energy (see Eq. (7.3)), we can as usually [11] consider two particles with the mass $m = E/c^2$, which have the distance of the reduced Compton wavelength $\lambda_C = \hbar c/E$. Then, the gravitation yields the potential $V = -G_N m^2/\lambda_C = -G_N E^3/c^5\hbar$. An upper limit for the correctness of this classical approach gives the assumption that this potential cannot exceed the limiting energy $E = E_{Pl} = \sqrt{\hbar c^5/G_N}$ (Planck energy (see Eq. (7.3))) because according to the indeterminacy principle the quantum fluctuations of the distance cause an energy uncertainty in order of magnitude of this Planck energy, so that it is not possible to describe these particles by a well-defined rest energy. Thus, because of $E_0(\mathrm{M}) = 6.849 \cdot 10^{26}\,\mathrm{eV}$, the rest energy of the magnetic monopoles, which is well-defined because of $E_0(\mathrm{M}) << E_{Pl}$, is connected with the Planck radius $\lambda_C = R_{Pl} = \sqrt{\hbar G_N/c^3}$ via their relativistic energy E_{Pl} (see Sec. 5.3 (e.g., Eq. (5.17) because of Eqs. (5.7), (5.10) and (7.1)).

In contrast to the large mass of the monopoles ($E_0(\mathrm{M}) = 6.849 \cdot 10^{26}\,\mathrm{eV}$), which is connected with the Planck radius (see above), we can assume that the small mass of the electron neutrino ($E_0(\nu_e) = 1.589 \cdot 10^{-3}\,\mathrm{eV}$) defines in first approximation an upper limiting value of the scale factor for the Friedmann-Lemaitre equations as the "final" state of the universe.

Thus, we assume that this "final" state proceeds from a blueshift (negative acceleration). Because of $\Omega_m = \{\Omega_{dm} + \Omega_\nu(\nu_\tau) + \Omega_\nu(\nu_\mu) + \Omega_\nu(\nu_e)\} + \Omega_b$, at $N(T) = 3.362644$, for this goal, we use the redshift condition of the matter-radiation equality (see Tables II and IV):

$$1 + z_{eq} = \frac{2\Omega_m}{N(T)\,\Omega_\gamma} = \\ = \frac{2\left(\{\Omega_{dm} + \Omega_\nu(\nu_\tau) + \Omega_\nu(\nu_\mu) + \Omega_\nu(\nu_e)\} + \Omega_b\right)}{N(T)\,\Omega_\gamma}, \qquad (7.5)$$

so that by Eq. (3.26) we can assume

$$1+z(\nu_e)=\frac{2\left\{\Omega_m-\left(\left\{\Omega_{dm}+\Omega_\nu(\nu_\tau)+\Omega_\nu(\nu_\mu)\right\}+\Omega_b\right)\right\}}{N(T)\,\Omega_\gamma}=$$

$$=\frac{2\Omega_\nu(\nu_e)}{N(T)\,\Omega_\gamma}=0.406^{+0.020}_{-0.025}\,. \tag{7.6}$$

Then, the neutrinos must be considered together with the radiation (see Eq. (2.12)). However, the matter-dominated universe expands for the redshift condition $1+z_{eq}>>1+z\geq 1$, i.e., the scale factor R increases. At $1+z\leq 1$, we have a blueshift, so that R decreases. Therefore, we assume that the blueshift $1+z(\nu_e)=0.406$ determines in first approximation a "final" state of the universe, where the particles do not move more practically, so that we must observe a (mean) negative acceleration, which "stops" effectively the remaining expansion as a result of the inertia of the particles. The values of this "final" state and of this mean negative acceleration are determined at the end of the next chapter. Here, we show also that this "final" process must be connected with a changing of the astronomical unit.

7.3 The values of the final state of universe and the mean negative acceleration

For Eq. (2.25), at $z_{eq}>>z>>1$, we can neglect Ω_Λ, so that the matter-dominated universe is described by the Friedmann equation of the form

$$\left(\frac{\dot{R}}{R}\right)^2=\Omega_m H_0^2\left(\frac{R_0}{R}\right)^3\,. \tag{7.7}$$

Eq. (7.7) has the solutions

$$R=(3/2)^{2/3}\,\Omega_m^{1/3}\,R_0(H_0\,t)^{2/3} \tag{7.8}$$

and

$$t=t(z)=\frac{2}{3\,H_0\left[\Omega_m(1+z)^3\right]^{1/2}}\,. \tag{7.9}$$

However, for Eq. (2.26), at $z << z_{eq}$, we cannot more neglect Ω_Λ, so that by Eq. (2.3) the matter-dominated universe is defined by

$$\left(\frac{\dot{R}}{R}\right)^2 = H_0^2(\Omega_m\left(\frac{R_0}{R}\right)^3 + \Omega_\Lambda) \tag{7.10}$$

with the solutions

$$\frac{R}{R_0} = \frac{1}{1+z} = \left(\frac{\Omega_m}{\Omega_\Lambda}\right)^{1/3}\left[\sinh(\tfrac{3}{2}\Omega_\Lambda^{1/2} H_0\, t)\right]^{2/3} =$$

$$= \left(\frac{\Omega_m}{\Omega_\Lambda}\right)^{1/3}\left[\frac{e^{\frac{3}{2}\Omega_\Lambda^{1/2} H_0 t} - e^{-\frac{3}{2}\Omega_\Lambda^{1/2} H_0 t}}{2}\right]^{2/3} \tag{7.11}$$

and

$$t = t(z) = \frac{2}{3 H_0\, \Omega_\Lambda^{1/2}} \ln \frac{\sqrt{\Omega_\Lambda (1+z)^{-3}} + \sqrt{\Omega_\Lambda (1+z)^{-3} + \Omega_m}}{\sqrt{\Omega_m}}. \tag{7.12}$$

Using Eqs. (7.9) and (7.12), we can form the equation

$$\left(\frac{\Omega_\Lambda}{\Omega_m}\right)^{1/2} \frac{1}{(1+z_\Lambda)^{3/2}} =$$

$$= \ln \frac{\sqrt{\Omega_\Lambda (1+z_\Lambda)^{-3}} + \sqrt{\Omega_\Lambda (1+z_\Lambda)^{-3} + \Omega_m}}{\sqrt{\Omega_m}}. \tag{7.13}$$

For the corresponding density parameters of Table IV, Eq. (7.13) yields the redshift condition

$$1 + z_\Lambda = 18.90^{+0.48}_{-0.49}, \tag{7.14}$$

where in Eqs. (2.25) or (2.26) the influence of the dark energy (Ω_Λ) begins for $z \leq 18.90$. Taking Eqs. (5.4) as well as (7.6), for the scale factor of the final state of the universe, we get

$$R = R(\nu_e) = \frac{R_0}{1 + z(\nu_e)} = (3.39^{+0.27}_{-0.23}) \cdot 10^{26}\ \mathrm{m}. \tag{7.15}$$

For the standard model, Eq. (7.12) gives $t(z(\nu_e)) = 9.016 \cdot 10^{17}\,\mathrm{s} = 28.57\,\mathrm{Gyr}$ (see Eq. (7.6)). In contrast to the standard model, the (present) exponential expansion (see Eq. (2.27)) yields the condition

$$\frac{R(\nu_e)}{R_0} = \frac{1}{1+z(\nu_e)} = \mathrm{e}^{\Omega_\Lambda^{1/2} H_0 (t_{\exp}(\nu_e) - t_0)}, \tag{7.16}$$

where $t_0 \equiv 4.358 \cdot 10^{17}\,\mathrm{s}$ (age of the present-day universe). Therefore, if we use the corresponding parameters of Table IV, Eq. (7.16) determines in first approximation the future age of the "final" state of the universe to $t_{\exp}(\nu_e) = 9.352 \cdot 10^{17}\,\mathrm{s} = 29.63\,\mathrm{Gyr}$.

By Eq. (7.14), for the beginning influence of the dark energy, we find its minimum scale factor

$$R = R_\Lambda = \frac{R_0}{1+z_\Lambda} = (7.28 \pm 0.32) \cdot 10^{24}\,\mathrm{m}. \tag{7.17}$$

Because of the expressions (7.15) and (7.17), which define the range of influence of the dark energy (Ω_Λ), for the mean negative acceleration (MNA), we must assume the average of their redshift conditions

$$1 + z_{\mathrm{MNA}} = \frac{R_0}{\sqrt{R_\Lambda R(\nu_e)}} = \left([1+z_\Lambda][1+z(\nu_e)]\right)^{1/2} = 2.77^{+0.10}_{-0.12}, \tag{7.18}$$

so that we obtain a corresponding effective equilibrium scale factor

$$R = R_{\mathrm{MNA}} = \frac{R_0}{1+z_{\mathrm{MNA}}} = (4.96^{+0.31}_{-0.27}) \cdot 10^{25}\,\mathrm{m}. \tag{7.19}$$

Therefore, by Eqs. (2.4) and (2.26), via Eqs. (7.18) and (7.19), for the matter-dominated universe ($P = 0$), the mean negative acceleration is effectively defined by

$$\begin{aligned} \ddot{R}_{\mathrm{MNA}} = a &= -\frac{1}{2} H_0^2 (\Omega_{\mathrm{m}} (R_0/R_{\mathrm{MNA}})^3 + \Omega_\Lambda) R_{\mathrm{MNA}} = \\ &= -\frac{1}{2} H_0 c \left[\Omega_{\mathrm{m}} (1+z_{\mathrm{MNA}})^2 + \Omega_\Lambda/(1+z_{\mathrm{MNA}})\right] = \\ &= (-8.71^{+0.76}_{-0.87}) \cdot 10^{-8}\,\mathrm{cm\,s^{-2}}. \end{aligned} \tag{7.20}$$

The value (7.20) agrees excellently with the observed [5] Pioneer (P) anomaly

$$\ddot{R}_{\mathrm{P}} = a_{\mathrm{P}} = (-8.74 \pm 1.33) \cdot 10^{-8}\ \mathrm{cm\ s^{-2}}. \tag{7.21}$$

This excellent agreement is an evidence for the correctness of $E_0(\nu_{\mathrm{e}})$ and $\Omega_\nu(\nu_{\mathrm{e}})$ as well as of the assumption of a "final" state of the universe. Consequently, Eq. (7.20) gives the significance of the electron neutrino for the universe.

With that, we have solved the mystery of the Pioneer anomaly [5, 20]. Thus, the thermal recoil pressure computer simulation [21] is doubtful because it explains the Pioneer anomaly as an unreal physical effect. We will return to this point at the end of Sec. 8.1.

Using the half of the expansion described for $\mathrm{k} = 0$ (see Sec. 6) by the Friedmann equation (see Eq. (2.3)), the (mean) negative acceleration is compensated by the half of the positive acceleration, which via Eqs. (2.3) and (2.26) is effectively given by

$$\begin{aligned}
&\frac{1}{2}\frac{\dot{R}^2_{\mathrm{MNA}}}{R_{\mathrm{MNA}}} = -\ddot{R}_{\mathrm{MNA}} = -a = \\
&= \frac{1}{2} H_0^2 (\Omega_{\mathrm{m}} (R_0/R_{\mathrm{MNA}})^3 + \Omega_\Lambda) R_{\mathrm{MNA}} = \\
&= \frac{1}{2} H_0 c \left[\Omega_{\mathrm{m}} (1+z_{\mathrm{MNA}})^2 + \Omega_\Lambda/(1+z_{\mathrm{MNA}})\right] = \\
&= (+8.71^{+0.76}_{-0.87}) \cdot 10^{-8}\ \mathrm{cm\ s^{-2}},
\end{aligned} \tag{7.22}$$

so that for $1+z_{\mathrm{MNA}}$ (see Eq. (7.18)) or at R_{MNA} (see Eq. (7.19)) via the sum of Eqs. (7.20) and (7.22) we obtain an effective equilibrium. The remaining half of the expansion of the Friedmann equation (see Eqs. (2.3) and (7.22)) must be responsible for a changing of the astronomical unit, to which we will return in Sec. 8.2.

7.4 The redshift values of the beginning, the half and the end of the reionization

Much information about the intergalactic medium (IGM), which permeates the space between the galaxies, has been obtained through its absorption of

light from distant quasars, whereby one of the most important tests of the presence of a diffuse component of the intergalactic neutral (mainly hydrogen (HI)) gas is the Gunn-Peterson effect [1]. This effect uses the fact that in the intergalactic neutral gas according to Ref. 1 the density of these HI atoms, defined by $n_{\mathrm{HI}}(z) \approx 2.42 \cdot 10^{-11} \tau(z) h \left\{ \Omega_\Lambda + \Omega_{\mathrm{m}} (1+z)^3 + \Omega_{\mathrm{r}} (1+z)^4 \right\} \mathrm{cm}^{-3}$ for $\mathrm{k} = 0$ (see Sec. 6), can be estimated by the measurement of its optical depth $\tau(z)$ from flux decrement in quasar spectra at the wavelength $\lambda_{\mathrm{Ly}\alpha} = 121.6\,\mathrm{nm}$ in $\mathrm{Ly}\alpha$ absorption (of the neutral hydrogen), which has a very large cross-section for

$$T_{\mathrm{IGM}} << T_{\mathrm{Ly}\alpha} = \frac{2\pi\hbar c}{k\,\lambda_{\mathrm{Ly}\alpha}} = 1.183 \cdot 10^5\,\mathrm{K}\,. \tag{7.23}$$

The observations show that at a redshift of order $1+z \approx 6$ the neutral hydrogen, left over from the time of recombination, becomes reionized by this ultraviolet light ($\lambda_{\mathrm{Ly}\alpha} = 121.6\,\mathrm{nm}$) from the massive stars (quasars) [1, 3].

For example, the condition (7.23) can be fulfilled by the neutrinos if they determine T_{IGM}. Thus, via Eqs. (3.27) to (3.29), analogously to Eq. (7.6), we assume that the redshifts z_{reion} of the neutrinos

$$z_{\mathrm{reion}}\left(\textstyle\sum_i \nu_i\right) = \frac{2\sum_i \Omega_\nu(\nu_i)}{N(T)\,\Omega_\gamma} - 1 = 14.27^{+0.37}_{-0.33}\,, \tag{7.24}$$

$$z_{\mathrm{reion}}(\nu_\tau) = \frac{2\,\Omega_\nu(\nu_\nu)}{N(T)\,\Omega_\gamma} - 1 = 11.60^{+0.31}_{-0.26} \tag{7.25}$$

and

$$z_{\mathrm{reion}}(\nu_\mu) = \frac{2\,\Omega_\nu(\nu_\mu)}{\dot{N}(T)\,\Omega_\gamma} - 1 = 1.263^{+0.036}_{-0.042} \tag{7.26}$$

determine the beginning, the half and the end of the reionization, respectively. This assumption is supported by the neutrino temperatures

$$T\left(\textstyle\sum_i \nu_i\right) = \left\{1 + z_{\mathrm{reion}}\left(\textstyle\sum_i \nu_i\right)\right\} T_0 = 41.62\,\mathrm{K}\,, \tag{7.27}$$

$$T(\nu_\tau) = \left\{1 + z_{\mathrm{reion}}(\nu_\tau)\right\} T_0 = 34.34\,\mathrm{K} \tag{7.28}$$

and

$$T(\nu_\mu) = \left\{1 + z_{\text{reion}}(\nu_\mu)\right\} T_0 = 6.168\ \text{K}\,, \tag{7.29}$$

since they fulfil the condition (7.23). Then, the neutrinos are coupled to the photons via $N(T) = 3.362644$ (see Eq. (2.12)). Therefore, our assumption shows the significance of these neutrinos for the universe.

The value (7.25) agrees excellently with the redshifts of the half reionization in the Tables II to IV, which were found on completely other ways. This fact is a strong argument for the correctness of the assumptions (7.24) and (7.26) as the beginning and the end of the reionization, respectively.

8 Flyby anomaly, astronomical unit changing and dark energy

8.1 The flyby anomaly

Using the (mean) negative acceleration $a = (-8.71^{+0.76}_{-0.87}) \cdot 10^{-8}\ \text{cm s}^{-2}$ (see Eq. (7.20)), we can explain the anomalous orbital-velocity differences ΔV_∞ (see below), denoted as flyby anomaly. They were observed during the Earth flybys by the Galileo, NEAR, Cassini, Rosetta and MESSENGER spacecraft, which were launched between December 1990 and September 2005 to Jupiter, to an asteroid, to a comet, to Saturn and Mercury, respectively. For these spacecrafts, at closest approach, all Earth flyby parameters are tabulated in Ref. [6].

For our goal, we perform the following considerations. The Earth rotation period is

$$t_\text{E} \cong 24\,\text{h} = 8.64 \cdot 10^4\,\text{s}\,. \tag{8.1}$$

Consequently, by the mean Earth equatorial radius $R_\text{Earth} = 6.378137 \cdot 10^6\,\text{m}$, we get the Earth circular orbit velocity

$$V_\text{E} \cong \frac{2\pi}{t_\text{E}} R_\text{Earth} = 463.83\ \text{m s}^{-1}\,. \tag{8.2}$$

However, the flyby anomaly cannot be explained by the Earth tangential (t) acceleration

$$a_t \approx \frac{V_E}{t_E} = 0.537\ \mathrm{cm\,s^{-2}} \tag{8.3}$$

because of $a_t >> a$. However, if the small Pioneer anomaly a_P (see Eq. (7.21)), which is identical with the negative acceleration a (see above), is a real effect, it must have a weak influence on the spacecrafts, which is calculated in Table V.

TABLE V. The most important Earth flyby parameters at the closest approach for Galileo, NEAR, Cassini, Rosetta and MESSENGER spacecraft (The quantities are explained in the text). [a)] For Galileo-II, the measured value ΔV_∞ is actually $-8\,\mathrm{mm/s}$, but it is reduced in magnitude after subtracting out an estimated atmospheric drag of $-3.4\,\mathrm{mm/s}$ [6].

Parameter	**Galileo-I**	**Galileo-II**	**NEAR**
Date	12/8/90	12/8/92	1/23/98
Height [km]	960	303	539
V_∞ [km/s]	8.949	8.877	6.851
δ_i [deg]	-12.52	-34.26	-20.76
δ_o [deg]	-34.15	-4.87	-71.96
ΔV_∞ [mm/s]	3.92 ± 0.3	-4.6 ± 1.0 [a)]	13.46 ± 0.01
t_{FB} [s]	$-4.781 \cdot 10^6$	$5.377 \cdot 10^6$	$-1.179 \cdot 10^7$
ΔV_{FB} [mm/s]	4.16	-4.68	10.3
$\bar{t}_{FB}$ [s]	$-4.485 \cdot 10^6$	$5.263 \cdot 10^6$	$-1.540 \cdot 10^7$

TABLE V, continued.

Parameter	Cassini	Rosetta	MESSENGER
Date	8/18/99	3/4/05	8/2/05
Height [km]	1175	1956	2347
V_∞ [km/s]	16.010	3.863	4.056
δ_i [deg]	-12.92	-2.81	31.44
δ_o [deg]	-4.99	-34.29	-31.92
ΔV_∞ [mm/s]	-2 ± 1	1.80 ± 0.03	0.02 ± 0.01
t_{FB} [s]	$2.216 \cdot 10^6$	$-1.034 \cdot 10^6$	$-2.907 \cdot 10^4$
ΔV_{FB} [mm/s]	-1.93	0.901	0.0253
$\bar{t}_{FB}$ [s]	$2.288 \cdot 10^6$	$-2.060 \cdot 10^6$	$-2.288 \cdot 10^4$

Because of the above-mentioned weak influence of the Pioneer anomaly, for the flyby (FB) anomaly of the spacecrafts, we can reasonably expect as a result of their orbit parameters at the closest approach that heuristically the "rotation periods t_{FB}" are approximately given by

$$t_{FB} \approx t_E \left(\frac{V_\infty}{V_E} \right)^2 (\cos\delta_0 - \cos\delta_i) \quad \text{(see Table V)}, \tag{8.4}$$

where V_∞ is the osculating hyperbolic excess spacecraft velocity, whereas δ represents the right declination of the incoming (i) and outgoing (o) osculating asymptotic spacecraft velocity vectors. Their experimental values were taken from Ref. [6] and are summarized in Table V. In Eq. (8.4), because of V_∞, we

must observe an increase of the "rotation period t_E" by the square ratios $(V_\infty/V_E)^2$, which are proportional to $(E_\infty/E_E)_{kinetic}$ at the spacecrafts. Likewise, in Table V, the measured anomalous flyby velocity differences ΔV_∞ [6] are given. Thus, by Eqs. (7.20) and (8.4), their (theoretical) flyby velocity differences ΔV_{FB}, which are also summarized in Table V, can be characterized semi-empirically by

$$\Delta V_{FB} \cong a t_{FB} = a t_E \left(\frac{V_\infty}{V_E}\right)^2 (\cos\delta_0 - \cos\delta_i) . \tag{8.5}$$

According to Table V, the comparison between the experimental values ΔV_∞ and our simple assumptions ΔV_{FB} (see Eq. (8.5)) yields only a maximum deviation of a factor 2. For the flyby "rotation periods", we find their "experimental" values $\bar{t}_{FB}$ via ΔV_∞ (see Table V) and a_P (see Eq. 7.21)) to

$$\bar{t}_{FB} = \frac{\Delta V_\infty}{a_P} . \tag{8.6}$$

Consequently, according to Table V, between $\bar{t}_{FB}$ (see Eq. (8.6)) and t_{FB} (see Eq. (8.4)), we observe likewise a maximum deviation of a factor 2.

Because the thermal recoil pressure computer simulation [21] cannot describe the flyby anomaly, our doubts about this computer simulation are justified (see also the next to last paragraph of Sec. 7.3). The excellent agreement between the theoretical and observed flyby data (see Table V) confirms our assumption of the Pioneer anomaly as a real effect.

8.2 The astronomical unit changing

An astronomical unit changing was observed by two independent researcher groups, analysing radio echoes from the planets [7, 8]. According to Krasinsky and Brumberg [7], the astronomical unit change was found to

$$\frac{d}{dt}\mathrm{AU} = (15 \pm 4)\ \mathrm{cm\,yr^{-1}}, \tag{8.7}$$

where $\mathrm{AU} = 1.49597870700(3) \cdot 10^{11}\ \mathrm{m}$ is the astronomical unit [10].

For the range $z_\Lambda \geq z \geq z(\nu_e)$, this astronomical unit changing can be explained by the remaining half of the expansion of the Friedmann equation at $\mathrm{k} = 0$ (see Sec. 6), since its other half of the expansion was used for the compensation of the mean negative acceleration (see also the last paragraph of Sec. 7.3). Therefore, for $1 + z_{\mathrm{MNA}}$ (see Eq. (7.18)) or at R_{MNA} (see Eq. (7.19)), in the matter-dominated universe, via Eqs. (2.3) and (2.26), a (mean) astronomical unit changing can be defined by

$$\frac{d}{dt}\mathrm{AU} = \frac{1}{2}\frac{\dot{R}^2_{\mathrm{MNA}}}{H_0 R_{\mathrm{MNA}}}\mathrm{corr(AU)} =$$

$$= \frac{1}{2} H_0 \left(\Omega_{\mathrm{m}} \left(\frac{R_0}{R_{\mathrm{MNA}}}\right)^3 + \Omega_\Lambda\right) R_{\mathrm{MNA}}\,\mathrm{corr(AU)}, \tag{8.8}$$

where the correction constant corr(AU) is necessary as a proportionality factor, since the radio echoes, which are observed on the surface of the earth, are reflected on the surface of the planets. Consequently, the radio signals run twice the distance $\Delta\mathrm{AU} = \mathrm{AU} - (R_{\mathrm{earth}} + R_{\mathrm{sun}})$, so that this correcture constant must be assumed as the symmetry condition

$$\mathrm{corr(AU)} = 2\frac{\mathrm{AU} - \Delta\mathrm{AU}}{R_0} =$$

$$= 2\frac{R_{\mathrm{earth}} + R_{\mathrm{sun}}}{R_0} = 2 \times (5.105 \pm 0.093) \cdot 10^{-18}, \tag{8.9}$$

where $R_{\mathrm{earth}} = 6.378137 \cdot 10^6\,\mathrm{m}$ and $R_{\mathrm{sun}} = (6.9551 \pm 0.0004) \cdot 10^8\,\mathrm{m}$ are the equatorial radii of the earth and the sun [10]. The denominator of this corr(AU) must be defined by the scale factor R_0 for the present-day universe

($z = 0$). Thus, by Eqs. (8.8) and (8.9), we find the (mean) astronomical unit changing to

$$\frac{d}{dt}\mathrm{AU} = c\left[\Omega_{\mathrm{m}}(1+z_{\mathrm{MNA}})^2 + \Omega_{\Lambda}/(1+z_{\mathrm{MNA}})\right]\frac{R_{\mathrm{earth}} + R_{\mathrm{sun}}}{R_0} =$$

$$= (2.521^{+0.18}_{-0.21})\cdot 10^{18}\,\mathrm{cm\,yr^{-1}}\,\frac{R_{\mathrm{earth}} + R_{\mathrm{sun}}}{R_0} = (12.9^{+1.2}_{-1.3})\,\mathrm{cm\,yr^{-1}}. \qquad (8.10)$$

The theoretical value (8.10) agrees excellently with the result (8.7) of the analysis of all available radiometric measurements in the time span 1961-2003 [7]. This result is in accordance with a later analysis of the solar-system anomalies in Ref. [9], which for the astronomical unit changing permits the limiting conditions $0 \le {}^{d}\!/_{dt}\,\mathrm{AU} \le 20\,\mathrm{cm\,yr^{-1}}$.

With that we have plausible explained the mystery of the astronomical unit changing.

8.3 The physical meaning of the effective influence of the dark energy

Our explanations of the measured Pioneer anomaly (see Sec. 7.3) and the observed astronomical unit changing (see Sec. 8.2) permit the assumption that the evolution of the universe ends in first approximation by a "final" state at $R(\nu_{\mathrm{e}}) = 3.39\cdot 10^{26}$ m (see Eq. (7.15)). Then, if we use instead of the Pioneer anomaly the (mean) astronomical unit changing (see Eq. (8.10)) which describes the scale factor changing per AU in the universe, the time span $\Delta\tau$ yields for R_0 as slow linear (lin) expansion of the universe after the exponential expansion:

$$R_{0\mathrm{lin}} = R_0\left(1 + \frac{\Delta\tau}{\mathrm{AU}}\,\frac{d}{dt}\mathrm{AU})\right) = R_0(1 + \Delta\tau \times 8.62\cdot 10^{-13}\,\mathrm{yr^{-1}}). \qquad (8.11)$$

Consequently, for the enormous time span of $\Delta\tau = 1.16\cdot 10^{9}\,\mathrm{yr}$, Eq. (8.11) gives only a relative changing of about

$$\frac{\Delta R_0}{R_0} = \frac{R_{0\text{lin}} - R_0}{R_0} = \frac{\Delta\tau}{\text{AU}}\frac{d}{dt}\text{AU} = 10^{-3}, \tag{8.12}$$

so that in first approximation Eq. (8.12) defines the "final" state of the universe (see above) because we have the same relative changing for $\Delta R(\nu_e)/R(\nu_e)$. This "final state is determined by the effective influence of the dark energy Ω_Λ via $1+z_{\text{MNA}}$ (see Eqs. (7.20) and (8.10)). Therefore, this "final" state shows the physical meaning of the effective influence of the dark energy Ω_Λ in Eq. (2.26) because in future the present exponential expansion, which is determined by the dark energy, gives way to a slow linear expansion of the universe.

However, for the future, in a time span $\Delta\tau \approx 200\,\text{yr}$, the changing of the astronomical unit via Eq. (8.11) with $R_0 \to \text{AU}$ is well measurable because we have here an AU changing of about $26\,\text{m}$ and the error of the present AU determination is only $3\,\text{m}$ (see after Eq. (8.7)). If in the future this conclusion can be confirmed, the Pioneer anomaly and the astronomical unit changing are uniquely proved, so that they can be counted to the most important astronomical discoveries within living memory.

9 Summary

Taking the results of the big bang model and the supersymmetric grand unified theories, we have shown the significance of the light neutrinos as well as the extremely heavy hypothetical magnetic monopoles for the universe. Using the results of the neutrino oscillation experiments together with cosmological data, we have presented an approximate solution for the neutrino problem (by the estimation of the neutrino masses and the neutrino densities of the universe). Via this estimation and by the magnetic neutrino moment of the standard SU(2)×U(1) electroweak theory, we have derived the masses of the X and Y gauge bosons. We have also obtained the mass of the

magnetic monopoles via the big bang model, so that in accordance with the particle physics we have exactly determined the coupling constant of the supersymmetric grand unified theories which characterize the early universe. Thus, using the "both" scale factors of absorption at the redshift "before" and after the inflation as different functions of the Hubble constant, we have obtained an exact and unique description of this inflation and its transition to the standard model, so that we have confirmed the presented solutions for the pressing problems of the standard cosmology as the horizon problem, the flatness problem, the monopole problem and the initial condition problem. This inflation is determined by the magnetic monopoles. We have found the exact value of the curvature for the universe. Via the matter-dominated universe and the exponential expansion, we have derived in first approximation the "final" state of the universe as a function of a blueshift via a negative acceleration determined by the electron neutrino, so that we have explained the Pioneer anomaly and the flyby anomaly via this mean negative acceleration as well as the astronomical unit changing. Via the neutrinos, we have obtained the redshift values for the beginning, the half and the end of the reioinization. We have explained the physical meaning of the effective influence of the dark energy via the "final" state of the universe. Therefore, in future, the (present) exponential expansion, which is determined by the dark energy, gives way to a slow linear expansion of the universe. All these results were mainly obtained by the big bang model, so that they show clearly the significance of the light neutrinos and the extremely heavy hypothetical magnetic monopoles for the universe.

10 Acknowledgment

We acknowledge Peter Ressel, who rewiewed critically the manuscript and provided several useful comments in the discussion.

References

[1] H. Mo, F. van den Bosch, and S. White, *GALAXY FORMATION AND EVOLUTION*, (Cambridge University Press, Cambridge, UK, 2010).

[2] K. Olive *et al.* [Particle Data Group], *Chin. Phys.* C**38**, 090001 (2014), [http://pdg.lbl.gov].

[3] S. Weinberg, *Cosmology* (Oxford University Press, New York, 2008).

[4] A. Unsöld and B. Baschek, *The New Cosmos*, (Springer, Berlin, Heidelberg, New York, 2005), 5th ed.

[5] J. D. Anderson, P. A. Laing, E. L. Lau, A. S. Liu, M. M. Nieto, and S. G. Turyshev, *Phys. Rev.* D**65**, 082004 (2002)

[6] J. D. Anderson, J. K. Campbell, J. E. Ekelund, J. Ellis, and J. F. Jordan, *Phys. Rev. Lett.* **100**, 091102 (2008)

[7] G. A. Krasinsky and V. A. Brumberg, *Celest. Mech. & Dyn. Astron.* **90**, 267 (2004)

[8] E. M. Standish, *The astronomical unit now* in D. W. Kurtz (ed.): *Transits of Venus: New Views of the Solar System and Galaxy*, Proceedings IAU Colloquium No. 196, 2004 (Cambridge University Press, Cambridge, UK, 2005), p. 163-179

[9] J. D. Anderson and M. M. Nieto, *Astrometric solar-system anomalies*, in S. A. Klioner, P. K. Seidelman and M. H. Soffel (eds.): *Relativity in Fundamental Astronomy*, Proceedings IAU Symposium No. 261, 2009 (Cambridge University Press, Cambridge, UK, 2010), p. 189-197

[10] J. Beringer *et al.* (Particle Data Group), *Phys.Rev.* D**86**, 010001 (2012), [http://pdg.lbl.gov]

[11] M. Treichel, *Teilchenphysik und Kosmologie* (Springer-Verlag, Berlin, Heidelberg, 2000)

[12] P. A. R. Ade et al., (Planck Collaboration I. and XVI.):
Planck 2013 results. I. Overview of products and scientific results, Astron. & Astrophys. **571**, A1 (2014), [http://arXiv.1303.5062v1];
Planck 2013 results. XVI. Cosmological parameters, Astron. & Astrophys. **571**, A16 (2014) [http://arXiv.1303.5076v1]

[13] J. Ellis, S. Kelley and D. V. Nanopoulos, *Phys. Lett.* B**260**, 131 (1991)

[14] P. Langacker and M. Luo, *Phys. Rev.* D**44**, 817 (1991)

[15] P. Langacker and N. Polansky, *Phys. Rev.* D**47**, 4028 (1993)
[16] T. Blazek, M. Carena, S. Raby and C. E. M. Wagner, *Phys. Rev.* D**56**, 6919 (1997)
[17] C. Berger, *Elementarteilchenphysik*, (Springer-Verlag, Berlin, Heidedelberg, 2002)
[18] A. Vilenkin and E. P. S. Shellard, *Cosmic Strings and other Topological Defects*, (Cambridge University Press, Cambridge, UK, 1994)
[19] K. Fujikawa and R. E. Shrock, *Phys. Rev. Lett.* B**45**, 963 (1980)
[20] H. Dittus and C. Lämmerzahl, *Physik Journal* **5**, 25 (2006)
[21] R. Rievers and C. Lämmerzahl, arXiv:1104.3985v2 [gr-qc], 5 May 2011

PARTICLES AND GENERAL COORDINATE TRANSFORMATIONS

Simon Davis
Research Foundation of Southern California
8861 Villa La Jolla Drive #13595
La Jolla, CA 92039 USA

Received April 3, 2017

Abstract

The effect of general coordinate invariance and the curvature of space-time on quantum field theory is investigated. Conditions for the CPT theorem to be valid in anti-de Sitter space-time are given. An action is constructed from the spin curvature and torsion required for a covariantly constant charge conjugation matrix.

PACS: 04.20.Gz, 11,30.Er

Keywords: *wedge, charge conjugation, covariant constancy, spin curvature*

Copyright © 2017 by Hadronic Press, Inc., Palm Harbor, FL 34684, USA

1. Introduction

Space-time quantization initially was formulated as a commutation relations of coordinate operators derived from the de Sitter group [1] to introduce a quantized spectrum through the eigenvalues of rotational generators in the spatial directions [2]. The origin of space-time through the matrix model, which provides a representation representation of a nonlocal field, is based on the dependence of the matrices representing the different coordinates. The extension to the theory of strings is based on $U(n)$ matrices, and therefore, a group symmetry is required for the extrapolation.

The description of quantum theories in terms of observables rather than states allows a characterization of locally covariant theories through $\mathcal{O}(\Sigma) = \mathcal{O}(M)$, where Σ is a Cauchy surface and $\mathcal{O}$ is the set of observables. Particle states can be defined consistently in globally hyperbolic space-times. The transformation from a particle to an antiparticle is defined to be the charge conjugation operator C, $T : \{t > 0\} \rightarrow \{t < 0\}$. The existence of a Cauchy surface invariant under T is sufficient for particle and antiparticles to be globally valid states. The CPT theorem can be proven to be valid for globally hyperbolic space-times.

It is known that covariant constancy of the charge conjugation condition in four dimensions requires the spin curvature to belong to $SO(3,2;\mathbb{C})$ [3]. The spatial extension from the tangent space on a manifold would be anti-de Sitter space. There is no substantial evidence of anti-de Sitter space, since bubble formation with anti-de Sitter interiors collapse gravitationally [4] and AdS geometries with three-dimensional hypersurfaces arising as solutions to string theory equations are not observed. Nevertheless, anti-de Sitter space will be found to satisfy the criteria for a geometrical background of quantum field theories with CPT invariance.

Several of the principles underlying constructive quantum field theory will be extended to anti-de Sitter space. The existence of a domain of holomorphicity for the operators will be established by extending the algebra to wedges in the embedding space of the anti-de Sitter manifold. The covariant constancy of the charge conjugation matrix will be demonstrated to be valid under conformal transformations to the globally hyperbolic Einstein state universe. Then a theory defined in terms of the spin curvature is given. It describes a coupling of a scalar and antisymmetric two-index field to gravity that occurs in string effective actions for a specific choicer of the spin torsion. Furthermore, there exists a nonlocal generalization which will have nonconserved charges.

2. The Conditions for the CPT Theorem in Globally Hyperbolic Space-times

In the Einstein static universe, either reflective boundary conditions are requested at $\mathcal{I}$ or two spacelike surfaces may be combined to give a Cauchy surface forthe devlopment of initial data and the solution to the field equation. The isometry group of $\mathbb{R}^1 \times S^3$ is $\mathbb{R}^1 \times SO(4)$. An extra three degrees of freedom would correspond to translations of the time axis along the spatial directions. However, the compactification of the noncompact space-times would prevent these degrees of freedom from being realized. The Einstein static universe is globally hyperbolic, and quantum theory can be formulated consistently on this manifold. Since $\mathbb{R}^1 \times SO(4) \subset SO(4,1)$, the gamma matrices in the formula for the spin curvature can be restricted to these corresponding to the subgroup. For example, $\{\gamma_5\} \times \{\gamma_{mn}\}$ might suffice for this gamma matrix algebra. The presence of γ_5 would introduce chirality into the model. A reversal of time and parity would occur simultaneously. Although antiparticles might be defined on the Einstein static universe, and scattering experiments may be undertaken with a particle moving forward in time with respect to a spacelike hypersurface and an antiparticle moving backwards in time in a neighbourhood of this surface, there could be interference from the development of data on the other spacelike hypersurface, located at a time $-\frac{\pi}{2}$ earlier which is complement in the Cauchy surface.

In Minkowski space-time, the parity, time reversal and charge conjugation operators can be chosen to be $P \sim \gamma_0$, $T \sim \gamma_1\gamma_3$ and $C \sim \gamma_2\gamma_0$. The set

$$\{1, P, T, PT, C, CP, CT, CPT\} \sim \{1, \gamma_0\gamma_0\gamma_3, \gamma_0\gamma_1\gamma_3, \gamma_2\gamma_0, \gamma_2\gamma_2\gamma_0\gamma_0\gamma_1\gamma_3, \gamma_2\gamma_2\gamma_3\} \quad (2.1)$$

which may be compared to the exterior sets of gamma matrices in the the Clifford algebras $Cl_{1,3}$ and $Cl_{4,1}$ is

$$\begin{aligned} Ext(Cl_{1,3}) &= \{1, \omega = \gamma_0\gamma_1\gamma_2\gamma_3, \gamma_1\gamma_3, \gamma_0\gamma_2, \gamma_0\gamma_1\gamma_3, \gamma_2, \gamma_0, \gamma_1\gamma_2\gamma_3\} \\ Ext(Cl_{4,1}) &= \{1, \gamma_{12345}, \gamma_{34}, \gamma_{125}, \gamma_{123}, \gamma_{45}, \gamma_{124}, \gamma_{35}\} \end{aligned} \quad (2.2)$$

The action of these operators on the Dirac equation may be given as follows. Let $U = \eta\gamma^0$ be the matrix such that $U\gamma_P U^{-1} = \gamma$ where $\gamma_P^\mu = (\gamma^0, -\vec{\gamma})$. The parity reversed wavefunction $\psi_P(x) = U\psi(x_P)$, with $x_P = (x^0, -x^i)$, would satisfy

$$(i(U\gamma_P U^{-1} \cdot \partial - m)\psi_P(x) = 0. \quad (2.3)$$

The similarity operator for time reversal is $U_T = i\gamma_3\gamma_1$ and $-U_T\gamma_T^* U_T^{-1} = \gamma$, where $\gamma_T = (-\gamma^0, \vec{\gamma})$, and equation for $\psi_T(x) = U_T(x_T)$ with $x_T = (-x^0, x^i)$ is

$$(i(-U_T\gamma_T^* U_T^{-1}) \cdot \partial - m)\psi_T(x) = 0. \tag{2.4}$$

If $B = i\eta_C\gamma^2$, such that $-B\gamma^* B^{-1} = \gamma$, and $\psi_C(x) = B\psi^*(x) = i\eta_C\gamma^2\gamma^0\bar{\psi}^T(x)$,

$$(-iB\gamma^* B^{-1} \cdot \partial - m)\psi_C(x) = 0. \tag{2.5}$$

The condition of the domain of holomorphicity allows the larger class of globally hyperbolic space-times. Each of these manifolds have conformal compactifications that can be embedded in the Einstein static universe. The wedge principle in Minkowski space-time [5] depends on a property following from the exponentiation of Lorentz generators. From the commutation relations are

$$[M_{\mu\nu}, M_{\rho\sigma}] = -ig_{\mu\rho}M_{\nu\sigma} + ig_{\mu\sigma}M_{\nu\rho} + ig_{\nu\rho}M_{\mu\sigma} - ig_{\nu\sigma}M_{\mu\sigma}, \tag{2.6}$$

$$[M_{0j}, M_{0k}] = -ig_{00}M_{jk} + ig_{0k}M_{j0} + ig_{j0}M_{0k} - ig_{jk}M_{00} = -iM_{jk}. \tag{2.7}$$

with the signature of the metric being $(+---)$. Similarly,

$$[M_{0j}, [M_{0j}, M_{0k}]] = -i[M_{0j}, M_{jk}] = -i(ig_{jj})M_{0k} = -M_{0k}. \tag{2.8}$$

By the identities, $e^{e^A B e^{-A}} = e^A e^B e^{-A}$ and $e^A B e^{-A} = B + [A,B] + \frac{1}{2!}[A,[A,B]] + ...$,

$$\begin{aligned} e^{isM_{0j}} e^{itM_{0k}} e^{-isM_{0j}} &= e^{itM_{0k} + istM_{jk} + it\frac{(is)^2}{2!}(-M_{0k}) + ...} \\ &= e^{it[cosh\ s\ M_{0k} + sinh\ s\ M_{jk}]}. \end{aligned} \tag{2.9}$$

Then

$$\begin{aligned} lim_{s\to\pm\infty} e^{isM_{01}} e^{2ire^{-|s|}M_{0j}} e^{-isM_{01}} &= lim_{s\to\pm\infty} e^{2ire^{-|s|}(cosh\ s\ M_{0j} + sinh\ s\ M_{ij})} \\ &= lim_{s\to\pm\infty} e^{ire^{-|s|}((e^{|s|}+e^{-|s|})M_{0j} \pm (e^{|s|}-e^{-|s|})M_{ij}} \\ &= e^{ir(M_{0j} \pm M_{ij})}. \end{aligned} \tag{2.10}$$

The analogue of M_{04} is $\frac{1}{2}(P^0 + K^0)$ in the conformal group of the boundary of conformally compactified anti-de Sitter space. Consider the null bivector $(e, f) \in \mathbb{R}^{2,s} \times \mathbb{R}^{2,s}$ with $e \cdot f < 0$. Let

$$\tilde{W}(e,f) = \{x \in \mathbb{R}^{2,s} | x^2 = R^2,\ e \cdot x > 0,\ f \cdot x > 0\} \tag{2.11}$$

If $\delta_{e,f} = (f \cdot x)e - (e \cdot x)f$,

$$\begin{aligned}(\delta_{e,f})^2 &= [(f \cdot x)e - (e \cdot x)f] \cdot [(f \cdot x)e - (e \cdot x)f] \\ &= -2(e \cdot f)(e \cdot x)(f \cdot x) > 0.\end{aligned} \tag{2.12}$$

since $e \cdot e = f \cdot f = 0$. The wedges can be defined to be

$$\begin{aligned}\tilde{W}_+(e,f) &= \{x \in \tilde{W}(e,f) | (\delta_{e,f}x)^0 > 0\} \\ \tilde{W}_-(e,f) &= \{x \in \tilde{W}(e,f) | (\delta_{e,f}x)^0 < 0\}.\end{aligned} \tag{2.13}$$

The modular group for a wedge algebra is given by a subgroup of the anti-de Sitter group which preserves the wedge, for a wedge $\tilde{W}_+(e,f)$, this is the subgroup of boost in the $e-f$ plane. Furthermore, in $\tilde{W}_+(f,e)$,

$$\begin{aligned}(\delta_{f,e}x)^0 &= [(e \cdot x)f - (f \cdot x)e]^0 \\ &= -[(f \cdot x)e - (e \cdot x)f]^0 < 0\end{aligned} \tag{2.14}$$

if $(\delta_{e,f}x)^0 > 0$. It follows that $\tilde{W}_+(f,e) = \tilde{W}_-(e,f)$. Similarly,

$$\delta_{-e,-f}(-x)^0 = [(-e(-x))(-f) - (-f(-x))(-e)]^0 = [(e(-x))f - (f(-x))e]^0 \tag{2.15}$$

Given that $-e \cdot (-x) > 0$ and $-f \cdot (-x) > 0$, $\tilde{W}_+(-e,-f) = -\tilde{W}_+(e,f)$.

The boundary between the two wedges will now be found. Let $(y_0, \vec{y}) = \frac{(-x_0, \vec{x})}{x_-}$ with $x_- = x_d - x_s$. The limit

$$\begin{aligned}lim_{|x_-|\to\infty}(y_0,\vec{y}) &= \left(0, ..., lim_{|x_-|\to\infty}\frac{|x_d|}{|x_-|}\right) \\ &= \left(0, ..., lim_{|x_-|\to\infty}\frac{|x_- + x_s|}{|x_-|}\right) = (0, ..., 0, 1).\end{aligned} \tag{2.16}$$

Let $e_\mu = (0, ...0, 1)$ and $f_\mu = (0, ..., 0, 1, -1)$. Then

$$\begin{aligned}e \cdot x &= -x_s + x_d > 0 \\ f \cdot x &= -x_s - x_d > 0\end{aligned} \tag{2.17}$$

since $x_d + x_s < 0$ and $x_d^2 - x_s^2 = (x_d + x_s)(x_d - x_s) < 0$. It follows that

$$x_0^2 - x_1^2 - ... - x_{s-1}^2 = R^2 + (x_s^2 - x_d^2) > R^2 \tag{2.18}$$

and

$$\delta_{e,f}x_d = (f \cdot x_d)e - (e \cdot x_d)f = -e - f = -2x_s. \tag{2.19}$$

Let $e_\mu = (1, 1, 0, ..., 0)$ and $f_\mu = (-1, 1, 0, ..., 0)$ such that

$$\begin{aligned} e \cdot x = x_0 - x_1 > 0 \\ f \cdot x = -x_0 - x_1 > 0. \end{aligned} \tag{2.20}$$

The region being covered is

$$R^2 = x_0^2 - x_1^2 - ... - x_{s-1}^2 - x_s^2 + x_d^2 < -x_s^2 + x_d^2 \tag{2.21}$$

and

$$\delta_{e,f} x_0 = (f \cdot x_0)e - (e \cdot x_0)f = -e - f = -2x_1. \tag{2.22}$$

In the five-dimensional embedding space of four-dimensional anti-de Sitter space,

$$\begin{aligned} e_0^2 + e_4^2 = e_1^2 + e_2^2 + e_3^2 \\ f_0^2 + f_4^2 = f_1^2 + f_2^2 + f_3^2, \end{aligned} \tag{2.24}$$

Since

$$\delta_{e,f} x = (f_0 x_0 - f_1 x_1 - f_2 x_2 - f_3 x_3 + f_4 x_4)e - (e_0 x_0 - e_1 x_1 - e_2 x_2 - e_3 x_3 + e_4 x_4)f, \tag{2.25}$$

and $(\delta_{e,f} x)^0 > 0$ if

$$\frac{e_4 x_4 - e_1 x_1 - e_2 x_2 - e_3 x_3}{f_4 x_4 - f_1 x_1 - f_2 x_2 - f_3 x_3} < \frac{e_0}{f_0} \tag{2.26}$$

and $(\delta_{e,f} x)^0 < 0$ if

$$\frac{e_4 x_4 - e_1 x_1 - e_2 x_2 - e_3 x_3}{f_4 x_4 - f_1 x_1 - f_2 x_2 - f_3 x_3} > \frac{e_0}{f_0}. \tag{2.27}$$

The boundary between the two wedges is given by

$$\begin{aligned} \frac{e_4 x_4 - e_1 x_1 - e_2 x_2 - e_3 x_3}{f_4 x_4 - f_1 x_1 - f_2 x_2 - f_3 x_3} = \frac{e_0}{f_0} \\ x_0^2 - x_1^2 - x_2^2 - x_3^2 + x_4^2 = R^2. \end{aligned} \tag{2.28}$$

It remains to be determined if a portion of anti-de Sitter space might contain $\tilde{W}_+$ and $\tilde{W}_-$ simultaneously, thereby preserving invariance under CPT. The order of the third cohomology group over $\mathbb{Z}_2$, $|H^3(M; \mathbb{Z}_2)|$, gives the number of piecewise linear structures [6]. When $H^3(M; \mathbb{Z}_2) = \phi$, $w_3 = 0$ and the manifold admits a global set of three-frames. The parallelizability of the manifold would be equivalent to a flat structure which is necessarily linear. The number of piecewise linear structures also refers to the number of patches of Minkowski space-time and anti-de Sitter regions to cover the manifold.

3. The Charge Conjugation Matrix in Curved Space

The charge conjugation matrix may be defined in curved space. It will be demonstrated that the properties of this matrix necessary for the CPT theorem continue to be valid under parallel transport along a curve in the space when the conditions of a vanishing covariant derivative are satisfied. Let μ be a curved space index, a be a Clifford algebra and A be a tangent space index. The covariant derivative of charge conjugation matrix C_{AB} [3] is

$$\begin{aligned}\nabla_\mu C_{AB} &= \partial_\mu C_{AB} - i\omega_\mu{}^D{}_A C_{DB} - i\omega_\mu{}^D{}_B C_{AD} \\ &= \partial_\mu C_{AB} + i\omega_\mu{}^D{}_A C_{BD} - i\omega_\mu{}^D{}_B C_{AD} \\ &= \partial_\mu C_{AB} + i\omega_{\mu BA} - i\omega_\mu{}^D{}_B C_{AD},\end{aligned} \tag{3.1}$$

where $\omega_\mu{}^A{}_B = \omega^a{}_\mu \Gamma_a{}^A{}_B$ with $\Gamma_a{}^A{}_B = \{\delta^A{}_B, \gamma_\mu{}^A{}_B . \gamma_{\mu\nu}{}^A{}_B, \tilde{\gamma}^A{}_B, \tilde{\gamma}^A{}_B\}$. Covariant constancy of the charge conjugation matrix requires

$$\partial_\mu C_{AB} = i\omega^a{}_\mu (\Gamma_{aAB} - \Gamma_{aBA}). \tag{3.2}$$

Since $\Gamma^{aA}{}_B \Gamma_b{}^B{}_A = 4\delta_a{}^b$,

$$\Gamma^{bBA} \partial_\mu C_{AB} = i\omega^a{}_\mu (4\delta^b{}_a \mp \delta^b{}_a) \tag{3.3}$$

where the minus sign corresponds to $\Gamma_{aAB} = \Gamma_{aBA}$ and the positive sign corresponds to $\Gamma_{aAB} = -\Gamma_{aBA}$. The matrices in the Clifford algebra are

$$\begin{aligned}\Gamma_{aBA} &= \{C_{BA}, \gamma_{\mu BA}, \gamma_\mu, \tilde{\gamma}_{\mu BA}, \tilde{\gamma}_{BA}\} \\ &= \{-C_{AB}, \gamma_{\mu BA}, \gamma_{\mu\nu BA}, \tilde{\gamma}_{\mu BA}, \tilde{\gamma}_{BA}\}\end{aligned} \tag{3.4}$$

The symmetry properties of the matrices may be checked. It can be shown that

$$\begin{aligned}C^A{}_B (\gamma_\mu)^B{}_C (C^{-1})^C{}_D &= -(\gamma_\mu^T)^A{}_D \\ C^{AB} (\gamma_\mu)_B C (C^{-1})^{CD}) &= -(\gamma^T)^{AD} \\ (\gamma_\mu)_{AC} (C^{-1})^C{}_D &= -(\gamma_\mu^T)_{AD} \\ (\gamma_\mu)_{AD} &= (\gamma_\mu^T)_{AD}\end{aligned} \tag{3.5}$$

and

$$
\begin{aligned}
([\gamma_\mu, \gamma_\nu]^T)_A{}^D &= [\gamma_\nu^T, \gamma_\mu^T]_A{}^D \\
&= [-C\gamma_\nu C^{-1}, -C\gamma_\mu C^{-1}]_A{}^D \\
&= (C\gamma_\nu C^{-1} C\gamma_\mu C^{-1} - C\gamma_\mu C^{-1} C\gamma_\nu C^{-1})_A{}^D \\
&= -C_{AB}(\gamma_\mu\gamma_\nu - \gamma_\nu\gamma_\mu)^B{}_C (C^{-1})^{CD} \\
&= -(\gamma_\mu\gamma_\nu - \gamma_\nu\gamma_\mu)_{AC}(C^{-1})^{CD} \\
&= (\gamma_\mu\gamma_\nu - \gamma_\nu\gamma_\mu)_{AC}(C^{-1})^{DC} \\
&= [\gamma_\mu, \gamma_\nu]_A{}^D
\end{aligned}
\tag{3.6}
$$

with the raising and lowering of indices through multiplication by C^{-1} and C respectively. Similarly,

$$
\begin{aligned}
(\tilde{\gamma}_\mu^T)_A{}^D &= -\frac{i}{3!}\varepsilon_{\mu\nu\rho\sigma}[(\gamma^\nu\gamma^\rho\gamma^\sigma)^T]_A{}^D \\
&= -\frac{i}{3!}\varepsilon_{\mu\nu\rho\sigma}[(-C\gamma^\rho C^{-1})(-C\gamma^r ho C^{-1})(-C\gamma^\nu C^{-1})]_A{}^D \\
&= \frac{i}{3!}\varepsilon_{\mu\nu\rho\sigma}(C\gamma^\sigma\gamma^\rho\gamma^\nu C^{-1})_A{}^D \\
&= -\frac{i}{3!}\varepsilon_{\mu\nu\rho\sigma}C_{AB}(\gamma^\nu\gamma^\rho\gamma^\sigma)^B{}_C(C^{-1})^{CD} \\
&= \frac{i}{3!}\varepsilon_{\mu\nu\rho\sigma}(\gamma^\nu\gamma^\rho\gamma^\sigma)_{AC}(C^{-1})^{DC} \\
&= -(\tilde{\gamma}_\mu)_A{}^D
\end{aligned}
\tag{3.7}
$$

and

$$
\begin{aligned}
(\tilde{\gamma}^T)_A{}^D &= \frac{1}{4!}\varepsilon_{\mu\nu\rho\sigma}[(\gamma^\mu\gamma^\nu\gamma^\rho\gamma^\sigma)^T]_A{}^D \\
&= -\frac{1}{4!}(C\gamma^\sigma\gamma^\rho\gamma^\nu\gamma^\mu C^{-1})_A{}^D \\
&= -\frac{1}{4!}\varepsilon_{\mu\nu\rho\sigma}C_{AB}(\gamma^\mu\gamma^\nu\gamma^\rho\gamma^\sigma)^B{}_C(C^{-1})^{CD} \\
&= \frac{1}{4!}\varepsilon_{\mu\nu\rho\sigma}(\gamma^\mu\gamma^\nu\gamma^\rho\gamma^\sigma)_{AC}(C^{-1})^{DC} \\
&= -(\tilde{\gamma})_A{}^D.
\end{aligned}
\tag{3.8}
$$

Let $\sigma_\mu = -\frac{i}{8}(C^{-1})^{BA}\partial_\mu C_{AB}$. Then

$$\begin{aligned}
\partial_\mu\sigma_\nu - \partial_\nu\sigma_\mu &= -\frac{i}{8}[\partial_\mu((C^{-1})^{BA}\partial_\nu C_{AB}) - \partial_\nu(((C^{-1})^{BA}\partial_\mu C_{AB})] \\
&= -\frac{i}{8}[\partial_\mu((C^{-1})^{BA}\partial_\nu C_{AB}) - \partial_\nu((C^{-1})^{BA}\partial_\mu C_{AB}) \\
&\qquad + (C^{-1})^{BA}(\partial_\mu\partial_\nu - \partial_\nu\partial_\mu)C_{AB}] \\
&= -\frac{i}{8}[-(C^{-1})^{BD}\partial_\mu C_{DE}(C^{-1})^{EA}\partial_\nu C_{AB} \\
&\qquad + (C^{-1})^{BD}\partial_\nu C_{DE}(C^{-1})^{EA}\partial_\mu C_{AB}] \\
&= -\frac{i}{8}[-\partial_\mu C^B{}_E\partial_\nu C^E{}_B + \partial_\nu C^B{}_E\partial_\mu C^E{}_B] \\
&= 0.
\end{aligned} \tag{3.9}$$

The commutator of two covariant derivatives on the charge conjugation matrix is

$$(\nabla_\mu\nabla_\nu - \nabla_\nu\nabla_\mu)C_{AB} = -i(\Omega^D{}_{A\mu\nu}C_{DB} + \Omega^D{}_{B\mu\nu}C_{AD}) + T^\rho{}_{\mu\nu}\nabla_\rho C_{AB}. \tag{3.10}$$

When $\nabla_\rho C_{AB} = 0$, $\Omega^D{}_{A\mu\nu}C_{DB} + \Omega^D{}_{B\mu\nu}C_{AB} = 0$ and $\Omega_{BA\mu\nu} + \Omega_{AB\mu\nu} = 0$. Since $\Omega_{AB\mu\nu}$ is symmetric in A, B,

$$\Omega^A{}_{B\mu\nu} = \frac{1}{2}\Omega^\rho{}_{\mu\nu}\gamma_\rho{}^A{}_B + \frac{1}{4}\Omega^{\rho\sigma}{}_{\mu\nu}\gamma_{\rho\sigma}{}^A{}_B. \tag{3.11}$$

and the set of Clifford algebra matrices $\{\gamma_\rho, \gamma_{\rho\sigma}\}$ generate $SO(3,2,\mathbb{C})$ [3].

The conformal transformation of the condition $\nabla_\mu C_{AB} = 0$ is equivalent if C_{AB} is viewed as a scalar. However, when it is considered to be a charge metric with a covariant derivative that contains a spin connection, it is acceptable to have

$$\tilde{\nabla}_C C_{AB} = \nabla_C C_{AB} + \Upsilon_A C_{CB} + \Upsilon_B C_{AC} \tag{3.12}$$

where $\Upsilon_A = \nabla_A log\ \Xi$ with Ξ being the conformal factor. Vanishiung of the covariant derivative of the charge conjugation matrix in the conformally related metric requires

$$\nabla_C C_{AB} + \Upsilon_A C_{CB} + \Upsilon_B C_{AC} = 0 \tag{3.13}$$

or

$$\partial_C C_{AB} - i\omega^a{}_C(\Gamma_{aAB} - \Gamma_{aBA}) + \Gamma_A C_{CB} + \Gamma_B C_{AC} = 0. \tag{3.14}$$

Multiplication by a Clifford algebra matrix gives

$$\Gamma^{bBA}\partial_C C_{AB} - i\omega^a{}_C\Gamma^a{}_C(\Gamma_{aAB} - \Gamma_{aBA}) + \Gamma^{bBA}(\Upsilon_A C_{CB} + \Gamma_B C_{AC}) = 0. \tag{3.15}$$

The spin connection term is nonvanishing when Γ^{bBA} is antisymmetric, which would cause the last term to be nonvanishing.

The solution to this equation is similar therefore to that of $\nabla_\mu C_{AB}$ in the uncompactified space-time. The conformal transformations of σ_μ and $\pi^\rho{}_\sigma = \frac{i}{8}\tilde{\gamma}^{\rho BA}\partial_\mu C_{AB}$ are given by

$$\begin{aligned}\tilde{\sigma}_C &= -\frac{i}{8}(C^{-1})^{BA}\partial_C C_{AB} - \frac{i}{4}(C^{-1})^{BA}\Upsilon_A C_{CB} \\ \tilde{\pi}^D{}_C &= -\frac{i}{8}\tilde{\gamma}^{DBA}\partial_C C_{AB} + \frac{i}{4}\tilde{\gamma}^{DBA}\Upsilon_A C_{CB}.\end{aligned} \tag{3.16}$$

The commutator of the covariant derivatives of the charge conjugation matrix is

$$(\{\tilde{\nabla}_\mu\tilde{\nabla}_\nu - \tilde{\nabla}_\nu\tilde{\nabla}_\mu)C_{AB} = -i(\tilde{\Omega}^D{}_{A\mu\nu}C_{DB} + \tilde{\Omega}^D{}_{B\mu\nu}C_{AD)} + T^\rho{}_{\mu\nu}\tilde{\nabla}_\rho C_{AB}. \tag{3.17}$$

When $\tilde{\nabla}_\rho C_{AB} = 0$, $\tilde{\Omega}_{BA\mu\nu} = \tilde{\Omega}_{AB\mu\nu}$ and

$$\tilde{\Omega}_{\mu\nu} = \frac{1}{2}\tilde{\Omega}^\rho{}_{\mu\nu}\gamma\rho^A{}_B + \frac{1}{4}\tilde{\Omega}^{\rho\sigma}{}_{\mu\nu}\gamma_{\rho\sigma}{}^A{}_B. \tag{3.18}$$

The holonomy group can be included in $SO(3,2,\mathbb{C})$ or the covering group $Sp(4;\mathbb{C})$. There are ten other equations for the charge conjugation matrix and scale factor

$$\begin{aligned}&\Gamma^{bBA}\partial_C C_{AB} = 0 \\ &-C_{AB}\partial_C\Gamma^{bBA} = -C_{AB}\nabla_C\Gamma^{bBA} = -\nabla_C\Gamma^b{}_A{}^A \\ &\qquad = 0\end{aligned} \tag{3.19}$$

either through Tr $\Gamma^b = 0$ or covariant constancy of the matrix.

4. An Action on a Curved Space admitting a Covariantly Constant Charge Conjugation Matrix

Consider the scale transformations

$$\begin{aligned}C'_{AB} &= re^{i\theta}C_{AB} \\ (C'^{-1})^{AB} &= \frac{e^{-i\theta}}{r}(C^{-1})^{AB}.\end{aligned} \tag{4.1}$$

Then

$$\begin{aligned}\sigma'_\mu &= -\frac{i}{8}(C'^{-1})^{BA}\partial_\mu C'_{AB} \\ &= -\frac{i}{8}\frac{e^{-i\theta}}{r}(C^{-1})^{BA}\partial_\mu(re^{i\theta}C_{AB}) \\ &= -\frac{i}{8}((C^{-1})^{BA}\partial_\mu C_{AB} + 4\frac{\partial_\mu r}{r} + 4i\partial_\mu\theta) \\ &= \sigma_\mu - \frac{i}{2}\partial_\mu(ln\ r) + \frac{1}{2}\partial_\mu\theta.\end{aligned} \tag{4.2}$$

If $\sigma_\mu = \varphi_\mu + i\chi_\mu$,

$$\begin{aligned}\varphi'_\mu &= \varphi_\mu + \frac{1}{2}\partial_\mu\theta \\ \chi'_\mu &= \chi_\mu - \frac{1}{2}\partial_\mu(ln\ r).\end{aligned} \tag{4.3}$$

Since the scalar part of the curvature remains zero, an action defined by the spin curvature would be invariant under these scale transformations. The covariant derivatives of the curved space-gamma matrices are

$$\begin{aligned}\nabla_\mu\gamma_\nu &= \phi\gamma_{\mu\nu} \\ \nabla_\mu\gamma_{\rho\sigma} &= \nabla_\mu\left(\frac{i}{2}[\gamma_\rho,\gamma_\sigma]\right) = \frac{i}{2}[\nabla_\mu\gamma_\rho,\gamma_\sigma] + \frac{i}{2}[\gamma_\rho,\nabla_\mu\gamma_\sigma].\end{aligned} \tag{4.4}$$

The commutator of the gamma matrix with the spin curvature tensor in $\nabla_\mu\gamma_\rho$ is given by

$$\begin{aligned}i[\Omega_{\mu\nu},\gamma_\rho] &= i\frac{1}{2}[\Omega^\sigma{}_{\mu\nu}\gamma_\sigma,\gamma_\rho] + i\frac{1}{4}[\Omega^{\sigma\tau}{}_{\mu\nu}\gamma_{\sigma\tau},\gamma_\rho] \\ &= \Omega^\sigma{}_{\mu\nu}\gamma_{\sigma\rho} + \frac{i}{4}\Omega^{\sigma\tau}{}_{\mu\nu}[\gamma_{\sigma\tau},\gamma_\rho] \\ &= \Omega^\sigma{}_{\mu\nu}\gamma_{\sigma\rho} + \frac{i}{4}\Omega^\sigma{}_\nu\cdot 2i(g_{\tau\rho}\gamma_\sigma - g_{\sigma\rho}\gamma_\tau) \\ &= \Omega^\sigma{}_{\mu\nu} - \Omega^\sigma{}_{\rho\mu\nu}\gamma_\sigma.\end{aligned} \tag{4.5}$$

The curvature equals

$$R^\sigma{}_{\rho\mu\nu} = -\Omega^\sigma{}_{\rho\mu\nu} - \phi^2(g_{\rho\mu}\delta^\sigma{}_\nu - g_{\rho\nu}\delta^\sigma{}_\mu) \tag{4.6}$$

and the torsion is

$$T^\sigma{}_{\mu\nu} = -\frac{1}{\phi}(\Omega^\sigma{}_{\mu\nu} - (\partial_\mu\phi\delta^\sigma{}_\nu - \partial_\nu\phi\delta^\sigma{}_\mu) \tag{4.7}$$

If $\phi \to 0$, $R^\sigma{}_{\rho\mu\nu} \to -\Omega^\sigma{}_{\rho\mu\nu}$ and $T^\sigma{}_{\mu\nu}$ either vanishes or becomes infinite unless $\Omega^\sigma{}_{\mu\nu} - (\partial_\mu\phi\delta^\sigma{}_\nu - \partial_\nu\phi\delta^\sigma{}_\mu) \propto \phi$.

By dimension counting, $R^{\sigma}{}_{\rho\mu\nu} \sim (length)^{-2} \sim (mass)^2$ and $T^{\sigma}{}_{\mu\nu} \sim (mass)$ such that

$$\Omega^{\sigma}{}_{\mu\nu} = k\phi^2\gamma^{\sigma}\gamma_{\mu\nu} + (\partial_{\mu}\phi\delta^{\sigma}{}_{\nu} - \partial_{\nu}\phi\delta^{\sigma}{}_{\mu}) \tag{4.8}$$

and $T^{\sigma}{}_{\mu\nu} \to 0$ as $\phi \to 0$. The Ricci scalar is

$$R = -\Omega - \phi^2(\delta^{\nu}{}_{\mu}\delta^{\mu}{}_{\nu} - g_{\rho\nu}g^{\rho\nu}\delta^{\sigma}{}_{\mu}\delta^{\mu}{}_{\sigma}) = -\Omega + 12\phi^2 \tag{4.9}$$

and

$$-\int d^4x\sqrt{-g}\Omega = \int d^4x\sqrt{-g}(R - 12\phi^2). \tag{4.10}$$

By Eq.(4.7),

$$\begin{aligned}\Omega^{\sigma}{}_{\mu\nu}\Omega_{\sigma}{}^{\mu\nu} &= (-\phi T^{\sigma}{}_{\mu\nu} + (\partial_{\mu}\phi\delta^{\sigma}{}_{\nu} - \partial_{\nu}\phi\delta^{\sigma}{}_{\mu}))(-\phi T_{\sigma}{}^{\mu\nu} + (\partial^{\mu}\phi\delta_{\sigma}{}^{\nu} - \partial^{\nu}\phi\delta_{\sigma}{}^{\mu})) \\ &= \phi^2 T^{\sigma}{}_{\mu\nu}T_{\sigma}{}^{\mu\nu} - 2\phi T^{\sigma}{}_{\mu\sigma}\partial^{\mu}\phi + 6\partial^{\mu}\phi\partial_{\mu}\phi\end{aligned} \tag{4.11}$$

and

$$\int d^4x\sqrt{-g}\Omega^{\sigma}{}_{\mu\nu}\Omega_{\sigma}{}^{\mu\nu} = \int d^4x\sqrt{-g}[\phi^2 T^{\sigma}{}_{\mu\nu}T_{\sigma}{}^{\mu\nu} - 2\phi T^{\sigma}{}_{\mu\sigma}\partial^{\mu}\phi + 6\partial^{\mu}\phi\partial_{\mu}\phi]. \tag{4.12}$$

Adding the two integrals gives

$$\int d^4x\sqrt{-g}[R - 12\phi^2 + \phi^2 T^{\sigma}{}_{\mu\nu}T_{\sigma}{}^{\mu\nu} - 2\phi T^{\sigma}{}_{\mu\sigma}\partial^{\mu} + 6\partial^{\mu}\phi\partial_{\phi}]. \tag{4.13}$$

Setting $T^{\sigma}{}_{\mu\nu} = 0$ yields

$$\int d^4x\sqrt{-g}[R + 6\partial^{\mu}\phi\partial_{\mu}\phi - 12\phi^2]. \tag{4.14}$$

which is the action of a scalar field minimally coupled to gravity. Let $T^{\sigma}{}_{\mu\nu} = \phi H^{\sigma}{}_{\mu\nu}$. Then the action is

$$\int d^4x\sqrt{-g}[R - 12\phi^2 + \phi^4 H^{\sigma}{}_{\mu\nu}H_{\sigma}{}^{\mu\nu} - 2\phi^2 H^{\sigma}{}_{\mu\sigma}\partial^{\mu}\phi + 6\partial^{\mu}\phi\partial_{\mu}\phi]. \tag{4.15}$$

When $H_{\mu\nu\rho}$ is the anti-symmetric field strength of a two-index field $B_{\mu\nu}$, the integral is

$$\int d^4x\sqrt{-g}[R - 12\phi^2 + \phi^4 H^{\sigma}{}_{\mu\nu}H_{\sigma}{}^{\mu\nu} + 6\partial^{\mu}\phi\partial_{\mu}\phi]. \tag{4.16}$$

Since $\Omega^{\sigma}{}_{\mu\nu}$ is the spin torsion and $T^{\sigma}{}_{\mu\nu} = \frac{1}{2}(\Gamma^{\sigma}{}_{\mu\nu} - \Gamma^{\sigma}{}_{\nu\mu})$ can be generalized to $\frac{1}{2}(\Gamma^{\sigma}{}_{\mu\nu}(x) - \Gamma^{\sigma}{}_{\nu\mu}(y))$, one might consider an action of the form

$$-\int d^4x\sqrt{-g}\Omega + \int d^4x\sqrt{-g(x)}\int d^4x\sqrt{-g(y)}\Omega^{\sigma}{}_{|m\omega}(x)K(x-y)\Omega_{\sigma}{}^{\mu\nu}(y). \tag{4.17}$$

The second integral is

$$\int d^4x\sqrt{-g(x)}\int d^4y\sqrt{-g(y)}\Big\{\phi(x)T^{\sigma}{}_{\mu\nu}K(x-y)\phi(y)T_{\sigma}^{\mu\nu}(y) - \phi(x)T^{\sigma}{}_{\mu\nu}(x)K(x-y)(\partial^{\mu}\phi(y)\delta_{\sigma}{}^{\nu}-\partial^{\nu}\phi(y)\delta_{\sigma}{}^{\mu}) - (\partial_{\mu}\phi(x)\delta^{\sigma}{}_{\nu}-\partial_{\nu}\phi(x)\delta^{\sigma}{}_{\mu}K(x-y)\phi(y)T_{\sigma}{}^{\mu\nu}(y) + 6\partial^{\mu}\phi K(x-y)\partial_{\mu}\phi(y)\Big\}. \tag{4.18}$$

When $K(x-y)$ is a symmetric function of x and y, it equals

$$\int d^4x\sqrt{-g(x)}\int d^4y\sqrt{-g(y)}\Big\{\phi(x)T^{\sigma}{}_{\mu\nu}(x)K(x-y)\phi(y)T_{\sigma}{}^{\mu\nu}(y) - 2\phi(x)T^{\sigma}{}_{\mu\nu}(x)K(x-y)(\partial^{\mu}\phi(y)\delta_{\sigma}{}^{\nu}-\partial^{\nu}\phi(y)\delta_{\sigma}^{\mu}) + 6\partial^{\mu}\phi(x)K(x-y)\partial_{\mu}\phi(y)\Big\}. \tag{4.19}$$

Nonlocal actions of scalar field are known to generate new charges that exist over a finite time interval as a result of nonconservation of the local charges.

5. Conclusion

The proof of the CPT theorem depends on several theorems in constructive quantum field theory. The existence of a domain of holomorphicity is valid for globally hyperbolic space-times. The wedge principle has been proven for anti-de Sitter space, where the boundary between the wedges has been described in the five-dimensional embedding space. It requires the existence of piecewise linear structure on the manifold, which would follow from the vanishing of the $H^3(M;\mathbb{Z}_2)$. The discrete operators representing charge conjugation, parity and time reversal may be defined on curved spaces. The condition of a vanishing covariant derivative is found to require the holonomy generators to belong to the complexification of the anti-de Sitter isometry group. The spin curvature and spin torsion on these manifolds have been evaluated and for the basis for an action describing the coupling of a scalar and anti-symmetric two-index field to gravity.

References

[1] H. S. Snyder, Quantized Space-Time, Phys. Rev. **71** (1947) 38-41.

[2] C. N. Yang, On Quantized Space-Time, Phys. Rev. **72** (1947) 874.

[3] J. P. Crawford, Spinor Metrics, Spin Connection Compatibility and Spacetime Geometry from Spin Geometry, Class. Quantum Grav. **20** (2003) 2945-2962.

[4] L. F. Abbott and S. Coleman, The Collapse of an Anti-de Sitter Bubble, Nucl. Phys. **B259** (1985) 170-174.

[5] H. J. Borchers, On Poincare Transformations and the Modular Group of the Algebra Associated with a Wedge, Lett. Math. Phys. **46** (1998) 295-301.

[6] R. Geoghegan and W. E. Haver, On the Space of Piecewise Linear Homeomorphisms of a Manifold, Proc. Amer. Math. Soc. **55** (1976) 145-151.

STUDY OF COMBUSTION OF COAL WITH MAGNEGAS AS AN ADDITIVE FOR IMPROVING COMBUSTION EFFICIENCY: A REVIEW OF PRESENT SCENARIO AND FUTURE SCOPE

Sachin Wazalwar[1], Vijay Tangde[2], Anil Bhalekar[2]
[1]Department of Applied Chemistry
Rajiv Gandhi College of Engineering
Research & Technology, Chandrapur
[2]Department of Chemistry
Rashtrasant Tukadoji Maharaj Nagpur University
Amravati Road Campus, Nagpur

Received November 6, 2016

Abstract

Fossil fuels are contributing the largest share in meeting up energy demands of urban lifestyle across the globe. May it be gasoline or coal, all sort of fossil fuels are drilled out of earth crust to burn on the earth surface creating a huge burden on air quality. Incomplete combustion of fossil fuels causes pollution of carbon monoxide and other gases. It also eats away the breathable oxygen from the atmosphere. Rampant use of coal in power sector causes problems adding to the global warming phenomenon. Many of the coal powered thermal power plants are used beyond its stipulated life span, with reduced efficiency, which results in incomplete combustion of fuel and emission of carbon monoxide. Santilli's discovery of magnecules is a boon in considerably reducing the above stated serious problems being faced by the mankind in particular and the adverse effects on the overall health of the earth in general. Amongst various proposed remedies the magnecules and magnehydrogen are seen to be best additives to fossil fuels which can effectively enhance the combustion efficiency of fossil fuels. The present paper discusses the enhancement in combustion efficiency of fossil fuels in terms of increased utility of carbon and improved quality of emission reducing the amount of obnoxious gases.

Based on invited talk at SIPS 2016, Santilli International Symposium on Sustainable Applications, Hainan Island, China, November 6 -10, 2016.

Copyright © 2017 by Hadronic Press, Inc., Palm Harbor, FL 34684, USA

INTRODUCTION

The new clean combustible gas, magnegas [1,2], developed by Italian-American Scientist Ruggero Maria Santilli [1,2], posses precisely a magnecular structure from which it has got its name. Clean water or even the sewage water can be converted to magnegas by systematic introduction to electric arc generating a high current in microseconds [3-5]. The gaseous product, so obtained, is unusual in behavior from its physical and chemical properties point of view [3]. It is a kind of short range polymeric product with two molecules of gas being bonded by a magnetic force of attraction than the conventional covalent bond. Structural detail of the properties of this gas is still a subject of discussions for about a decade. Spectroscopic results and their interpretations are of great interest of the chemists. This is mainly due to the characteristics of this new matter which are beyond the scope of interpretation of many spectroscopic and chromatographic instruments available in market. But apart from all these discussions, the most striking feature of Magnegas is that it is proving to be a promising fuel of the 21st century. So far, the success of this fuel is reported as alternative fuel in automobile sector [3-5]. Some high energy gas fuelled fields like metal cutting tools are also working successfully on this fuel.

Another potential direction of energy studies of magnegas is that the hybrid of this fuel with fossil fuels is expected to show enhanced combustion efficiency. Magnetized hydrogen from magnegas burns with elevated temperature and helps in complete combustion of carbon in coal and hydrocarbon in gasoline. Thus Hy-Diesel, Hy-Gasoline, Hy-Coal are the new age terms coined by Santilli [5].

The scope of the present paper is to discuss the possibilities of a technology to use magnegas as an additive to coal in order to enhance the combustion efficiency of coal. Another equally important aspect of study is to estimate the environmental benefits of using magnegas and/or magnehydrogen as additive to reduce the emission of green house gases and limit suppress the global warming phenomenon in its long term use.

PRESENT GLOBAL ENERGY SCENARIO

The whole world is thriving for energy in terms of electricity for industrial and agricultural development. Electricity is one of the fundamental forms of energy of modern world. From industrial production to basic amenities and luxurious life, everything is dependent on electricity. Major part of the electricity comes from coal and nuclear power plants. But rampant use of fossil fuels like coal is a cause of worry for future. A water heater uses about two tons of coal a year. And a refrigerator consumes half-ton a year [6-8]. Even though many of us don't ever see coal, we use several tons of it every year! The rapid depleting reservoirs of coal along with dirty nature of this cheap fuel are a cause of worry for whole world due to increasing pollution and global warming from emitted gases.

Use of fossil fuels like gasoline, diesel and coal is causing a huge loss to the ecosystem across entire globe. These fuels are limited in stock and the way we are burning them, is leaving them incompletely burnt. Thus it is a dual loss in terms of energy as well environmental damage. Automobile and electricity generation are the two important sectors using large quantity of fossil fuel. Out of the two, electricity generation is at the top! Coal-fired power plants are largest emitter of majority green house gases. Switching over to natural gas is one of the possible ways for coal fired power plants, but limited supply of natural gas does not meet the requirements in developing countries. In such case, coal remains favorite fuel for generation of power in most of the largely populated countries. Coal-fired power plants currently fuel 41% of global electricity [7-10].

Coal produces 44 % of the total electricity of United States and also contributes as single largest source of pollution [7]. 68% of the total electricity of India comes from coal fired power plants [8,10]. In US, up to 353 coal-fired generators in 31 states (out of a national total of 1,169) are

ripe for retirement, equal to a total of 59 gigawatt of power generating capacity. Collectively they represent as much as 18 percent of the country's coal-generating capacity and approximately six percent of the nation's power [8,9]. In 2011, approximately 42 percent of United State's electricity was produced by burning coal [7]. But by 2012, more than three-quarters of coal-fired power plants of U.S. have outlived their 30-year life span, with 17 percent being older than half a century. Most are inefficient, operating far below both their power generation potential and the most efficient coal units on the power grid. More or less similar is the situation in all other nations obtaining large share of the electricity from coal.

PROBLEM WITH COMBUSTION OF FOSSIL FUELS

In all, the fossil fuel combustion is a serious cause for damage of environmental conditions. Limited and steeply depleting sources of fossil fuels along with pollution due to combustion are causing great worry for the future health scenario of all living beings.

The extremely serious environmental problems caused by the disproportionate combustion of fossil fuels are well documented by Prof. R. M. Santilli as follows [4]:

(1)The combustion of fossil fuels releases in our atmosphere about sixty millions metric of tons carbon dioxide CO_2 per day that are responsible for the first large environmental problem known as "global warning" or "green house effect" [10,11]. Of these only 30 million metric tons are estimated to be recycled by our ever decreasing forests. This implies the release in our atmosphere of about thirty million metric tons of unrecycled green house gases per day, which release is the cause of the "global warming" now visible to everybody through climactic episodes such as floods, tornadoes, hurricanes, etc. of increasing catastrophic nature.

(2) The combustion of fossil fuels causes the permanent removal from our atmosphere of about 21 million metric tons of breathable oxygen per day, a second, extremely serious environmental problem known as "oxygen depletion."[4]. Even though not disclosed by political circles and newsmedia, the very admission of an "excess" CO_2 in our atmosphere (that is, CO_2 no longer recycled by plants) is an admission of oxygen depletion because the "O_2 in the excess CO_2" was originally breathable oxygen. Hence, by recalling the atomic weight of CO_2 and O_2, we have the value $32/44 \times 30 \times 10^6 = 21.8 \times 10^8$ tons of lost oxygen per day.

(3)The combustion of fossil fuels releases in our atmosphere about fifteen million metric tons of carcinogenic and toxic substances per day [4]. This third, equally serious environmental problem is euphemistically referred to by the news media as "atmospheric pollution", while in reality it refers to the primary source of the widespread increase of cancer in our societies. For instance, it has been established by various medical studies (generally suppressed by supporters of the oil cartel) that unless of genetic origin, breast cancer is due to the inhaling of carcinogenic substances in fossil fuels exhaust. These studies have gone so far as to establish that breast cells are very receptive to a particular carcinogenic substance in fossil fuel exhaust. After all, responsible citizens should remember and propagate (rather than myopically suppress) the fact that the U. S. Environmental Protection Agency has formally admitted that diesel exhaust is carcinogenic.

PROBLEM WITH COMBUSTION OF COAL FOR POWER

Combustion of coal is associated with emission of significant quantity of volatile matter and carbon monoxide. This is a loss in terms of energy and also causing pollution due to release of green house gases (CHs and CO).

As listed in Annexure A of Kyoto Protocol, the six major greenhouse gases are Carbon dioxide (CO_2); Methane (CH_4); Nitrous oxide (N_2O); Hydro fluorocarbons (HFCs); Per-fluorocarbons (PFCs); and Sulphur hexafluoride (SF_6) [9]. Out of these six gases, three most common gases in significantly large quantity are emitted from coal fired power plants. In burning fossil fuel like coal, about 60% of the energy in the original fuel is literally thrown through the fluke, and so is

the related cost, due to the notoriously poor combustion [8]. Thus, majority of the combustible and energetic content is lost unutilized in the process.
In addition, majority of the old power plants lack essential modern pollution controls, so they damage public health. The sulfur they emit causes acid rain. The mercury they release poisons waterways and fish and causes neurological damage in children [9]. The soot they emit creates smog that causes lung disease, premature death, and triggers asthma attacks [10,11]. Burning coal demands billions of gallons of cooling water from vulnerable rivers and lakes, and leaves behind vast quantities of toxic ash residuals, while coal mining causes extensive and lasting damage both to human health and the natural environment [12].
If we look into the exact process through a deeper eye, it is seen that the coal, when heated up, gets converted into the carbon monoxide at first. Then the CO is converted to CO_2. Also, at the same time, some of the carbon combines with hydrogen to form volatile HCs. CO and HCs being gases, tend to escape out of the combustion chamber where there is a need to convert maximum gaseous content into their final oxidation products to get maximum energy. However, in reality, only part of the carbon monoxide is converted into its dioxide and a very few of the volatile matter is burnt. Thus the emission is largely containing carbon monoxide and HCs which are a waste of energy on one side and a cause of pollution and global warming on the other side.
Conversion of CO to CO_2 in atmosphere causes thermal pollution due to exothermic nature of this conversion. Depletion of breathable oxygen in the ambient air adds to the gravity of the problem. 18 to 20 ton of coal is burnt for generation of 1 MW energy. Thus a 2000 MW power plant burns about 40000 ton of coal per day and release a huge volume of gases in atmosphere.
Initial generation of heat in furnace causes formation of volatile matter. Further conversion of coal leads to formation of CO. Both of these gases are vulnerable to move upward and thus cause release along with emission. Although, black carbon is not directly emitted from the coal fired power plant in routine condition, but the possibility cannot be ruled out for smaller coal burning units like potteries and brick production.
Most of the Indian coal-fired power plants emit about 1 ton CO_2 per MW. Observed range of data obtained from Central Electricity Authority (CEA) for the year 2012-13 for all coal-fired power plants show a range of 0.9 to 2.1 ton specific emission of CO_2. Despite all the evils associated with combustion of coal, it can't be discarded altogether because of the issues of economy associated with it. Evaluation of the economic competitiveness of coal generators and comparison of the cost of electricity from individual coal-fired electricity generating units with the cost of electricity generated from an average natural gas power plant shows that cleaning the combustion of coal in coal fired power plants will be costlier. Specifically, if a coal-fired generator— after installing any needed pollution controls—would be more expensive to operate than a typical cleaner-burning and more efficient natural gas combined-cycle [6].
A graphical representation of the SPM emitted from a power plant over a period of 4 years show the exact scenario of emission.
Figure 1 and Figure 2 depict 20 readings from a period of about 4 years showing the emission exceeding prescribed limits on many occasions. Both of these units are about 30 years old.
Despite numerous problems associated with combustion of coal, still we cannot think of scrapping all coal fired power plants, because coal is the cheapest of all other energy sources. Being solid, it is easy in handling and operations as compared to natural gas which is cleaner to coal. Further, location of coal reservoirs adds a lot to the geographical restrictions of the economy of coal fired power plants. In India, there are large coal reservoirs available in central Indian states. These coal reservoirs invite coal fired power plants to these regions and no other alternate fuel can meet up this requirement in any other part of the country.

Table 1. Year wise electricity generation and CO_2 emission from coal fired power plants in India [15].

Sr. No.	Year / Factor	2008-09	2009-10	2010-11	2011-12	2012-13
1	**Net Generation (GWh)**	467298.3811	495,343	516,877	562,991	633,793
2	**Absolute Emissions (tCO_2)**	510877863.2	534154395.8	554,435,897	596,550,869	666,699,576
3	**Specific Emissions ($t\ CO_2/MWh$)**	1.18	1.17	1.19	1.14	1.14

Thus it is more positive approach to think of a cleaner additive to coal than going for alternate fuel. Additive which is not restricted to any geographical area will be more helpful for economy and cleaner process of coal fired power plants.

It is known in chemistry that hydrogen is the best additive to improve combustion, with consequential improvement of the environmental quality of the exhaust. In fact, hydrogen has the biggest flame temperature and speed among all known fuels. Consequently, the injection of hydrogen as an additive in the flame of fossil fuels burns the uncombusted component of the exhausts in a way proportional to the used percentage of hydrogen. But, use of hydrogen as additive has several limitations and restrictions. Limitations are mainly due to cost and difficulty in handling.

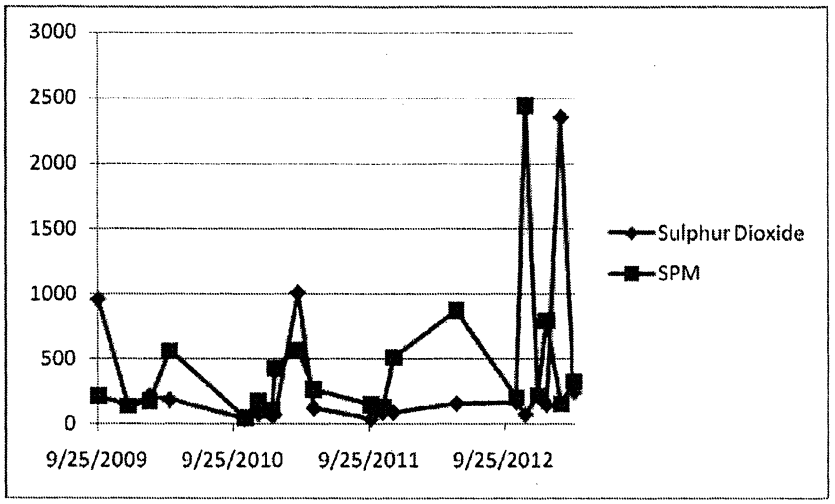

Figure 1. Graphical representation of emission of SO_2 and SPM from a 250 MW unit-1 of Chandrapur Super Thermal Power Plant. The X-axis showing dates of collection and Y-axis represents emission in mg/Nm^3 (Year of commissioning-1983)

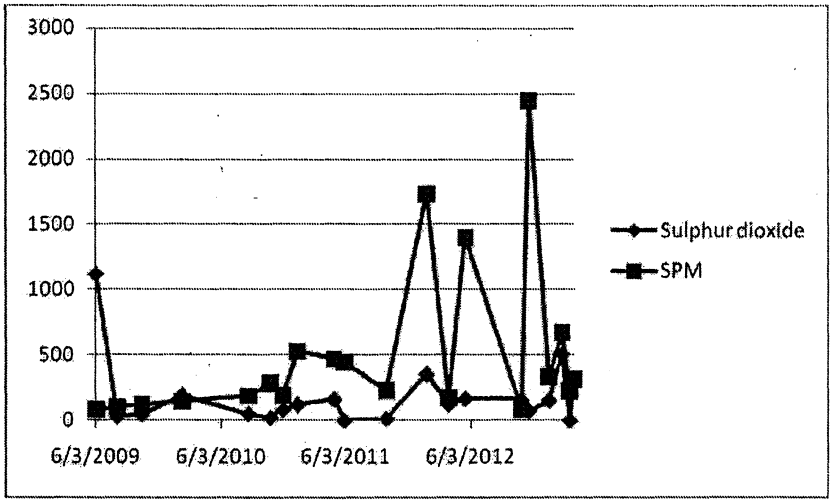

Figure 2. Graphical representation of emission of SO_2 and SPM from a 250 MW unit-2 of Chandrapur Super Thermal Power Plant. The X-axis showing dates of collection and Y-axis represents emission in mg/Nm^3 (Year of commissioning-1984)

MAGNEGAS- THE BEST OPTION FOR HYDROGEN AS ADDITIVE AT PRESENT

Looking at the energy requirement of world and our dependency on coal for power, it seems to have no direct alternative any next morning. Continuing with the same scenario of combustion of this dirty fuel will create a miserable environmental situation in next one or two decades only.
Coal is and will be the major and cheap source of power generation in many countries. India, a developing country, and a $1/6^{th}$ population of globe, is largely dependent on coal as a major source of energy for generation of electricity. Out of 1,50,000 MW of total energy capacity, approximately 78,000 MW comes from coal fired thermal power plants. These power plants are mainly situated in places where there is ample coal under the earth surface. Burning coal itself is a dirty process with heavy emission of green house gases. Further coal mining has its own adverse effect on land and water in the area which ultimately ruins the agriculture and causes rehabilitation of people. One of the serious problems in burning coal for electricity is the incomplete combustion that results in loss of at least 30% fuel as uncombusted hydrocarbon, hence lesser thermal efficiency and increased cleaning cost of exhaust system and pollution control. As the data of emission shows significant quantity of carbon monoxide emitting out, it is a multi directional loss to the environment. Excavation of fossil fuel itself is against environmental balance and incomplete combustion causes decreased combustion efficiency along with heavy release of poisonous gas, carbon monoxide. Further conversion of carbon monoxide to oxide in the atmosphere is causing thermal pollution. Hence the priority need is clean combustion of the existing fossil fuel and utilizing the maximum available carbon of the fuel. This can be done by injecting magnegas [3, 4, 13] along with the conventional fossil fuel.
The property of magnecules[3,4] to undergo magnecular combustion[1-4] with high energy output is due to weak magnecular bond. This is exploited for the industrial development of new clean fuels such as magnegas. MagneGas is a good additive for the cleaning of fossil fuel exhaust because:

1. When produced from the recycling of water-base liquid wastes, magnegas contains about 65% hydrogen, thus qualifying as an effective additive to improve fossil fuel combustion;
2. The remaining components of magnegas are rich in oxygen, thus helping to alleviate the large oxygen depletion caused by fossil fuel combustion and

The cost of magnegas is competitive over that of fossil fuel, particularly when produced by the electric power plants, because of the reduced cost of electricity and the possibility of producing magnegas from the recycling of city sewage, with a consequential income that covers most of the operating costs of PlasmaArcFlow Recyclers.
Therefore, it is a high time to come up with a realistic solution to clean the combustion of coal in power and other small coal using sectors like brick making to cement and metallurgical industries.
The only viable option is to add a suitable additive for cleaner co combustion process. Pure hydrogen gas can meet up the thermodynamic requirements but it is not viable due to safety and economical reasons. Therefore, magnegas can prove to be a better additive for co combustion with coal.
Magnegas can be synthesized on site by using any source of water and applying the famous technique pioneered by Prof. R. M. Santilli.

The magnegas can be used along with coal as additive for effective co combustion. Flame temperature of magnegas is upto 10500 F which helps in combustion of all the carbon and traces of nitrogen and sulphur to their final oxidation products in the combustion chamber itself. This ensures complete combustion of carbon to generate maximum energy. It also helps to burn all the volatile matter formed due to internal reaction of carbon and hydrogen from coal. Localized combustion of all combustible elements from coal is the main objective which can be best fulfilled by using magnegas as an additive for co combustion with coal. Some experiments are already conducted by Magnegas Corp. in collaboration with various partners across Europe, U.S. and Australia and they have reported a positive outcome of the experimental trials [3].
Magnegas achieves a flame temperature of about 3800^{O}C. This high temperature helps in combustion of all combustible matter, thus enhancing the energy output of process. Further, it is also observed in the earlier studies that co combustion of magengas has reduced the carbon dioxide emission by about 30 to 40% and reduced emission of carbon monoxide [3].
Below mentioned is a tabulated interpretation of the results of combustion of coal in comparison with co-combustion of magnegas and coal.

Table 1. Comparison of flue gases and stack temp in combustion of coal and coal+magnegas, Courtesy: www.magengas.com/reports/cocombustion [3].

Factor	**Coal**	**Coal+Magnegas**
Oxygen	11%	13%
Carbon Dioxide(CO2)	15%	9%(40%)
Carbon monoxide (CO)	58ppm	28ppm (52%)
Nitrous oxide (NOx)	160ppm	46ppm (71%)
Stack temp	3710^{0} C	~2990^{0} C
	6700 F	5400 F

As magnehydrogen would be more energetic than magnegas due to resemblance of MH with hydrogen, magnehydrogen can be used in place of magnegas as a refinement to the co combustion experiment. The first independent experimental verification of the new species of Santilli MagneHydrogen was achieved in October 11, 2011, by D. Day [14-16] of the Eprida Laboratory, 3020 Canton Road Suite 104, Marietta, GA, via the use of a VSA station for the separation of MH from MG, the use of a GC-TCD for the measurement of the percentage of hydrogen in the separated gas, and the use of conventional methods for the measurement of molecular weight. In this way, Day achieved a species of MH with about 97.5% pure Hydrogen, while having 3.89 times the specific weight of H_2, and a consequential energy content of 1167 BTU/scf.

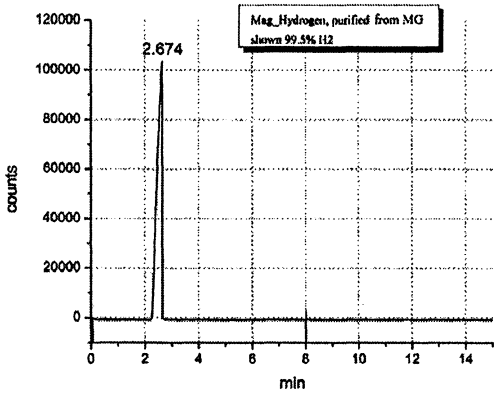

Figure 3. GC-TCD scan of MagneHydrogen showing no appreciable difference of MH with pure hydrogen [13].

As reported by Prof. Yang [3] from an industrial viewpoint, it is sufficient to achieve a species of MH with at least 3.3 the specific weight of H_2 to have the same energy content of 1000 BTU/scf of Natural Gas (NG). In fact, under said conditions, MH would avoid the current needs to liquefy Hydrogen in order to achieve a sufficient range, since MH can be compressed like NG. Additionally, the magnecular structure of MH avoids the traditional seepage of Hydrogen through the walls [14, 15], thus allowing long term storage that is currently prohibited by molecular Hydrogen due to current environmental laws.

Magnehydrogen is a cluster species and about 7.4 times heavier than hydrogen. This anomaly to conventional gaseous molecules helps in reducing the leakage of these novel species from pipeline. Permeability issues needs to be answered while passing hydrogen through pipeline but magnehydrogen has a advantage due to its polymeric nature. Moreover, energetically it is equivalent to hydrogen and generates a high flame temperature which can prove key to cleaner combustion of coal.

Thus magnehydrogen is the closest choice to replace hydrogen as an additive and in some physical properties discussed above, it is even better to hydrogen.

Indian coal is known for its high ash content. Coal-fired power plants generate a huge quantity of ash which is an environmental problem. As per the estimates Magnegas Corporation based on studies conducted at their place, there is an elimination of particulate matter when using magnegas with coal as additive. This estimate is a source of hope for cleaning the combustion of coal-fired power plants in many states of India. Central Indian coal mines deliver a coal with ash as high as 38 to 40% and the fly ash emitting from the coal-fired power plants is a cause of land, soil and air pollution in the area.

The high temperature generated due to addition of magnegas can facilitate chemical gasification reaction occur easily in a reactor. Mixing of pulverized coal can enhance the ability of process. Even biomass and combustible garbage can be burnt with this additive. The high temperature attained inside the combustion place must be converting the ash into glass slag kind of material.

A power plant of 2340 MW capacity using high ash central Indian coal consumes 40 to 45 thousand ton coal per day. The average ash content in this coal is 35%. Estimated ash per annum is ~5100000 ton/yr. Ash generation per annum as reported by this power plant ~3600000 ton/yr. Thus ~1500000 ton/yr is the fly ash generation. Assuming 98.5% efficiency of ESP, ash liberated through stack in the atmosphere is 22500 ton/yr. This ash deposits in the surrounding area and pollute the ecological factors like lake, small water streams and farmland.

With addition of the magnegas, the conversion of ash into fusible mass will minimize the pollution due to fly ash.

As carbon will be converted in totality to its dioxide, the total obtainable energy will be increased. This, in fact, is the goal of overall process which will increase the energy efficiency of the coal combustion process.

As CO is highly reactive and it is difficult to measure the enthalpy of formation of CO practically by calorimeter, a simple calculative approach is described below [16].

$C\ (graphite) + \frac{1}{2}\ O_2 \rightarrow CO\ (g)\quad \Delta H_1 = ?$

$CO\ (g) + \frac{1}{2}\ O_2 \rightarrow CO_2\ (g)\quad \Delta H_2 = -283.0\ kJ/mol$

$C\ (graphite) + O_2 \rightarrow CO_2\ (g)\quad \Delta H_3 = -393.5\ kJ/mol$

Hess's law gives:

$\Delta H_1 = \Delta H_3 - \Delta H_2 = -393.5 + 283.0 = -110.5\ kJ/mol$

For every elemental carbon released in stack as carbon monoxide, we are gaining 110.5kJ/mol and loosing 283.0 kJ/mol of energy. Thus, loss amounts to 256% per mol.

This loss would be eliminated with the addition of magnegas which helps in complete combustion of carbon to CO_2.

Many metallurgical processes use heat liberated in operations to generate power. Increased waste heat due to magnegas as additive can be used effectively. An example of the availability of waste heat is given as follows [17,18]:

In a furnace, the exhaust gases are leaving the furnace at 900°C at the rate of 2100 m^3/hour. The total heat recoverable at 180°C final exhaust can be calculated as

$Q = V \times \rho \times C_p \times \Delta T$

Q is the heat content in kcal

V is the flow rate of the substance in m^3/hr

ρ is density of the flue gas in kg/m^3

C_p is the specific heat of the substance in kcal/kg °C

Heat available (Q) = 2100 x 1.19 x 0.24 x (900-180) = 4,31,827 kcal/hr

Not only the metallurgical operations but the small power plants also utilise the waste heat thrown out of the stack. The term "combined cycle" describes the combination of two thermodynamic cycles, with the gas turbine (Brayton cycle) burning natural or synthetic gas from coal/residuals/oil, and its hot exhaust gas powering a small steam power plant (Rankine cycle). Combined Cycle Power Plants (CCPPs) can achieve a thermal efficiency higher than 60% today, compared to single cycle gas power plants which are limited to efficiencies of around 35 to 42% [19]. In place of natural gas, coal fired power plant using pulverized coal can also work on two cycles to increase electricity output. Also, when the total heat content in waste heat recovery is dependent on difference in temperature (ΔT), 8 to 9 times increase due to addition of magnegas will certainly increase the efficiency of waster recovery process.

In developing countries like India, there is a great deal of disparity in urban and rural life quality. In India, 42 percent of rural households use kerosene for lighting. By contrast, about 93 percent of urban households use electricity for lighting and only about 6 percent use kerosene. On average, a rural household receives six hours of electricity supply from the grid during the off-peak period (usually afternoon and night). The cost of lighting a rural household includes the cost of grid supply and the cost of kerosene. The loss of electricity in grid is also significant to be noted [20].

Distributed power generation in small capacity can serve the purpose of extending availability of electricity to rural households. This will also save losses in distribution and local employment generation is possible for rural population.

There are a few small capacity power plants established on cooperative basis in few states of India. The village community uses locally available coal, biomass and other combustible waste to generate power of few kW which is sufficient to meet their electricity requirement. These power plants are based on a crude, steam engine principle, and can't be equipped with modern pollution control facility. The overall economy does not permit use of costly ESPs.

If such small power plants are supplied with magnegas, which can be generated on site, it will help to increase the combustion efficiency of original fuel. It will also improve the quality of emission, thereby, supporting clean atmosphere.

The old age power plants of less capacity can also be run on coal + magnegas hybrid fuel to improve the efficiency of combustion. As these power plants are not suitable to be equipped with modern pollution control facility, they are emitting beyond permissible limit. Scale up of the present experimental results obtained by Magnegas Corporation can give a good solution to improve the economy of these power plants.

A bottom up model for combustion of coal with magnegas was proposed by the authors and it is still under consideration for experiments. This model study will mainly focus on Indian coal and thermal power units in India. The outcome of study can help to devise a scaled up process of co combustion of magengas and coal which can serve the purpose of all coal-firing industries in India. Apart from larger coal based power plants, there are many captive to micro power plants operated on co operative basis in villages. These power plants meet up the energy requirement of those villages. Due to lack of any sophisticated emission controlling technologies, these power plants emit a high amount of poisonous gases like CO_2, CO and NOx. Due to low stack height of these steam engine based power units, the workers are exposed to poor health and environmental conditions. The clean up aimed with co combustion of coal with magengas can provide better environmental conditions to workers in small coal fired units.

CONCLUSION

In the present paper we discussed the possibilities of using magnegas as an additive to coal in order to enhance the combustion efficiency of coal. To justify the need of novel fuel like magnegas, initially we have discussed the present scenario of energy sources and their fulfilment, problems associated with combustion of fossil fuels especially coal and their effects leading to global warming and oxygen depletion and need of mankind to find alternate fuels due to devastating effects of burning fossil fuels. Then with the short introduction to the new fuel magnegas which posses the magnetically bonded molecules and magnecules and hence justified the lower energy for its combustion called as "magnecular combustion" when used independently as well as mixed with coal as an additive for its complete and clean combustion. The present scenario of coal fired power plants and the emission statistics can be improved by introduction of magnegas as additive. As data in table 2 shows reduction in CO2 emission by 40% with use of magnegas as additive, the average specific emission from Indian coal fired power plants can be reduced from ~1.18 to ~0.62. Hence its has been emphasized in this paper that the priority need is clean combustion of the existing fossil fuel and utilizing the maximum available carbon of the fuel which can be done by injecting magnegas along with the conventional fossil fuel.

ACKNOWLEDGEMENT

Authors are thankful to Thunder Energy Coporation, FL, USA for financial support towards travel and registration grants for academic events of our participation. We are also grateful to Prof. R. M. Santilli for his generous support and provision for access of his established facts for verification and studies.

REFERENCES

[1] R. M. Santilli, "The new fuels with magnecular structure" International Academic Press, (2008). http://www.i-b-r.org/docs/Fuels-Magnecular-Structure.pdf

[2] R. M. Santilli, "The novel magnecular species of hydrogen and oxygen with increased specific weight and energy content", Int J Hydrogen Energy (2003); 28:177-96, http://www.santillifoundation.org/docs/Santilli-38.pdf.

[3] Y. Yang, J. V. Kadeisvili, and S. Marton, "Experimental Confirmation of the New Chemical Species of Santilli Magnehydrogen", Int. J. Hydrogen Ener., **38**, 5003, (2013).

[4] Gandzha and J. Kadisvily, "New Science for a New Era", Sankata Printing Press, Nepal, (2001).

[5] http://magnegas.com/hy-fuels" ***http://magnegas.com/hy-fuels***.

[6] U.S. Department of Energy, http://www.fe.doe.gov/education/energylessons/coal/gen_coal.html http://www.worldcoal.org/coal/uses-of-coal/coal-electricity/ http://www.ucsusa.org/clean_energy/coalvswind/c01.html

[7] Ripe for Retirement, "The Case for Closing America's Costliest Coal Plants, Union of Concerned Scientists", November 2012.

[8] Energy Information Administration (EIA). 2012a. "Electric power monthly. February 2012 with data through December 2011". Washington, DC: U.S. Department of Energy. Online at http://www.eia.gov/electricity/monthly/current_year/february2012.pdf.

[9] UNEP 2012, "The Emissions Gap Report 2012. United Nations Environment Programme (UNEP)", Nairobi.

[10] Environmental Protection Agency (EPA) 2012, "Mercury: Basic information", Washington, DC. Online at http://www.epa.gov/mercury/bout.htm, accessed February 28, 2012.

[11] Environmental Protection Agency (EPA) 2010a, "Federal implementation plans to reduce interstate transport of fine particulate matter and ozone; proposed rule", 40 CFR Parts 51, 52, 72, et al. Federal Register 75, August 2. Online at http://www.gpo.gov/ fdsys/pkg/FR-2010-08-02/pdf/2010-17007.pdf.

[12] National Research Council (NRC) 2010, "Hidden costs of energy: Unpriced consequences of energy production and use", Washington, DC: National Academies Press, 2010. http://www.nap.edu/catalog.php?record_id=12794.

[13] Publication of reports by Central Electricity authority (2009-13)

[14] R. M. Santilli, "The novel magnecular species of hydrogen and oxygen with increased specific weight and energy content", Int J Hydrogen Energy, 28 (2010) 177-96. http://www.santillifoundation.org/docs/Santilli-38.pdf

[15] R. M. Santilli, "The new fuels with magnecular structure" International Academic Press, (2008). http://www.i-b-r.org/docs/Fuels-Magnecular-Structure.pdf

[16] John Kotz, Paul Triechel, John Townsend, "Chemistry and Chemical Reactivity", Volume 1, Seventh Edition, Thomson Brooks/Cole.

[17] ***http://www.beeindia.in/energy_managers_auditors/*** documents/guide _books/2Ch8.pdf

[18] D. A. Reay, E and F. N. Spon, "Heat Recovery Systems", London, (1979).

[19] Klaus Willnow (Siemens), "Energy Efficient Solutions for Thermal Power Plants, Energy Efficiency Technologies", Annex III, Technical Report, WEC Knowledge Network, World Energy Council, August 2013.

[20] The World Bank, "Empowering Rural India: Expanding Electricity Access by Mobilizing Local Resources Analysis of Models for Improving Rural Electricity Services in India through Distributed Generation and Supply of Renewable Energy", South Asia Energy Unit, Sustainable Development Department. 2010.

HADRONIC JOURNAL 40, 85 - 95 (2017)

CONNECTION PRESERVING MAPS AND SOME APPLICATIONS

Feray Bayar and Ayhan Sarioğlugil
Ondokuz Mayis University
Faculty of Sciences and Arts
Department of Mathematics
55139, Samsun, Türkiye
feraybayar@gmail.com, ayhans@omu.edu.tr, sarioglugil@gmail.com

Received March 10, 2017

Abstract

The aim of this paper is to investigate the applications of connection preserving maps on Riemannian manifolds.

Keywords: Connection Preserving Map, Conformal Map, Riemannian Manifold

Copyright © 2017 by Hadronic Press, Inc., Palm Harbor, FL 34684, USA

1.Introduction

It is well known that modern geometry was born when Riemann first separated the concept of geometry from the concept of space. The geometry was redesigned according to the topological concepts by Riemann. In this geometry, the geometric structures which are named as manifold by Riemann play an important role. One of the geometric structures added in this new geometry is the concept of the linear connection. Classically, a connection was defined by Christoffel (1869) to be a set of symbols $\{^{k}_{ij}\}$ or Γ^{k}_{ij} . The modern view point was finally formulated about 1950 by Koszul. Other the important geometric structure is the concept of the Riemann metric.The notion of a Riemannian metric dates back to Riemann's 1854 lecture. The association of a connection is due to Levi-Civita, [7]. Properties of connection preserving and conformal maps in n- dimensional C^{∞} −manifolds were given by N. J. Hicks in 1963, [4]. He proved that a conformal map f which defined between C^{∞} class differentiable manifolds M and M′ is connection preserving if and only if f is a homothety, [4].Furthemore, N. J. Hicks studied the connection preserving spray maps, [5]. He investigated the finding necessary and sufficient conditions for a spray map to be connection preserving.Then F. Erkekoğlu studied the differential geometry of the connection preserving maps,[3]. C. Tezer showed that for $n \neq 3,7$ a conformal diffeomorphism of S^n into itself admits no invariant connection except the trivial case where it admits an invariant Riemannian metric,[9]. Besides, S. T. Pamuk proved that the results in [9] without any restiriction on the dimension of spheres, [8].

In this paper we investigated the applications of connection preserving map on Riemannian manifolds.This paper is organized as follows: Section 2 gives some basic concepts of the Riemann geometry. In the third section the geometry of Riemannian manifolds under the connection preserving maps will be investigated.

2.Preliminaries

Riemannian metric is a tensor field g of type (0,2) which is symmetric and positive-definite for all $X, Y \in \chi(M)$. A manifold M with Riemannian metric g is called a Riemannian manifold and denoted by (M, g) or M,[10].
A connection ∇ on M will be a C^{∞} covariant differentation operator assigning

to C^∞ vector fields X and Y (with common domain A) a C^∞ vector field $\nabla_X Y$ (on A) such that

$$\begin{cases} 1.\ \nabla_X(Y+Z) = \nabla_X Y + \nabla_X Z \\ 2.\ \nabla_{(X+Y)} Z = \nabla_X Z + \nabla_Y Z \\ 3.\ \nabla_{hX} Y = h\,\nabla_X Y \\ 4.\ \nabla_X(hY) = X(h)Y + h\,\nabla_X Y \end{cases} \tag{1}$$

where Z is a C^∞ vector fields on A and h is a C^∞real valued function on A.The torsion tensor $T(X,Y)$ and curvature tensor $R(X,Y,Z)$ of a connection are defined by

$$T(X,Y) = \nabla_X Y - \nabla_Y X - [X,Y] \tag{2}$$

and

$$R(X,Y,Z) = \nabla_X \nabla_Y Z - \nabla_Y \nabla_X Z - \nabla_{[X,Y]} Z \tag{3}$$

for all $X,Y,Z \in \chi(A) \subset \chi(M)$, [3]. If $T \equiv 0$ we have

$$[X,Y] = \nabla_X Y - \nabla_Y X \tag{4}$$

On Riemannian manifold M there exists one and only one affine connection ∇ that satisfies vanishing torsion tensor and parallel metric g. The connection ∇ is called the Riemannian connection, [10].
The curvature tensor R satisfies the equations

$$R(X,Y)Z + R(Z,X)Y + R(Y,Z)X = 0 \tag{5}$$

and

$$(\nabla_X R)(Y,Z) + (\nabla_Y R)(Z,X) + (\nabla_Z R)(X,Y) = 0. \tag{6}$$

These equations are called first and second Bianchi identity, respectively, [10]

Let $\{x_1, x_2, \ldots, x_n\}$ be the local coordinate system on M .Then the vector system$\{\frac{\partial}{\partial x_k} = \partial_k : 1 \le k \le n.\}$ is the standard basis of $\chi(M)$. Thus, for all $\nabla_{\partial_i}\partial_k \in \chi(M)$ we can write as, [1],

$$\nabla_{\partial_i}\partial_j = \sum_{k=1}^{n} \Gamma_{ij}^k \partial_k, 1 \leq i,j,k \leq n$$

Here Γ_{ij}^k are called the Christoffel Symbols(or connection coefficients) and defined by

$$\Gamma_{ij}^k\} = g(\nabla_{\partial_i}\partial_j, \partial_k). \tag{7}$$

Let the vector system $\{\partial_1, \partial_2, \ldots, \partial_n\}$ be an orthonormal frame of the tangent spaces $T_M(P)$. Then

$$Ric(X,Y) = \sum_{k=1}^{n} g(R(\partial_k, X)Y, \partial_k) \tag{8}$$

defines a global tensor field Ric of type (0,2), called the Ricci curvature tensor of M. Using the Ricci tensor Ric, the scalar curvature r is defined by, [1],

$$r = \sum_{k=1}^{n} Ric(\partial_k, \partial_k) \tag{9}$$

For all $X, Y, Z, W \in \chi(M)$ the Riemannian-Christoffel curvature tensor of type (0,4) is defined by, [2],

$$K(X,Y,Z,W) = g(X, R(Z,W)Y). \tag{10}$$

Let X and Y be two linearly independent vectors at a point. The sectional curvature $K(\pi)$ for the plane section spanned by X and Y is defined by, [2]

$$K(\pi) = ((K(X,Y,X,Y))/(g(X,X)g(Y,Y) - [g(X,Y)]^2)). \tag{11}$$

Let (M,g) and (M',g') be C^∞-Riemannian manifolds, and $f: M \to M'$ be a C^∞-map. For Jacobian map f_* of f, if there is a C^∞-real-valued function $G > 0$ on M for any P in M, then

$$g'(f_*X, f_*Y) = G(P)g(X,Y) \tag{12}$$

for all $X, Y \in \chi(M)$; f is called conformal, [2]. Here if G is a constant function, f is homothety. If $G = 1, f$ is an isometry. Let M and M′ be C^∞-manifolds with connections ∇ and ∇', respectively. A C^∞map $f: M \to M'$ is connection preserving if

$$f_*(\nabla_X Y) = \nabla'_{f_*X} f_* Y \tag{13}$$

for all vector fields X and Y, [4]. Let M and M' be n-dimensional C^∞ −connected Riemannian manifolds, and let f be a C^∞-conformal map of M

into M' with G. Then f is Riemannian connection preserving map if and only if f is homothety, [4].

Thus, we can give the following corollary.

Corollary 1: Let M and M' be n −dimensional C^∞-connected Riemannian manifolds, and let f be a connection preserving map. Then we have

$$f_*([X,Y]) = [f_*X, f_*Y]. \tag{14}$$

Other words, the connection preserving map f preserves the Lie derivative £. Namely,

$$f_*(£_{X}(Y)) = £_{f_*X} f_*Y.$$

Proposition1: Let M and M' be n − dimensional Riemannian manifolds with Riemannian curvature tensor R and R', respectively. If $f: M \to M'$ is connection preserving map, then

$$f_*(R(X,Y)Z) = R'(f_*X, f_*Y)f_*Z \tag{15}$$

for all $X, Y, Z \in \chi(M)$, [4].

Let M and M' be n −dimensional Riemannian manifolds. In this study, we focused on the following question. If there is a connection preserving map defined between M and M', then which geometric properties of manifolds are invariant or not. Furthermore, we describe a map which preserves connection and then see that the image of a hyperbolic paraboloid surface generate an elliptic paraboloid surface under this map.

3. Geometry of Riemannian manifolds under connection preserving maps

Throughout this section, we will denote M and M' as n −dimensional Riemannian manifolds.

Theorem 1: Let $f: M \to M'$ be a C^∞-map. Assume that Γ_{ij}^k and Γ'^k_{ij} are Christoffel symbols of M and M', respectively. If f is connection preserving map, then we obtain

$$\Gamma_{ij}^k = \Gamma'^k_{ij}, \quad 1 \leq \mathrm{i,j} \leq \mathrm{n}. \tag{16}$$

Proof: Let ∇ and ∇' be Riemannian connections on M and M', respectively. Then we have

$$\nabla_{\partial_i}\partial_j = \sum_{k=1}^{n} \Gamma_{ij}^{k}\, \partial_k \,, 1 \le i,j,k \le n\,. \tag{17}$$

where $\chi(M) = Span\{\partial_1, \partial_2, \ldots, \partial_n\}$, $\frac{\partial}{\partial_{x_k}} = \partial_k$.

From (13) we have

$$f_*\left(\nabla_{\partial_i}\partial_j\right) = \nabla'_{f_*\partial_i} f_*\partial_j. \tag{18}$$

Substituting (17) into (18), we get

$$\sum_{k=1}^{n} \Gamma_{ij}^{k}\, f_*(\partial_k) = \nabla'_{f_*\partial_i} f_*\partial_j.$$

On the other hand we have

$$\nabla'_{f_*\partial_i} f_*\partial_j = \sum_{k=1}^{n} \Gamma'^{k}_{ij} f_*\partial_k \tag{19}$$

where $\chi(\mathrm{M}') = Span\{f_*\partial_k : 1 \le \mathrm{k} \le \mathrm{n}\}$.

From (18) and (19) we get

$$\Gamma_{ij}^{k} = \Gamma'^{k}_{ij}$$

This is completed the proof.

Theorem 2: Let $f: M \to M'$ be a conformal map. Suppose that K and K' are Riemannian-Christoffel curvature tensors of M and M',respectively. If f is connection preserving map, then we get

$$K'(f_*X, f_*Y, f_*Z, f_*W) = G(P)K(X,Y,Z,W) \tag{20}$$

for real-valued $G > 0$ function and all $P \in M$.

Proof: From (10) the Riemannian-Christoffel curvature tensor K' of M' is

$$K'(f_*X, f_*Y, f_*Z, f_*W) = g'(f_*X, R'(f_*Z, f_*W)f_*Y) \tag{21}$$

where $f_*X, f_*Y, f_*Z, f_*W \in \chi(\mathrm{M}')$.

Substituting (15) into (21) we get

$$K'(f_*X, f_*Y, f_*Z, f_*W) = g'\big(f_*X, f(R(Z,W)Y)\big).$$

On the other hand, since f is a conformal map, we obtain

$$K'(f_*X, f_*Y, f_*Z, f_*W) = G(P)K(X,Y,Z,W)$$

for real-valued $G > 0$ function and all $P \in M$. This is completed the proof.

Thus, we can give the following corollary.

Corollary 2: Let $f: M \to M'$ be a connection preserving map. In this case, if f is a homothety, we have

$$K'(f_*X, f_*Y, f_*Z, f_*W) = \delta K(X,Y,Z,W), \delta = \text{const.}$$

Theorem 3: Let $f: M \to M'$ be a connection preserving map. For all $X, Y, Z \in \chi(M)$ we have the following:

(i) Jacobi identity is invariant under the map f.

(ii) First Bianchi identity is invariant under the map f.

(iii) Second Bianchi identity is invariant under the map f.

Proof: (i) For all $X, Y, Z \in \chi(M)$ we have as Jacobi identity of M

$$[X,[Y,Z]] + [Y,[Z,X]] + [Z,[X,Y]] = 0. \tag{22}$$

Applying the map f_* to the both side of (22) we get

$$f_*([X,[Y,Z]] + [Y,[Z,X]] + [Z,[X,Y]]) = f_*(0).$$

or

$$f_*([X,[Y,Z]]) + f_*([Y,[Z,X]]) + f_*([Z,[X,Y]]) = 0. \tag{23}$$

By (14), we obtain

$$f_*([X,[Y,Z]]) = [f_*X, f_*([Y,Z])] = [f_*X, [f_*Y, f_*Z]] \tag{24}$$

$$f_*([Y,[Z,X]]) = [f_*Y, f_*([Z,X])] = [f_*Y, [f_*Z, f_*X]] \tag{25}$$

$$f_*([Z,[X,Y]]) = [f_*Z, f_*([X,Y])] = [f_*Z, [f_*X, f_*Y]] \tag{26}$$

Substituting (24), (25) and (26) into (23) we get

$$f_*([X,[Y,Z]]) + f_*([Y,[Z,X]]) + f_*([Z,[X,Y]]) = 0.$$

This is completed the proof.

(ii) For all $X, Y, Z \in \chi(M)$, the first Bianchi Identity of M is

$$R(X,Y)Z + R(Z,X)Y + R(Y,Z)X = 0 \tag{27}$$

Applying the map f_* to the both side of (27) we get

$$f_*(R(X,Y)Z + R(Z,X)Y + R(Y,Z)X) = f_*(0)$$

or

$$f_*(R(X,Y)Z) + f_*(R(Z,X)Y) + f_*(R(Y,Z)X) = 0. \tag{28}$$

By (15), we obtain

$$f_*(R(X,Y)Z) = R'(f_*X, f_*Y)f_*Z \tag{29}$$

$$f_*(R(Z,X)Y) = R'(f_*Z, f_*X)f_*Y \tag{30}$$

$$f_*(R(Y,Z)X) = R'(f_*Y, f_*Z)f_*X. \tag{31}$$

Substituting (29), (30) and (31) into (28) we get

$$R'(f_*X, f_*Y)f_*Z + R'(f_*Z, f_*X)f_*Y + R'(f_*Y, f_*Z)f_*X = 0$$

Hence, the first Bianchi Identity is invariant under the map f.

(iii) Let ∇ and ∇' be Riemannian connections on M and M', respectively. The second Bianchi Identity of M is

$$(\nabla_X R)(Y,Z) + (\nabla_Y R)(Z,X) + (\nabla_Z R)(X,Y) = 0. \tag{32}$$

for all $X, Y, Z \in \chi(M)$.

Applying the map f_* to the both side of (32) we get

$$f_*((\nabla_X R)(Y,Z) + (\nabla_Y R)(Z,X) + (\nabla_Z R)(X,Y)) = f_*(0)$$

or

$$f_*((\nabla_X R)(Y,Z)) + f_*((\nabla_Y R)(Z,X)) + f_*((\nabla_Z R)(X,Y)) = 0. \tag{33}$$

By (14) and (16) we find

$$f_*\left((\nabla_X R)(Y,Z)\right) = \nabla'_{f_*X} f_*\big(R(Y,Z)\big) = \nabla'_{f_*X} R'(f_*Y, f_*Z) \tag{34}$$

$$f_*\left((\nabla_Y R)(Z,X)\right) = \nabla'_{f_*Y} f_*\big(R(Z,X)\big) = \nabla'_{f_*Y} R'(f_*Z, f_*X) \tag{35}$$

$$f_*\left((\nabla_Z R)(X,Y)\right) = \nabla'_{f_*Z} f_*\big(R(X,Y)\big) = \nabla'_{f_*Z} R'(f_*X, f_*Y). \tag{36}$$

Substituting (34), (35) and (3.22)6 into (33) we get

$$\nabla'_{f_*X} R'(f_*Y, f_*Z) + \nabla'_{f_*Y} R'(f_*Z, f_*X) + \nabla'_{f_*Z} R'(f_*X, f_*Y) = 0.$$

This is completed the proof.

Lemma 1: Let $f: M \to M'$ be a connection preserving map. Suppose that ∇ and ∇' are Riemannian connections on M and M', respectively. Then we obtain

$$f_*\big(\nabla^{(n)}{}_X Y\big) = (\nabla')^{(n)}{}_{f_*X} f_* Y \quad , \mathrm{n} \in \mathbb{Z}, \tag{37}$$

for all $X, Y \in \chi(M)$.

Proof: We will do the proof by inductive method.

Step 1: For $n = 1$, (37) is correct,since

$$f_*(\nabla_X Y) = \nabla'_{f_*X} f_* Y.$$

Step 2: Suppose that (37) is correct for $n = k$,that is

$$f_*(\nabla^{(k)}{}_X Y) = (\nabla')^{(k)}{}_{f_*X} f_* Y \tag{38}$$

Step 3: Prove that (39) is correct for $n = k + 1$,that is

$$f_*\big(\nabla^{(k+1)}{}_X Y\big) = (\nabla')^{(k+1)}{}_{f_*X} f_* Y.$$

Since $\nabla^{(k+1)}{}_X Y = \nabla^{(k)}{}_X(\nabla_X Y)$ we can write

$$f_*\big(\nabla^{(k+1)}{}_X Y\big) = f_*\Big(\nabla^{(k)}{}_X(\nabla_X Y)\Big). \tag{39}$$

By using (14), we get

$$f_*\big(\nabla^{(k+1)}{}_X Y\big) = (\nabla')^{(k)}{}_{f_*X} f_*(\nabla_X Y) = (\nabla')^{(k)}{}_{f_*X}\big(\nabla'_{f_*X} f_* Y\big)$$

or

$$f_*\left(\nabla^{(k+1)}{}_X Y\right) = (\nabla')^{(k+1)}{}_{f_*X} f_* Y.$$

This is completed the proof.

Example 1: Let M be a hypersurface in E^3 given by

$$M \ldots . \varphi(u,v) = (u,v,uv).$$

$f: E^3 \to E^3$ defined by

$$f(x,y,z) = (y^2, xy, xy).$$

is a connection preserving map for $f(M) = M'$. So we have

$$M' \ldots . (f \circ \varphi)(u,v) = (v^2, uv, uv).$$

Let show the parametric equation of M as implicit form. So we have

$$g(x,y,z) = z - xy = 0.$$

From here we get

$$gradg = (-y,-x,1).$$

Suppose that $X = (-x,y,0)$ and $Y = (1,0,y)$ are vector fields on $\chi(M)$. We will show the equality

$$f_*(\nabla_X Y) = \nabla'_{f_*X} f_* Y$$

is correct. The matrix corresponding to the Jacobian map f_* of f is

$$J = \begin{bmatrix} 0 & 2y & 0 \\ y & x & 0 \\ y & x & 0 \end{bmatrix}. \tag{40}$$

On the other hand, we get

$$\nabla_X Y = (0,0,y).$$

Then we have

$$f_*(\nabla_X Y) = J\nabla_X Y = (0,0,0). \tag{41}$$

Similarly we obtain

$$f_*X = (2y^2, 0, 0)$$

and

$$f_*Y = (0, y, y).$$

From here we have

$$\nabla'_{f_*X} f_*Y = (0,0,0). \tag{42}$$

Combining (41) and (42) we get

$$f_*(\nabla_X Y) = \nabla'_{f_*X} f_*Y.$$

Then, f is a connection preserving map.

References

[1] Chavel, I., Riemannian Geometry, Cambridge University Press, New York, 2006.

[2] Chen, B., Geometry of Submanifolds, Marcel Dekker Inc. , New York, 1973.

[3] Erkekoğlu, F.,Koneksiyon Koruyan Dönüşümlerin Diferensiyel Geometrisi, MSc, Gazi Üniversitesi,Ankara, Türkiye, (1986).

[4] Hicks, N. J., Connexion Preserving , Conformal and Parallel Maps, Michigan Math. J. 10,(1963), 295-302.

[5] Hicks, N. J., Connexion Preserving Spray Maps, Illinois J. Math., Vol. 10, (1966),661-679.

[6] Millman, R. S. &Parker, G. D., Elements of Differential Geometry, Prentice-Hall Inc. , New Jersey, 1977.

[7] Millman, R. S. & Stehney, A. K., The Geometry of Connections,The American Mathematical Monthly, Vol. 80, No. 5 (1973), pp. 475-500.

[8] Pamuk, S. T.,Connection Preserving Conformal Diffeomorphism of Spheres, MSc, Middle East Technical University, Ankara, Türkiye, (2002).

[9] Tezer, C., Sur les transformations conformes de la sphere admettant une connexion invariante, Indag. Mathem., N. S., 11 (3), (2000),467-475.

[10] Yano, K. & Kon, M., Structures on Manifolds, World Scientific Publishing Co. Pte. Ltd., Singapore, 1984.

MAGNECULAR STRUCTURE OF NEW CLEAN FUELS

Chandrashekhar P. Pandhurnekar
Department of Applied Chemistry
Shri Ramdeobaba College of Engineering and Management
Nagpur, India

Received November 6, 2016

Abstract

Clean energies should be our strategies to conserve life-life cycle as a symbiotic connection of all biological forms and as a self-producing beauty. In this industrial era, use of clean fuels such as Magnegas^{TM} can be one of the most appropriate step in attaining the sustainability which not only reduce the emission of harmful exhaust in the atmospheric air but moreover releases oxygen which ultimately enhance the breathing quality of the air. All the conventional fuels more or less release carbon dioxide and other carcinogenic gases during their combustion; and also cause permanent removal of oxygen from atmosphere. Excessive industrial uses of the conventional fossil fuel comprising the conventional covalent bonding in the recent past showing visible effects to everybody through climactic episodes such as floods, tornadoes, hurricanes, changes in local seasonal timing, etc. Such associated problems with uses of fossil fuels prompted Professor R. M. Santilli to discover new chemical species having a new type of bonds which are much weaker than covalent bonds. In memoir of the Italian-American physicist, R. M. Santilli presented for the first time, the theoretical and experimental evidence on the existence of the new chemical species of magnecules defined as clusters of individual atoms (H; O; C; etc.), diatomic radicals (HO; CH; etc.) and ordinary molecules (H_2; CO; H_2O; etc.) bonded together by attractive forces. In this presentation, different topics which are shortly covered are: basics of hadronic chemistry, Santilli's model of hydrogen and water molecules using hadronic chemistry, conception of Santilli's magnecules, magnecular structure of H_3 and O_3, experimental verifications, industrial applications of fuels with Magnecular structures.

Based on invited talk at SIPS 2016, Santilli International Symposium on Sustainable Applications, Hainan Island, China, November 6 -10, 2016

Copyright © 2017 by Hadronic Press, Inc., Palm Harbor, FL 34684, USA

INTRODUCTION

Anthropogenic climate change presents a serious threat to the health, prosperity, and stability of human communities, to the stability and existence of non-human species and ecosystems, and to international political and military stability [1-3]. Human health is affected by higher temperature via impacts on heat waves, drought, fires, floods and storms, and indirectly by ecological disruptions brought on by climate change including shifting patterns of disease [4]. National responsibilities for global warming can be assigned under the premise that fossil fuel CO_2 emissions are the primary issue for long-term warming. Carbon released in fossil fuel burning will not be naturally removed from the climate system for millennia [5]. CH_4, N_2O, O_3 and other gases also contribute to human-made climate change, but CO_2 contributes about 80% of the increase of GHG climate forcing in the past two decades and much of the increase of the other 20% is related to fossil fuel mining or fossil fuel use. Current fossil fuel CO_2 emissions are shown in **Figure 1(a)**. China is the largest source of current emissions, with the United States second and India a rapidly growing third. However, climate change is accurately proportional to cumulative emissions **Figure 1(b)**.

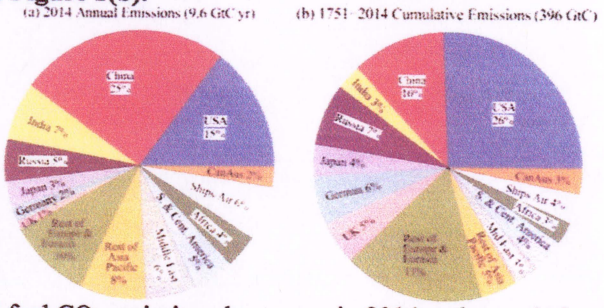

Figure 1. Fossil fuel CO_2 emissions by source in 2014 and cumulative 1751–2014 [6].

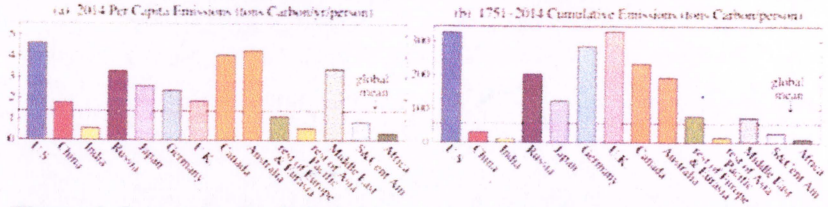

Figure 2. Per capita fossil fuel CO_2 emissions in 2014 and cumulative [6].

The United States and Europe, including their portions of air and ship emissions, are each responsible for more than one-quarter of the climate change, China about 10% and India about 3%. Consumption-based accounting for emissions increases this disparity between developed and developing country emissions. Per capita fossil fuel emissions (**Figure 2(a)**) and cumulative emissions (**Figure 2(b)**) provide a useful perspective on emission responsibilities. Despite China's high current emissions, on a per capita basis they remain lower than many western nations, and slightly larger than the global average. Cumulative per capita emissions by China are an order of magnitude smaller than US emissions, and India's cumulative per capita emissions are even smaller. International cooperation in generating more affordable carbon-free energies is needed, or economic development in many nations will continue to be based on fossil fuels, despite pollution and climate impacts [6].

However, the fossil fuel resources upon which industry is heavily dependent are limited in available quantities and are expected to be close to depletion in the near future. The unprecedented popularity and successful utilization of petroleum and coal resources observed in the twentieth century may decline in the ending of twenty first century or next century due to lack of resources availability, thus making prospects for future sustainability seen grim. Public appetites for convenient and alternative fuel sources and superior high performance materials are, however, growing. Therefore, additional and alternative sources for fuels not only be developed further but also needed for immediate commercial exploitation. Use of alternative fuels is no longer a matter for the future; it is realistic issue of the present [7].

If usable energy or deliverable power is the final product to be desired, alternate sources for energy may strongly and directly affect the lifestyle of the consumers, as well as their energy consumption pattern. A good alternative fuel available in the market is Magnegas^{TM} and Aquygen^{TM}, new fuels having magnecular bonding, developed by Prof. R. M. Santilli, which primarily consists of bonds of magnetic types enabling pollution free and environmentally benign emission of exhaust. In this review paper, different topics which are shortly covered are: basics of hadronic chemistry, Santilli's model of hydrogen and water molecules using hadronic chemistry, conception of Santilli's magnecules, magnecular structure of H_3 and O_3, experimental verifications, industrial applications of fuels with Magnecular structures.

BASICS OF HADRONIC CHEMISTRY

R. M. Santilli and D. D. Shillady introduced the iso-chemical model of the hydrogen (**Figure 3**) [8], water (**Figure 4**) [9] and other molecules which permitted the achievement, apparently for the first time in chemistry, of a numerical representation of binding energies, electric and magnetic moments, as well as other molecular features exact to the desired digit. The new models also achieve the first restriction of valence correlations to electron pairs, as established experimentally, exhibits perturbative series converging dramatically faster than those of quantum chemistry (with consequential major reduction of computer time), and resolve other vexing problems of current molecular chemistry. These results were achieved by assuming that two valence electrons couple themselves into a singlet state at short distances, called iso-electronium, with a new, strongly attractive force due to the deep overlapping of the electron wave packets. The new strong valence force produced are non-linear (in the wave functions), non-local (e.g. of integral type) and non-potential (e.g. of contact zero-range) type. Also, the new force can be thought as the previously missing molecular equivalent of the nuclear strong interactions. Being non-linear, non-local and non-potential, the new strong valence force cannot be represented with the Hamiltonian alone, thus requiring at least one second operator. As such, the new strong valence force is outside any dream of scientific treatment via conventional quantum mechanics and chemistry, since the latter are strictly linear, local and potential. In view of these limitations, new mathematical, physical and chemical theories had to be worked out for the invariant treatment of the new strong valence force. These new formulations are known under the name of hadronic mechanics, super-conductivity and chemistry and are reviewed in detail in monograph [10].

Hadronic chemistry is based on the lifting of the basic unit, from its simple value I = +1 currently used in chemistry (and dating back to biblical times) to the most general possible integro-differential operator of hermitean or non-hermitean, single-valued or multi-valued character, with corresponding lifting of all possible conventional associative products A x B among generic quantities A, B (such as numbers, functions, operators, etc.)

$$I = +1 \to \hat{I} = \hat{I}\,(t, r, p, \psi, \partial_k \psi, ...) = 1/\hat{T},$$
$$A \times B = A \hat{\times} B = A \times \hat{T} \times B,$$
$$I \times A = A \times I = A \to \hat{I} \hat{\times} A = A \hat{\times} \hat{I}$$

with corresponding lifting of the entire mathematical and physical structure of conventional theories. All conventional linear, local and potential effects are represented with the usual Hamiltonian, while all non-linear, non-local and non-potential effects are represented with the generalized unit $\hat{I}$. Consequently, hadronic chemistry has various branches, called iso-, geno- and hyper-chemistry which are characterized, correspondingly, by single valued hermitean, single-valued non-hermitean, and multi-valued non-hermitean generalized units. These branches are used for the invariant treatment, respectively, of closed-isolated systems with non hamiltonian internal effects, open-irreversible systems, and irreversible multi-valued biological structures [11].

Santilli-Shillady strong valence bond (1999)

To provide a conceptual outline, consider the conventional quantum mechanical equation in relative coordinates and reduced mass for two electrons in singlet coupling as,

$$(p^2/m + e^2/r)\, \psi(r) = E\, \psi(r), \qquad (1)$$

where m is the electron mass. The above equation shows the *repulsive* Coulomb force between the *point-like charges* of the electrons. But the electrons have *extended wave packets* of the order of 1 fm whose mutual penetration, as necessary for the valence bond, causes *non-linear, non-local and non-potential interactions* at the foundations of hadronic mechanics (see the preceding chapter). The only known possibility fo an invariant representation of these interactions is to exit from the class of unitary equivalence of Eq. (1) via an iso-unitary transformation that, for simplicity, we present below in its *projection* into a conventional non-unitary form

$$UU^\dagger \neq I,\ UU^\dagger = I^* = 1/T\,, \qquad [2]$$

$$U\,[(p^2/m + e^2/r)\, \psi(r)]\, U^\dagger =$$

$$= [\,(Up^2U^\dagger)/m + (e^2/r)UU^\dagger]\, (UU^\dagger)^{-1}\, [U\psi(r)U^\dagger] =$$

$$= [1/m)p^*\, T\, p^*\, T + e^2/r\,]\, \psi^*(r) = E'\, \psi^*(r), \qquad [3]$$

where one should note the different eigenvalue E' from the value E of Eq. (1) (due to the general non-commutativity of the Hamiltonian and the iso-unit).

At this point, Santilli and Shillady introduce the following realization of the non-unitary transform, that is, of the *fundamental iso-unit of hadronic chemistry,* Eq. (4) of FHC,

$$UU^\dagger = I^* = 1/T = e^{\{[\psi(r)/\psi^*(r)] \int \psi\dagger_1(r)\, \psi_2(r)\, d3(r)\}} = 1 + [\psi(r)/\psi^*(r)] \int \psi^\dagger{}_1(r)\, \psi_2(r)\, d^3(r) + ... \qquad [4]$$

where ψ and ψ^* are the solutions of the unitary and non-unitary equations, and ψ_k, k = 1,2, are the conventional quantum mechanical wave functions of the two electrons. It is evident that, as desired, the above iso-unit represents interactions that are: non-linear, because dependent in a non-linear way in the wave functions; nonlocal, because inclusive of a volume integral; and non-potential, because not representable with a Hamiltonian. Additionally, for all mutual distances between the valence electrons greater than 1 fm, the volume integral of Eq. (4) is null with the crucial limit

$$\text{Lim}_{r \text{ bigger 1 fm}} I^* = 1, \qquad [5]$$

under which hadronic chemistry recovers quantum chemistry identically and uniquely. As it was the case for hadronic mechanics, hadronic chemistry merely provides a form of "completion" of quantum chemistry at short distances much along the celebrated intuition by Einstein, Podolsky and Rosen. Santilli and Shillady solved the above equations in all details. First, by inserting iso-unit (Eq. 4) in Eqs. (3), they obtained the iso-equation here projected on a conventional Hilbert space

$$[p^2/2m' + e^2/r - V_o e^{-br}/(1 - e^{-br})]\, \psi^*(r) = E'\psi^*(r), \qquad [6]$$

where m' represents the iso-renormalization of the mass caused by non-potential interactions, and one recognizes the emergence of the *attractive Hulten potential*

$$V_{\text{Hulten}} = V_o e^{-br}/(1 - e^{-br}), \qquad [7]$$

But the Hulten potential is known to behave like the Coulomb potential at short distances and be much stronger than the latter. Therefore, Eq. (6) admits the excellent approximation

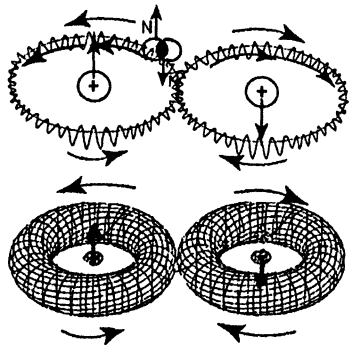

Figure 3. A schematic view of the magnetic fields of the isochemical model of the hydrogen molecule with isoelectronium assumed to be a stable quasi-particle. The top view represents the molecule at absolute zero degree temperature with polarization of the orbit in a plane, while the bottom view represents the molecule at ordinary temperature with a polarization of the orbit within a toroid. In both cases there is the disappearance of the total intrinsic magnetic moments of the electrons because they are coupled in the isoelectronium with antiparallel spin and magnetic moments due to Pauli's exclusion principle. The lack of contribution of the intrinsic magnetic moments of the electrons persists even when the isoelectronium has dimension much bigger than 1 fm, because the antiparallel character of the spins and magnetic moments persists, resulting in an average null total intrinsic magnetic moment of the electrons. Therefore, the biggest magnetic moment of the hydrogen molecule which can be obtained via polarizations is that of the electrons orbits. Note, as recalled, the oo-shaped (also called figure eight) configuration has been recently proved in mathematics to be one of the most stable solutions of the N-body problem.

$$[p^2/2m' - V' e^{-br}/(1 - e^{-br})] \psi^*(r) = E' \psi^*(r), \qquad [8]$$

where the new constants V' reflects the "absorption" of the repulsive Coulomb potential by the much stronger *attractive* Hulten potential.

In this way, Santilli and Shillady achieved for the first time in the history of chemistry [8], a valence coupling between two identical electrons in singlet coupling with a strongly attractive force, as requested by experimental evidence, which model is today known as the *Santilli-Shillady strong valence bond.*

As it is well known, according to quantum chemistry, the hydrogen molecule is a *four body* system comprising two protons and two electrons with conventional equation for the molecule at rest, that is, the two protons are considered as rest as conventionally done

$$[p_1^2/2m_1 + p_2^2/2m_2 + e^2/r_{12} - e^2/r_{1a} - e^2/r_{1b} - e^2/r_{2a} - e^2/r_{2b} + e^2/R] \psi(r) = E \psi(r), \qquad [9]$$

where: 1, 2 represents the two electrons; a, b represent the two protons; and R is the distance between the protons. Due to its four-body character, the above equation, does not admit any

analytic solution; misses at least 2% of the binding energy; and predicts that the hydrogen molecule is paramagnetic due to the evidence independence of the electrons.

The repetition of the non-unitary transform of the preceding section yield *the iso-chemical model of the hydrogen molecule as a four-body system*

$$[p_1^2/2m'_1 + p_2^2/2m'_2 - V^* e^{-br}/(1 - e^{-br}) + e^2/R]\, \psi^*(r) = E'\, \psi^*(r), \qquad [10]$$

showing the appearance of the Santilli-Shillady strong valence bond of Hulten type that "absorbs" all coulomb potentials, where m' represents the iso-renormalized mass of the electrons.

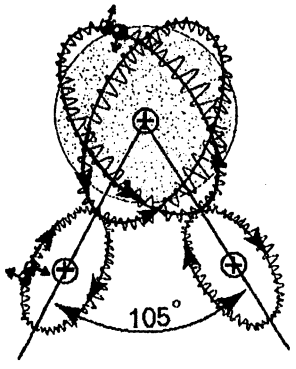

Figure 4. A schematic view of the proposed isochemical model of the water molecule here depicted at absolute zero degrees temperature and in the absence of any motion for the case of fully stable isoelectronium. It should be stressed that at ordinary temperature rotational motions recover the conventional space distribution, thus recovering the conventional "Mickey Mouse" configuration of the water. Also, the model is presented in terms of the orbits of the valence electrons (rather than in terms of density distributions). The fundamental assumption is that the two valence electrons, one per each pair of atoms, correlate themselves into two bonded singlet states at short distance we have called isoelectronia, one per each diatomic radicals H-O, which states are assumed to be mostly stable (see the text for the mostly unstable case). The water molecule is then reducible to two intersecting H-O diatomic radicals with a common O-atom. The only orbits yielding a stable water molecule are those in which each isoelectronium describes a oo-shaped orbit around the respective two nuclei of the H- and O-atoms. The isoelectronia are then responsible for the attractive force between the atoms. The binding energy is instead characterized by the oo-shaped orbits of the isoelectronia around the respective two nuclei, conceptually represented in this figure via a standing wave for a particle of spin 0 and charge -2e. Note that, in the absence of molecular motions, the orbits of the two isoelectronia are perpendicular to the H-O-H plane, thus confirming a characteristic of the water molecule. Conventional exchange, van der Waals and other forces remain admitted by the model when the isoelectronia are mostly unstable. The model permits a representation of: 1) the "strong" value of the molecular bond; 2) the reason why the H O molecule has only two hydrogen atoms and one oxygen atom; 3) a representation of the binding energy, electric and magnetic moments accurate to several digits; and other advances studied in the text. The above model of the H-O diatomic radicals is then extendable to other H-based diatomic radicals, such as H-C.

CONCEPTION OF SANTILLI'S MAGNECULES

Santilli magnecules in gases, liquids, and solids consist of stable clusters composed of conventional molecules, and/or diatomic radicals, and/or individual atoms bonded together by opposing magnetic polarities of toroidal polarizations of the orbits of at least the peripheral atomic electrons when exposed to sufficiently strong external magnetic fields, as well as the polarization of the intrinsic magnetic moments of nuclei and electrons [**Figure 5**] [12]. A population of magnecules constitutes a chemical species when essentially pure, i.e., when molecules or other species are contained in very small percentages in a directly identifiable form.

Magnecules are also called:
A) *elementary* when only composed of two molecules; If the conventional valence bond is denoted with the symbol "–" and the new magnetic bond with the symbol "×", examples of elementary magnecules in gases and liquids are respectively given by
$\{H-H\} \times \{H-H\}$, $\{O-O\} \times \{O-C-O\}$, etc., (11)
$\{C_{15}-H_{20}-O\} \times \{C_{15}-H_{20}-O\}$, etc.; (12)
B) *magneplexes* when entirely composed of several identical molecules; examples of magneplexes in gases and liquids are respectively given by
$\{H-H\} \times \{H-H\} \times \{H-H\} \times \ldots$, etc., (13)
$\{H-O-H\} \times \{H-O-H\} \times \ldots$, etc.; (14)
C) *magneclusters* when composed of several different molecules and examples of magneclusters are given by

$\{H-H\} \times \{C-O\} \times \{O-C-O\} \times \{C=O\} \times .$, etc. (15)
$\{C_{13}-H_{18}-O\} \times \{C_{14}-H_{12}-O_3\} \times \{C_{15}-H_{20}-O\} \times \ldots$,etc. (16)

A generic representation of a gas magnecules requires the presence of individual atoms and diamers (diatomic), such as:

$\{H-H\} \times \{C-O\} \times H \times \{H-O-H\} \times C \times \{H-O\} \times \ldots$, etc, (17)

Santilli magnecules are characterized by, or can be identified via the following main features [13]:
I) Magnecules primarily exist at large atomic weights where not expected, for instance, at atomic weights which are ten times or more the maximal atomic weight of conventional molecular constituents;
II) Magnecules are characterized by large peaks in macroscopic percentages in mass spectrography, which peaks remain unidentified following a search among all existing molecules;
III) Said peaks admit no currently detectable infrared signature for gases and no ultraviolet signature for liquids other than those of the conventional molecules and/or diatomic radicalss constituting the magnecule;
IV) Said infrared and ultraviolet signatures are generally altered (a feature called "mutation") with respect to the conventional versions, thus indicating an alteration (called infrared or ultraviolet mutation) of the conventional structure
of diatomic radicalss generally occurring with additional peaks in the infrared or ultraviolet signatures not existing in conventional configurations;
V) Magnecules have an anomalous adhesion to other substances, which results in backgrounds (blank) following spectrographic tests which are often similar to the original scans, as well as implying the clogging of small feeding lines with consequential lack of admission into analytic instruments of the most important magnecules to be detected;

VI) Magnecules can break down into fragments under sufficiently energetic collisions, with subsequent recombination with other fragments and/or conventional molecules, resulting in variations in time of spectrographic peaks (called time mutations of magnecular weights);
VII) Magnecules can accrue or lose during collision individual atoms, dimmers or molecules; and other anamolous properties.

One of the most important features of magnecules is their anomalous release of energy in thermochemical reactions, in view of its evident importance for the industrial development of new clean fuels such as magnegas [14]. This feature is crucially dependent on the existence within the magnecules of individual atoms, such as H, C and O, and/or individual diatomic free radicals, such as H–O and H–C. In fact, at the breakdown of the magnecules due to combustion, these individual atoms and diatomic free radicals couple themselves into conventional molecules via known exothermic reactions such as

$$H + H \rightarrow H_2 + 105 \text{ Kcal./mole}, \quad (18)$$
$$C + O \rightarrow CO + 255 \text{ Kcal/mole}, \quad (19)$$
$$H{-}O + H \rightarrow H_2O + 28 \text{ Kcal/mole, etc.}, \quad (20)$$

with consequential release during combustion of a large amount of energy that does not exist in fuels with a conventional molecular structure.

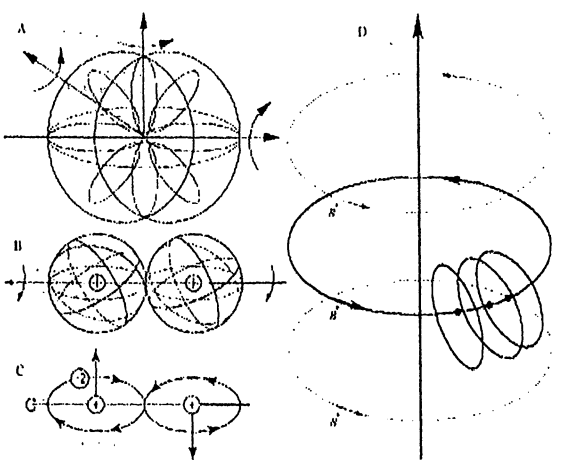

Figure 5. A schematic view of the main mechanism underlying the creation of magnecules, here illustrated for the case of the hydrogen molecule. It consists in the use of sufficiently strong external magnetic fields which can progressively eliminate all rotations, thus reducing the hydrogen molecule to a configuration which, at absolute zero degrees temperature, can be assumed to lie in a plane. The planar configuration of the electron orbits then implies the manifestation of their magnetic moment which would be otherwise absent. The r.h.s. of the above picture outlines the geometry of the magnetic field in the immediate vicinity of an electric arc as described in the text for the case of hadronic molecular reactors. Note the circular configuration of the magnetic field lines around the electric discharge, the tangential nature of the symmetry axis of the magnetic polarization of the hydrogen atoms with respect to said circular magnetic lines, and the consideration of hydrogen atoms at orbital distances from the electric arc 10^{-8}cm, resulting in extremely strong magnetic fields proportional to $(10^{-8})^{-2}= 10^{16}$ Gauss, thus being ample sufficient to create the needed polarization.

Finally, magnecules are called:
i) *isomagnecules* when having all single-valued characteristics and being reversible in time, namely, when they are characterized by isochemistry;
ii) *genomagnecules* when having all single-valued characteristics and being irreversible in time, namely, when they are characterized by genochemistry; and
iii) *hypermagnecules* when having at least one multi-valued characteristic and being irreversible in time, namely, when they are characterized by hyperchemistry.

MAGNEHYDROGEN™ AND MAGNEOXYGEN™

The conventional molecular hydrogen and oxygen gases can be turned into a new species with magnecular structure here called MagneHydrogen™ and MagneOxygen™ [15]. The aspect important for the hypothesis of MagneH and MagneO is that the toroidal polarization of the orbits of the electrons of the individual H atoms, plus the polarization of the intrinsic magnetic moments of nuclei [16-18] and electrons in the H molecule is sufficient for the creation of the desired new chemical species with bigger specific weight, because the new bonds can occur between pairs of individual H atoms [**Figure 6**].

The creation of MagneOxygen™ is expected to be considerably simpler than that of MagneHydrogen™ because oxygen is paramagnetic, thus having electrons free to acquire an overall magnetic polarity which is absent for the case of MagneHydrogen™.

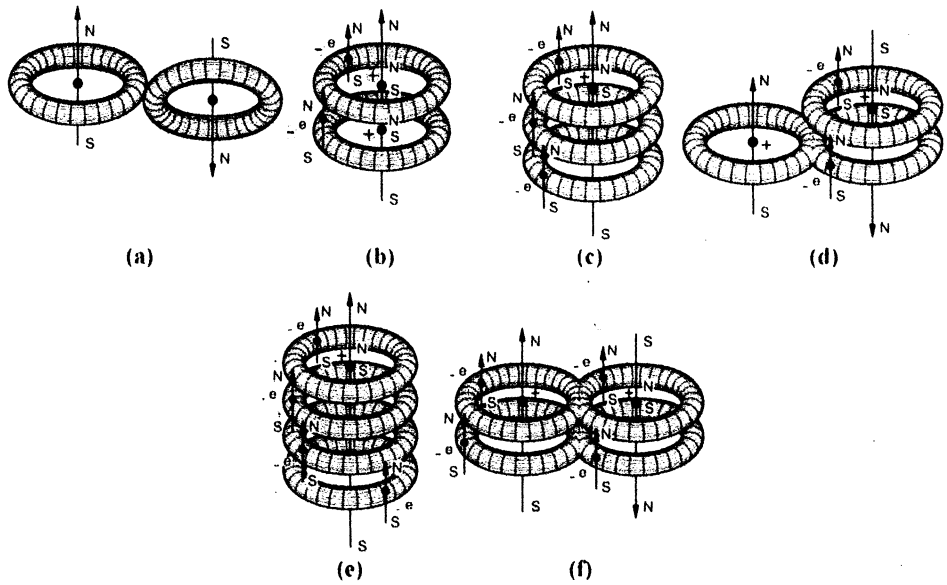

Figure 6. A conceptual rendering of the cluster MH_2 in which MH is predicted as being composed by part of the molecular species H—H (**Fig. 6a**) and part by the magnecular species H × H (**Fig. 6b**); the cluster MH_3 in MH which is predicted as being composed by magnecular species H × H × H (**Fig. 6c**) and H—H × H (**Fig. 6d**); the cluster MH_4 in MH which is predicted as being composed by the magnecular species H × H × H × H (**Fig. 6e**), H—H × H—H (**Fig. 6f**) and H—H × H × H (not shown for simplicity).

Under the assumption that the original gases are essentially pure, MagneHydrogen™ can be schematically represented as follows:

$(H_\uparrow - H_\downarrow) \times H_\uparrow$,

$(H_\uparrow - H_\downarrow) \times (H_\uparrow - H_\downarrow)$,

$(H_\uparrow - H_\downarrow) \times (H_\uparrow - H_\downarrow) \times H_\uparrow$, *etc.*

While MagneO can be schematically represented as given below:

$(O_{\uparrow} - O_{\downarrow}) \times O_{\uparrow}$,
$(O_{\uparrow} - O_{\downarrow}) \times (O_{\uparrow} - O_{\downarrow})$,
$(O_{\uparrow} - O_{\downarrow}) \times (O_{\uparrow} - O_{\downarrow}) \times O_{\uparrow}$, *etc.*
where the arrows now indicate possible polarizations of more than one electron orbit.

It has been proved after a series of experiments that the combustion of MagneH and MagneO releases more energy than the combustion of conventional H and O gases.

It then follows that
I) the use for internal combustion engines of MagneH with a sufficiently high specific weight is expected to eliminate liquefaction, yield essentially the same power as that produced with gasoline, and produce a dramatic decrease of operating costs;
II) the use of MagneH and MagneO in fuel cells is expected to yield a significant increase of voltage, power and efficiency; and
III) the use of liquefied MagneH and MagneO as fuels for rocket propulsion is expected to permit an increase of the payload, or a decrease of the boosters weight with the same payload.

EXPERIMENTAL VERIFICATION OF MAGNECULES

Memoir [13] then presented a considerable experimental evidence on the existence of the new species of magnecules for a gas created via the above reviewed method. The verification was achieved via the use of a GC-MS/IRD, namely, a Gas Chromatographer Mass Spectrometer equipped with an InfraRed Detector. Santilli's main experimental argument is that all gas chromatographic equipment available in the late 1990s had been conceived and established for the detection of conventional molecular species. The only possibility available at the time of memoir [13] to ascertain the existence of the new species of magnecules was that of subjecting the same injection, first for detection via the GC-MS and then detection via the IRD (**Figure 7** and **Figure 8**). The identification of clear clusters in the GC-MS that have no IR signature establishes the existence of magnecules since their bond is stable at ambient temperature, but weaker than the valence bond, thus having no IR signature. The magnecular nature of the bond was then confirmed by the arc method for its creation. Santilli insisted that it was impossible to achieve the same results in a resolutory way via two separate instruments due to the impossibility of matching scans in the GC-MS with scans in a separate IRD without any ambiguities.

```
Information from Data File:
File       : C:\HPCHEM\1\DATA\0618004.D
Operator   : NAW
Acquired   : 18 Jun 98    1 01 pm using AcqMethod VOC_TRMS
Sample Name: TOUP'S TECH
Misc Info  : 1ML LOOP; 10C @ ULTRA COLUMN
Vial Number: 1
CurrentMeth: C:\HPCHEM\1\METHODS\DEFAULT.M
```

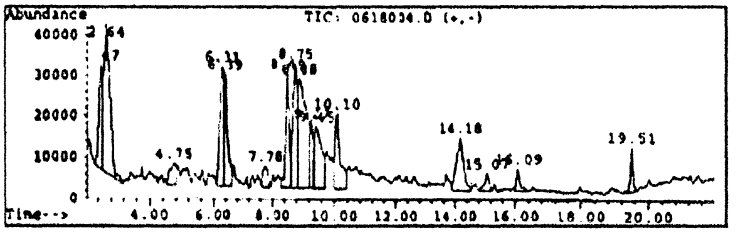

Retention Time	Area	Area %	Ratio %
Total Ion Chromatogram			
2.474	1753106	5.386	33.724
3.644	5091514	15.641	95.000
4.754	641528	1.971	11.974
6.307	2737769	8.411	51.098
6.350	2211258	6.793	41.272
7.782	592472	1.820	11.058
8.490	2357396	7.242	43.999
8.754	2786829	8.565	51.977
8.882	5357812	16.460	100.000
9.265	1123809	3.452	20.975
9.448	2421234	7.438	45.191
10.098	1946292	5.979	36.326
14.177	2129791	6.543	39.751
15.073	435208	1.337	8.123
16.085	389822	1.198	7.276
19.509	577433	1.774	10.777

Figure 7. A reproduction from memoir [13] of the GC-MS peaks between 40 and 400 a.m.u. on a gas with a magnecular structure obtained on June 19, 1998, by analysts Louis A. Dee and Norman Wade of the branch of National Technical Systems (NTS) located at the McClellan Air Force Base in North Highland, near Sacramento, California. The test was done on a type of magnegas produced via an electric arc between graphite electrodes submerged in tap water. Therefore, only the CO_2 peak was expected to appear in the scan in a macroscopic percentage.

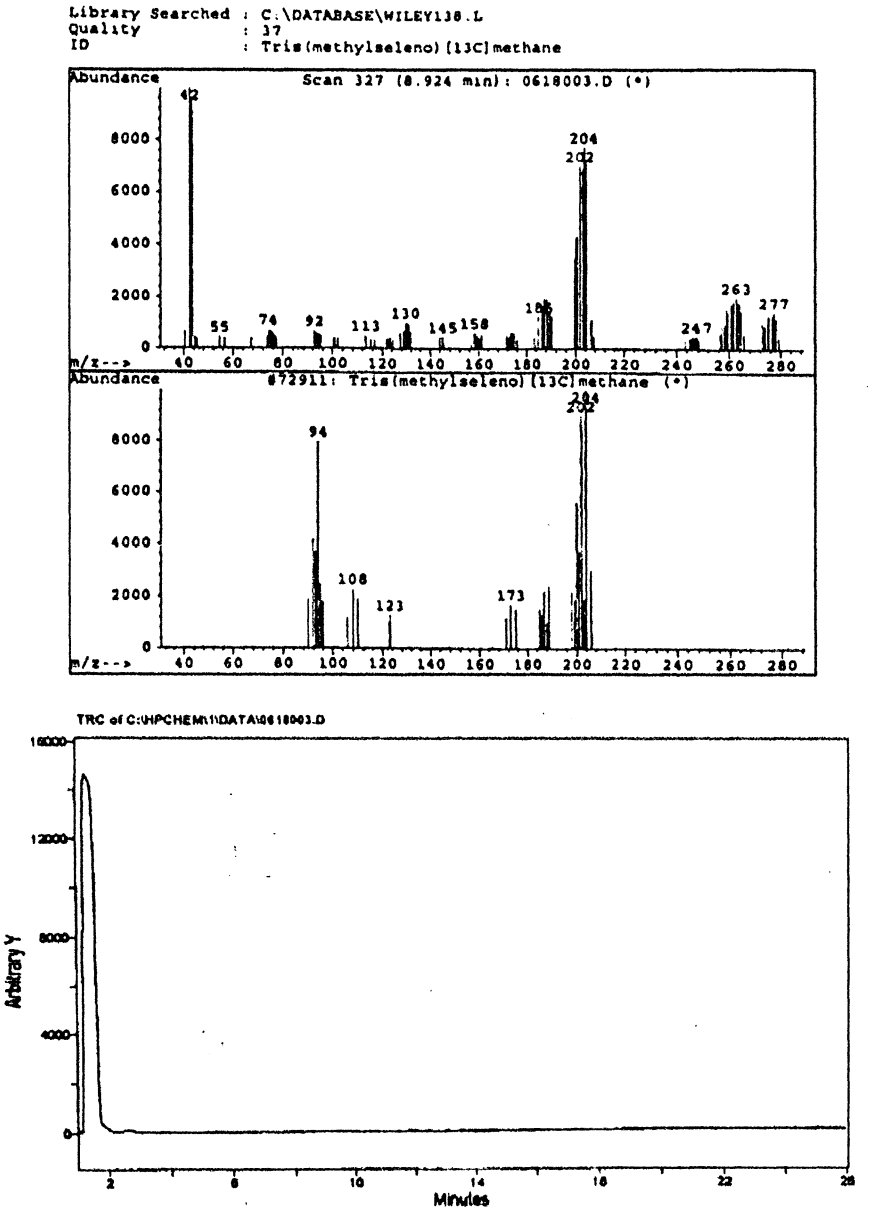

Figure 8. A representation (top view) from memoir [13] of the first experimental evidence at NTS laboratories that the peaks of (Figure 7) are "unknown" because of a lack of identification by the computer among 500, 000 known molecules. The same situation occurred for all remaining peaks of (Figure 7). A reproduction (bottom view) from memoir [1] on the scan of (Figure 7) obtained via the IRD component of the GCMS/IRD providing the first experimental evidence on the lack of IR signature of the GC-MS peaks of (Figure 7). In fact, the above IRD scan establishes the existence of large clusters that have no IR signature at all, thus dismissing valence bonds since they would require perfectly spherical clusters that are essentially impossible at large a.m.u. The only identified IR signature is that for the conventional molecule CO_2, but the latter refers to the constituents of the peaks of (Figure 7), because it is not identified as an isolated detectable species.

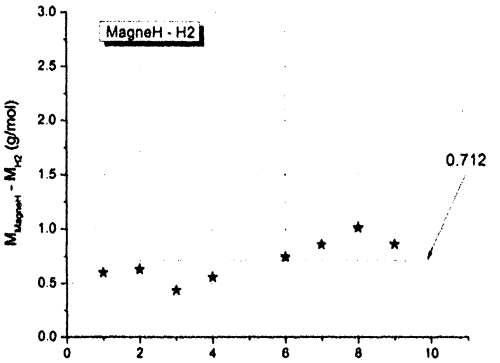

Figure 9. Statistical measurements on the molecular weight of MH with respect to that of H, which is represented by the abscissa, showing that the former is about 35% heavier than the latter, namely, the anomaly is about ten times the statistical error [19].

DATE TESTED	9/5/2012		
QUANTITY TESTED	2		
PACKAGE TYPE	standard		
SAMPLE	ID	EQ09012	EQ02171
Mass	2	177,131	150,391
Mass	3	93,300	77,390
Mass	4	354,930	397,630
Mass	5	373	242
Mass	6	20,779	16,402
Mass	12	1,208	753
Mass	13	73	70
Mass	14	4,517	3,051
Mass	15	641	518
Mass	16	4,393	2,411
Mass	17	9,362	3,121
Mass	18	39,386	12,362
Mass	19	5,922	2,123
Mass	20	17,950	4,954
Mass	22	178	0
Mass	24	239	0
Mass	26	1,043	236
Mass	27	466	320
Mass	28	43,690	28,234
Mass	29	1,186	881
Mass	30	1,305	382
Mass	31	228	0
Mass	32	7,328	5,828
Mass	40	469	337
Mass	42	137	0
Mass	43	459	456
Mass	44	11,546	8,718
Mass	45	399	375
Mass	46	137	0
Mass	73	320	336

Figure 10. A scan of two species of MG done with IVA 110A showing anomalous chemical species from 2 a.m.u. to at least 150 a.m.u., here reduced for simplicity to 73 a.m.u. The above analysis confirms the existence of MH in MG because all species up to 11 a.m.u. can only be MH due to the lack of He and other gases in MG at low a.m.u [19].

Yang *et al.* [19] recently published important research papers in which the experimental confirmation of new chemical species of MagneHydrogen™ has been reported. The first independent experimental verification of the new species of Santilli MagneHydrogen was achieved via the use of a VSA station for the separation of MH from MG, the use of a GC-TCD for the measurement of the percentage of Hydrogen in the separated gas, and the use of conventional methods for the measurement of molecular weight (**Figure 9** and **Figure 10**). Experimentally it was confirmed that MH posses about 97.5% pure Hydrogen, while having 3.89 times the specific weight of H_2, and a consequential energy content of 1167 BTU/scf.

The second experimental verification of Santilli Magne-Hydrogen was achieved using a Vacuum Swing Adsorption (VSA) for the separation of MH from MG, and GC-TCD for the measurement of the conventional Hydrogen content, and a highly accurate balance for the measurement of the molecular weight of MH (**Figure 11**). It was established that the above identified species has the molecular weight of 2.71 a.m.u., thus being 35% heavier than conventional Hydrogen [20].

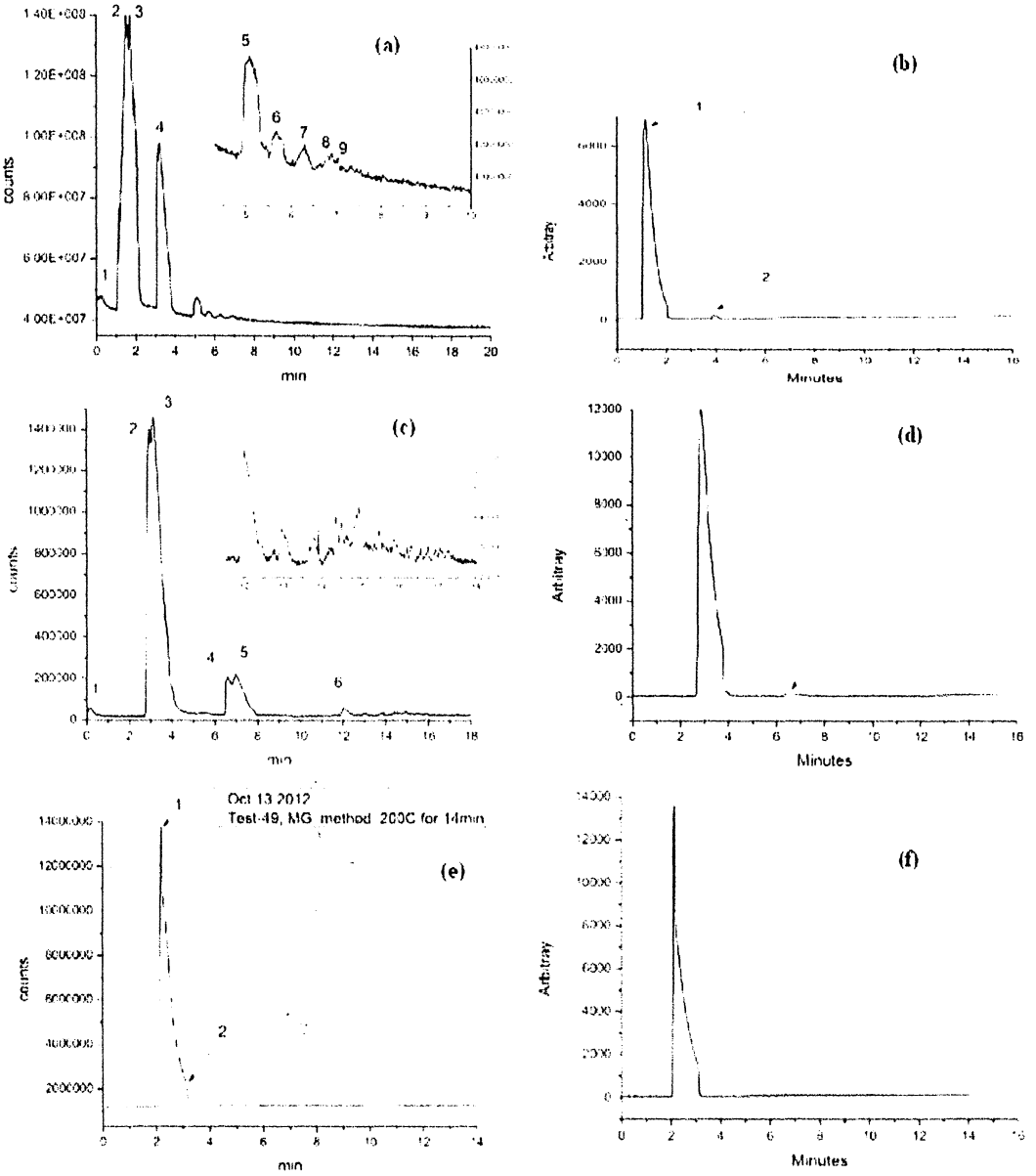

Figure 11. Representative scans achieved by Yang *et al.* on November 8, 2012, via the GC-MS/IRD described in the test. The top view presents a GC-MS scan from 1 a.m.u. to 500 a.m.u. with the column operated at 100 C and the use of 22 minutes elusion time (Figure 11a). The tests were conducted on filtered and compressed MagneGas synthesized from ethylene glycol. In Figure 11b, we present the IRD of the same gas and the same injection which provides experimental confirmation for the presence in MagneGas of clusters without an IR signature, thus confirming the main claim of memoir [13], namely, the existence in nature of bonds other than those based on valence (Figure 11c). Scans obtained via the same GC-MS/IRD, the same 22 minutes elusion time, and the same magnecular gas as those for (Figure 11a), but with the column operated at 400^0 C. In the top view, we present a GC-MS scan showing a decrease of the magnecular species of (Figure 11a) due to the increased temperature of the column, thus

confirming the dependence of the detection of magnecules from the column temperature first identified by Santilli [13]. Figure 11d shows IRD scan confirming the absence of IR signatures for magnecular species and in Figure 11e, scans obtained via the same GC-MS/IRD, the same 22 minutes elusion time, and the same magnecular gas as those for (Fig. **6**), but with the column operated at 200^0 C has been shown. The top view presents a GC-MS scan showing the disappearance of magnecules, thus confirming Santilli's claim [13] that magnecular clusters admit a temperature (the Curie temperature) at which magnetic bonds disappear [20].

Table I. Chemical constituents present in Magnegas2™		
Component name	CAS No.	Percentage (vol./vol.)
Hydrogen	1333-74-0	50-60
Ethane	74-84-0	9-15
Carbon Monoxide	630-08-0	8-12
Ethylene	74-85-1	7-12
Methane	74-82-8	4-8
Trace Gases	NA	2-3
Carbon Dioxide	124-38-9	1-2

Yang *et al.* carried out large variety of tests with different magnecular gases, different equipment and different procedures, wherein they confirmed the results postulated by Prof. R. M. Santilli in his memoir. The few results are summarized as follows [19, 20]:

1. Characterization of magnecules by weakly bonded individual atoms, diatomic radicalss, and conventional molecules;
2. Stability of magnecules at ambient temperature;
3. Progressive reduction of magnecules with the increase of the temperature;
4. Termination of magnecules at a suitable Curie temperature;
5. Detection of magnecular clusters under a suitably selected and operated GC-MS; etc.

The theoretical confirmation of MagneHydrogen consisting individual hydrogen atom bonded together and having stable clusters under a new internal attractive forces originating from the toroidal polarization of orbitals of atomic electrons when placed in strong magnetic fields has been done by various researchers recently [21-27].

INDUSTRIAL APPLICATIONS OF FUELS WITH MAGNECULAR STRUCTURE

Magnegas

The new species of magnecules consisting of the gaseous fuel [28] produced and sold worldwide under the trade name of MagneGas™ (MG) by the U. S. publicly traded company Magnegas Corporation (see www.magnegas.com for details). Plasma Arc Flow reactor [**Figure 12**] use a submerged DC arc to achive complete recycling of liquid waste into a clean burning combustible gas called MG, heat usable via exchangers, solid precipitates. The MagneGas process converts liquid waste into a cost competitive and clean burning fuel that is interchangeable with natural gas. It has the lowest greenhouse gas emissions when compared to fossil fuel and can be used for metal cutting, electricity production, cooking, heating, or powering natural gas automobiles.

Plasma Arc Flow Recycle can recycle (i) City Sewage and/or Sludge, (ii) Automotive Liquid Waste, (iii) Liquid Animal Waste, (iv) Oil Based Liquid Waste, (v) Glycerin & Bio-Fuel By-Products, (vi) Paint & Thinner Waste, and (vii) Petroleum and Petroleum By-Products.

As per the details available, the chemical composition of Magnegas2™ is as depicted below in **Table 1**. Because of Magnecular structure, this gas shows some very interesting properties which has been proved in different experiments, such as:

Figure 12. 100KW Plasma Arc Mobile Recycler

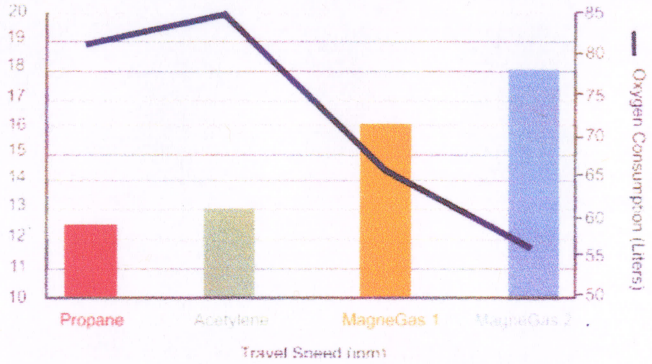

Figure 13. Travel speed cutting 2-inch steel

- **MagneGas 2** has a higher temperature than both propane and acetylene
- **MagneGas 2** is made of a renewable source.
- **MagneGas 2** cuts both faster and cleaner with little to no slag
- **MagneGas 2** releases less smoke

MagneGas™ is an innovative green gas that is a replacement to acetylene. As well as being both safer and more cost effective than acetylene, it also cuts faster and cleaner. MagneGas™ also improves the performance of equipment and the productivity of employees by concentrating the heat at the precise point of the cut, this creates a higher quality cut. MagneGas™ is safer because there is limited flashback during cuts and has a lower toxicity than acetylene. Since MagneGas™ costs less than acetylene and uses less oxygen it is very cost competitive and saves users money.

MagneGas 2 can cut 2 inch steel at a rate of 18 inches per minute [**Figure 13**].

- 38% faster than Acetylene.
- 44% faster than Propane.

MagneGas 2 uses oxygen more efficiently, saving money on both oxygen and gas.

- 34% less than34% less than Acetylene.
- 31% less than Propane.

Aquygen™ gas:

Santilli then provided theoretical experimental evidence [29] on a third industrial application of the new species of magnecules, here referred to the gas commercially produced via certain electrolyzers and essentially consisting of 2/3 Hydrogen and 1/3 Oxygen, which contains a small percentage of H and O magnecular clusters. Under these conditions, Santilli suggested in Ref. [5] the name of HHO (although a similar gas produced via a different electrolyzer is known as Brown's gas). American company Hydrogen Technology Applications, Inc., which company is the owner of all intellectual rights and is currently producing and selling the HHO gas on a world wide basis under the commercial name of Aquygen™ (see *www.hytechapps.com/products.html* for more details). Aquygen™ gas supplements standard vehicle fuels such as gasoline and diesel, increasing BTUs while decreasing emissions.

The Model 1500 Aquygen® Gas Generator **[Figure 14]** runs on water and electricity only! It produces a stable hybrid hydrogen-oxygen gas, with many unique properties. The generator provides a superior gas for most conventional brazing, soldering and metal cutting operations.

Aquygen® gas has been shown to increase combustion efficiency in coal-fired furnaces leading to a dramatic decrease in fuel consumption and significant reduction in emissions, including CO_2, CO, NO_x, SO_x, and fly-ash **[Figure 15]**. Preliminary testing carried out at Western Research Institute (WRI), the leading energy research entity located in the number-one coal-producing state in the nation which has earned a name for reliable emissions testing and monitoring at power plants, showed an increase in furnace temperature upon the introduction of Aquygen® gas (A) and the ability to obtain the same furnace temperature with a decreased coal feed rate (B).

Figure 14. The Model 1500 Aquygen® Gas Generator

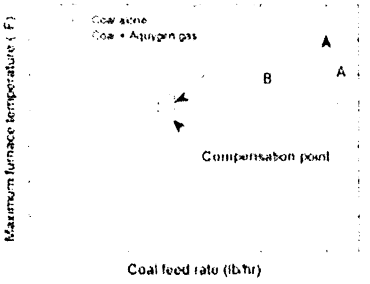

Figure 15. Variation in the maximum furnace temperature against fuel burnt under varied condistion

An electrolyzer which decomposes distilled water into a new fuel composed of hydrogen, oxygen and their molecular and magnecular bonds, called HHO. The electrolyzer can be used to provide the new combustible gas as an additive to combustion engine fuels or in flame or other generating equipment such as torches and welders. The new combustible gas is comprised of clusters of hydrogen and oxygen atoms structured according to a general formula H_mO_n wherein m and n have null or positive integer values with the exception that m and n can not be 0 at the same time, and wherein said combustible gas has a varying energy content depending on its use. The first remarkable feature of the special electrolyzers of this invention are their efficiencies. For example, with the use of only 4 Kwh, an electrolyzer rapidly converts water into 55 standard cubic feet (scf) of HHO gas at 35 pounds per square inch (psi). By using the average daily cost of electricity at the rate of $0.08/Kwh, the above efficiency implies the direct cost of the HHO gas of $0.007/scf. It then follows that the HHO gas is cost competitive with respect to existing fuels. The second important feature of the HHO gas is that it exhibits a "widely varying energy content" in British Thermal Units (BTU), ranging from a relatively cold flame in open air, to large releases of thermal energy depending on its use. This is a direct evidence of fundamental novelty in the chemical structure of the HHO gas.

In fact, all known fuels have a "fixed energy content" namely, a value of BTU/scf that remains the same for all uses. Also, the variable character of the energy content of the HHO gas is clear evidence that the gas has a magnecular characteristic in its structure, rather than a molecular structure, namely, that its chemical composition includes bonds beyond those of valence type.

The third important feature of the HHO gas is that it does not require any oxygen for its combustion since it contains in its interior all oxygen needed for that scope. By recalling that other fuels require atmospheric oxygen for their combustion, thus causing a serious environmental problem known as "oxygen depletion", the capability to have combustion without any oxygen depletion renders the HHO gas particularly important on environmental grounds.

Another important feature of the HHO gas is that it bonds to gaseous fuels (such as natural gas, magnegas fuel, and other fuels) and liquid fuels (such as diesel, gasoline, liquid petroleum, and other fuels) by significantly improving their thermal content as well as the environmental quality of their exhaust.

REFERENCES

[1]Intergovernmental Panel on Climate Change, 2013. *Climate Change 2013: The Physical Science Basis, Summary for Policy Makers*, WG1Contribution to IPCC AR5.
[2]Intergovernmental Panel on Climate Change. Intergovernmental Panel on Climate Change, 2014a. *Climate Change 2014: Synthesis Report, Summary for Policymakers*. Intergovernmental Panel on Climate Change, Geneva.
[3]R. Heede and N. Oreskes, Potential emissions of CO and methane from proved reserves of fossil fuels: An alternative analysis, *Global Environmental Change*, 36 (2016), 12–20.
[4] K. D. Lafferty, The ecology of climate change and infectious diseases. *Ecology*, 90 (2009), 888–900.
[5]J. G. Canadell, C. L. Quéré, M. R. Raupach, C. B. Field, E. T. Buitenhuis, P. Ciais, T. J. Conway, N. P. Gillett, R. A. Houghton and Gregg Marland, Contributions to accelerating atmospheric CO_2 growth from economic activity, carbon intensity, and efficiency of natural sinks, *PNAS*, 104 (2007), 18866-18870.
[6]J. Hansen and M. Sato, Regional climate change and national responsibilities, *Environ. Res. Lett.*, 11 (2016), 034009.
[7]S. Lee, J. G. Speight and S. K. Loyalka, *Handbook of Alternative Fuel Technologies, Second Edition*. 2015, CRC Press, chapter 1.
[8]R. M. Santilli and D. D. Shillady, A new iso-chemical model of the hydrogen molecule, *International Journal of Hydrogen Energy*, 24 (1999), 943-956.
[9]R. M. Santilli and D. D. Shillady, A new isochemical model of the water molecule, *International Journal of Hydrogen Energy*, 25 (2000), 173-183.
[10]R. M. Santilli, *Foundations of Hadronic Chemistry with Applications to New Clean Energies and Fuels*, 2001, Kluwer Academic Publishers, Dordrecht, The Netherlands.
[11]R. M. Santilli, *The New Fuels with Magnecular Structure*, 2008, International Academic Press, Palm Harbor, Florida, U. S. A.
[12]I. Gandzha, and J. Kadeisvily, *New Sciences for a New Era. Mathematical, Physical Discoveries of Ruggero Maria Santilli*, 2011, Sankata Printing Press, Kathmandu, Nepal.
[13]R. M. Santilli, Theoretical prediction and experimental verifications of the new chemical species of magnecules, *Hadronic Journal*, 21 (1998), 789-894.
[14]R. M. Santilli, and A. K. Aringazin, The structure and combustion of Magnegas, *Hadronic Journal*, 27 (2000), 299-330.
[15]R. M. Santilli, The novel magnecular species of hydrogen and oxygen with increased specific weight and energy content, *International Journal of Hydrogen Energy*, 28 (2003), 177-196.
[16]A. K. Aringazin and M. G. Kucherenko, Estimate of the polarized magnetic moment of the isoelectronium in the hydrogen molecule, *Hadronic Journal*, 21 (1998), 895-902.
[17]A. K. Aringazin and M. G. Kucherenko, Exact variational solution of the restricted three- body Santilli-Shillady model of the hydrogen molecule, *Hadronic Journal*, 23 (2000), 1-56.
[18]A. K. Aringazin, Toroidal configuration of the orbit of the electron of the hydrogen atom under strong external magnetic fields, *Hadronic Journal*, 24 (2001), 134-172.
[19]Y. Yang, J. V. Kadeisvili and S. Morton, Experimental Confirmations of Santilli's Magne-Hydrogen, *International Journal of Hydrogen Energy*, 38 (2013) 5003-5008.
[20]Y. Yang, J. V. Kadeisvili and S. Morton, Additional Experimental Confirmations of the New Chemical Species of Santilli Magnecules, *Open Physical Chemistry Journal*, 5 (2013), 1-16.
[21]C. P. Pandhurnekar, Advances on Alternative Fuels with Santilli Magnecular Structure, *International Journal of Alternative Fuels*, 17 (2015)1132-1144.
[22]S. P. Zodape, Novel Chemical Species of Santilli's Magnegas, *AIP Conference Proceedings*, 1648 (2015), 510022.
[23]C. P. Pandhurnekar, Studies on the new fuels with Santilli magnecular structure and their industrial applications, *AIP Conference Proceedings*, 1648 (2015), 510015.

[24]S. S. Wazalwar, V. M. Tangde and A. A. Bhaleka, Study of Combustion of Coal with Magnegas as Additive for Improved Combustion Efficiency: A Review of Present Scenario and Future Scope, AIP Conference Proceedings 1648 (2015), 510021.
[25]S. P. Zodape, Novel Chemical Species of Santilli's Magnegas in Hadronic Chemistry, *AIP Conference Proceedings*, 1648 (2015), 510022.
[26]C. P. Pandhurnekar, Studies on the new fuels with Santilli magnecular structure and their industrial applications, *AIP Conference Proceedings*, 1648 (2015), 510015.
[27]R. M. Santilli, The novel magnecular species of hydrogen and oxygen with increased specific weight and energy content, *International Journal of Hydrogen Energy*, 28 (2003), 177-196.
[28]R. M. Santilli, A new gaseous and combustible form of water, *International Journal of Hydrogen Energy*, 31 (2006), 1113-1128.